MOLECULAR ANALYSES OF UNTRANSLATED REGIONS OF HIBISCUS LATENT SINGAPORE VIRUS

CAO SHISHU
(MSc, Huazhong Agri. Uni., China)

A THESIS SUBMITTED FOR
THE DEGREE OF DOCTOR OF PHILOSOPHY
DEPARTMENT OF BIOLOGICAL SCIENCES
NATIONAL UNIVERSITY OF SINGAPORE

2007

Acknowledgements

I am greatly indebted to my supervisor, Professor Wong Sek Man, for his professional guidance, continuous encouragements and support. I would like to thank my thesis committee members A/P Zhang Lian Hui from Institute of Molecular and Cell Biology and Dr. Song Jianxing from Biochemistry Department for their guidance and support.

I would also like to thank Dr. Ichiro Maruyama, former Principal Investigator of Genome Institute of Singapore for his guidance during my study in his lab. My thanks also go to A/P Li Tianhu, Chemistry Department of NUS, who guided me to carry out some of my experiments in his lab. I would like to thank Professor Peter Palukaitis, Scottish Crop Research Institute, U.K., for his suggestions and encouragements during his visit to Singapore.

I appreciate the following friends and members in my lab who have helped me a lot during my study: Li Weimin, Meng Chunying, Luo Qiong, Cheng Ao, Lim Chinchin, Yang Jing, Zhang Xin, Srinivasan KG, Pang Junxiong, Vincent, Bak Xiao Ying, Teh Yufen, Sunil KT and all those who have helped me and those I forgot to mention here.

Sincere appreciation goes to Mr. Chong Ping Lee for providing necessary items for my research work and those persons in-charge of the DNA sequencing facilities in DBS.

Lastly and most importantly, I would like to thank the National University of Singapore for awarding me a research scholarship, which makes my dream to study in Singapore possible.

TABLE OF CONTENTS

LIST OF PUBLICATIONS

- **Cao, SS** and S M Wong, "5', 3' RNA-RNA interaction facilitates both poly(A) tail-dependent and poly(A) tail-independent translation of *Hibiscus latent Singapore virus* mRNA". International Conference on the Frontiers of Plant Molecular Biology (p50) (22 - 24 May 2006). Changsha, Hunan, China.
- **Cao SS**, Wang HH, Luhur A and Wong SM. (2005). Yeast expression and characterization of SARS-CoV N protein. J. Virol. Methods 130: 83-88.

LIST OF ABBREVIATIONS

Viruses

AMV	*Alfalfa mosaic virus*
BMV	*Brome mosaic virus*
BSMV	*Barley stripe mosaic virus*
BYDV	*Barley yellow dwarf virus*
DENV	*Dengue virus*
EMCV	*Encephalomyocarditis virus*
FMDV	*Foot and mouth disease virus*
HAV	*Hepatitis A virus*
HCRSV	*Hibiscus chlorotic ringspot virus*
HCV	*Hepatitis C virus*
HLSV	*Hibiscus latent Singapore virus*
ORSV-S1	*Odontoglossum ringspot virus, Singapore isolate*
PVX	*Potato virus X*
RCNMV	*Red clover necrotic mosaic virus*
SHMV	*Sunn-hemp mosaic virus*
STNV	*Satellite Tobacco necrosis virus*
TBSV	*Tomato bushy stunt virus*
TEV	*Tobacco etch virus*
TMV-Cr	*Tobacco mosaic virus, strain crucifer*
TNV	*Tobacco necrosis virus*
ToMV	*Tomato mosaic virus*

TYMV	*Turnip yellow mosaic virus*
WNV	*West Nile virus*

COMMON TERMS

aa(s)	Amino acid(s)
ARE	AU-rich element
CP	Coat protein
CPE	Cytoplasmic polyadenylation element
eIF(s)	Eukaryotic translation initiation factors
eRF(s)	Eukaryotic release factors
GFP	Green fluorescent protein
GUS	β-Glucuronidase
IRES(s)	Internal ribosome entry site(s)
IRE	Irion response element
IRP	Irion response protein
MP	Movement protein
nt(s)	Nucleotide(s)
ORF(s)	Open reading frame(s)
PABP	Poly-A binding protein
PARS	Poly- A rich sequences
PKR	RNA-dependent protein kinase
PTB	Pyrimidine tract binding protein
RdRp	RNA dependent RNA polymerase
RRM	RNA recognition motif

sgRNA	Subgenomic RNA
SBP	Selenocysteine-binding protein
TLS	t-RNA-like structure
UTR (s)	Untranslated region(s)
UPD	upstream pseudo-knotted domain

LISTS OF FIGURES

Lists of Tables

Summary

Hibiscus latent Singapore virus (HLSV) is a new tobamovirus recently reported. The genome contains a 5'- and a 3'-untranslated region (UTR). In this study, the functions of 5'UTR and 3'UTR in regulating gene expression were analyzed by *in vitro* and *in vivo* assays. In wheat germ extract and *kenaf* protoplasts, the presence of both 5'UTR and 3'UTR enhanced luciferase activity. Predicted stem loops between 5'UTR and 3'UTR could form nine nucleotide base-pairing which could enhance translation. At the same time, an internal poly(A) tract in the 3'UTR interacted with its 5'cap to form a predicted "closed loop" in enhancing its translation. Therefore, it is suggested that the interaction between the 5'- and 3'-UTRs could promote both poly(A) -dependent and poly(A)-independent translation in HLSV. This study also showed that the length of the internal poly(A) tract and the polyadenylation signal sequence were important for infectivity of HLSV in *Nicotiana benthamiana*. Lastly, HLSV 3'UTR was able to enhance IRES translation tested *in vitro.*

CHAPTER 1

LITERATURE REVIEW

1.1 Introduction

Hibiscus latent Singapore virus (HLSV) is a plant virus recently reported from Singapore (Srinivasan et al., 2002, 2005). The genome of the virus contains a 5' untranslated region (UTR) and a 3'UTR. In this study, we have characterized the functions of the 5'UTR and 3'UTR through molecular analysis methods. The effect of 3'UTRs on the viral coat protein expression and the systemic movement in *N. benthamiana* was analyzed. 5'UTR and 3'UTR interaction in regulating the luciferase reporter gene translational process, and regulating HLSV IRESs-driven translational process were analyzed in detail.

1.1.1 *Hibiscus latent Singapore virus*

According to the serological relatedness, virus morphology, host range and genome organization, HLSV belongs to the genus tobamovirus which is one of the very well characterized groups of viruses (Srinivasan et al., 2003). HLSV caused no visible disease symptoms on hibiscus plant. The virus was co-purified with another plant virus called *Hibiscus chlorotic ringspot virus* (HCRSV). When the virus was tested in other plants, it caused chlorotic local lesion disease symptom on *Chenopodium quinoa* and a curly and mild mosaic leave disease symptom on *Nicotiana benthamiana*. The virus was also tested in other plants. Experimental results showed that the virus could only infect the above mentioned three plant species (Srinivasan et al., 2005).

The genus tobamovirus consists of 22 species (Lewandowski, 2005) and can be classified into 3 sub-groups based on their host range and genome organization.

Complete sequences and partial sequences of several tobamoviruses have been reported (Goelet et al., 1982; Ohno et al., 1984; Solis and Garcia-Arenal., 1990; Ikeda et al., 1993; Alonso et al., 1991; Chng et al., 1996; Lartey et al., 1995; Meshi et al., 1981; Silver et al., 1996; Tan et al., 2000; Ugaki et al., 1991; Srinivasan et al., 2002, 2005; Adkins et al., 2003). Crop losses due to various viral epidemics are documented. Various compilations of crop loss data which may help in predicting global estimates of crop losses are reported (Waterworth and Hadidi, 1998). Tobamovirus-related reduction in crop yields has been estimated to be 30-35% in tobacco and 15-30% in cucumber (Sutic et al., 1999). Also tobamoviruses are well characterized viruses and have been a useful tool for understanding the basic processes of virus infection, multiplication and their survivals. Modern molecular biological techniques have helped us to gain insights into the genome organization and expression strategies of different viruses, which in turn lead to the discovery of methods to overcome the crop losses resulting from virus epidemics as well as the exploitation of viruses as vectors for expressing therapeutic proteins (Hamamoto et al., 1993; Wu et al., 2003).

HLSV was determined to have a close serological relationship with *Tobacco mosaic virus* (TMV) (Srinivasan et al., 2002). The antiserum raised against HLSV coat protein could cross react with TMV coat protein but not *Sunn hemp mosaic virus* (SHMV) or *Odontoglossum ringspot virus*-Singapore isolate (ORSV-S1). Both HLSV and TMV have similar genome organization but with differences in their 3'UTR. In TMV, the 3'UTR consists of an upstream pseudo-knotted domain (UPD) followed by a t-RNA-like structure (TLS) at the 3' terminus. In HLSV, it is an internal poly(A) tract followed by the TLS.

1.1.2 The genome organization of HLSV

HLSV is a positive-strand RNA virus and its genome (Genbank Accession No. NC 008310) contains a 5'UTR, encodes a RNA dependent-RNA polymerase (RdRp) on replicase,a movement protein (MP)and a coat protein (CP), contains a 3'UTR. The 5'UTR contains 58 nucleotide and is predicted to be a stem-loop structure by M-fold (ΔG= -11.8 kcal/mol). The 5'UTR contains a $(CAA)_n$ repeat sequence, which is quite similar with the TMV 5'UTR-a $(CAA)_n$ repeat sequence. The 3'UTR is a 77-96 nt poly(A) tract followed by a TLS at the 3' terminus. The 3'UTR ended with the tri-nucleotides CCA as a replication site (Singh and Dreher, 1998). The whole genome of HLSV is 6474 nucleotides.

During virus replication in plants, the major ORFs, for example, RdRp, MP or CP, are believed to perform important function in the process of viral infection, which was analyzed in other tobamoviruses (Asurmendi et al., 2004; Fujiki et al., 2006; Yamaji et al., 2006). Besides the major ORFs in the viral genome, there are also UTRs. These regions can not be neglected since they are also a part of the genome. They may function as a replication or translational regulator. For example, studies on the TMV 5'UTR found that it is an AU rich and $(CAA)_n$ repeat sequence which can enhance translation (Gallie et al., 1987). The 3'UTR of TMV is an UPD followed by a TLS sequence. Studies have shown that the UPD of TMV can function similar to a poly(A) tail to enhance translation (Gallie and Walbot, 1990). In HLSV, 5'UTR and 3'UTR were also present. The 3'UTR is a unique feature, which is totally different from all other tobamoviruses. Its 3'UTR contains an internal poly(A) tract, followed by a TLS sequence. Till now, this unique 3'UTR was only reported in *barley stripe mosaic virus* (BSMV) genome in plant viruses

(Gustafson et al., 1989), but the length of the internal poly(A) tract in BSMV is less than that in HLSV. In the genome of HLSV, there is a putative polyadenylation signal sequence (AAUAUA) in the CP coding region, which is 105 nt upstream the internal poly(A) tract. This sequence encodes two amino acids (N and I) of the CP. It may be a regulator for the latter internal poly(A) tract. The whole genome organization of HLSV is shown as Fig.1.1. Instead of other elements in the genome, HLSV 5'and 3'UTRs were the main focus in this study. In the following part of this review, the roles of UTRs will be focused on.

1.2 Roles of viral untranslated regions

1.2.1 Function as untrtanslated regions of mRNAs

1.2.1.1 Regulation of viral RNA stability

Viral RNAs are a special kind of mRNA. Their UTRs could have the same functions as the UTRs of mRNAs. From the various studies on mRNAs, clues as to the function of UTRs could be found and similar functions of UTRs of viral RNA could be deduced. Studies showed that the poly(A) tails of mRNAs could be involved in the turnover or degradation of mRNAs (Decker and Parker, 1995; Jacobson and Peltz, 1996). A poly(A) tail could stabilize electroporated mRNAs two to four folds in tobacco protoplasts (Gallie, 1991), and by shortening the poly(A) tail in many mRNAs, degradation of them begun (Jacobson and Peltz, 1996). The poly(A)-binding proteins (PABP) plays key roles in the metabolism of polyadenylated RNAs. Studies have shown that bound PABP can protect mRNAs *in vitro* against attack by 3'–5' exonucleases (Bernstein et al., 1989). This suggests that the poly(A) tails interacts with PABP to form a RNA-protein

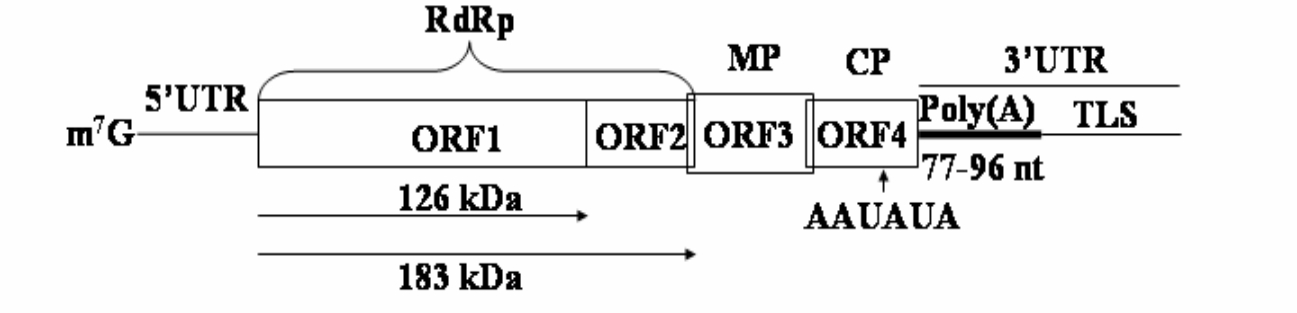

Fig. 1.1 Genome organization of HLSV, with 6474nt in length. 5'UTR is 1-58nt; RdRp is 59-4975nt; MP is 4965-5813; CP is 5800-6291nt. 3'UTR is 6292-6474 when the poly(A) is considered to be 77nt.

complex, which could help to stabilize the mRNA.

The 3'UTR can influence mRNA stability in either a positive or negative way (Decker and Parker, 1995; Jacobson and Peltz, 1996). There are AU-rich elements (AREs) that are found in the 3'UTRs of many mammalian mRNAs, such as those mRNAs encoding transcription factors. The AREs vary considerably in sequence, but most commonly contain multiple copies of the pentanucleotide AUUUA. Also there are a number of proteins that bind to AREs have been reported (Jacobson and Peltz, 1996). Some of these bindings are involved in accelerating degradation of mRNA. Others bindings can also protect mRNA from degradation. It shows the multiple roles of 3'UTR on the mRNA turnover, which could be regulated specifically by AREs (Peng et al., 1998).

In a study (Decker and Parker, 1995), it is observed that the mRNAs possessing specific protein binding sites can be protected from degradation by bound proteins. For example, the 3'UTR of the mammalian transferrin receptor mRNA contains five iron-responsive elements (IREs) which afford protection against ribonuclease cleavage. Also the IREs are bound by IRE-binding protein (Klausner et al., 1993).

In plant mRNAs, it has been demonstrated that AREs are able to act as instability signals. In the study, a synthetic AUUUA repeat was placed in the 3'UTR of two reporter mRNAs (Ohme-Takagi et al., 1993). Another report has also identified the stability determinant in the 3'UTR of an auxin-induced mRNA (Gil and Green, 1996).

1.2.1.2 Modulation of translational expression

1.2.1.2.1 Translational control mechanisms

The molecular mechanisms and control processes that regulate translation are complex. They can be subdivided into two groups, global and transcript-specific control. Global control enables vertebrate cells to utilize strategies that offer co-regulation of manyexpressed transcripts. In cellular responses such control is used to a threatening stress, such asultraviolet irradiation, viral infection or nutrient starvation. For examples, double-stranded RNA-dependent protein kinase (PKR) inhibits global protein synthesis by phosphorylation of the eIF2 a-subunit (eIF2a) (Dever, 2002). The other control is thetranscript-specific control. In the transcript-specific control, the synthesis of a functional related protein is usually regulated in response to metabolic perturbation. In most cases of transcript-specific control, cellular mRNA-binding proteins can bind to a cis-element in the UTR of the target transcript which resulted in translational repression or activation. For example, binding of the IRE-binding protein to the 5'UTR IRE of ferritin is a best-understood mechanism of translational control by trans-acting factors. Since this study is related to translation regulation by viral UTRs, mechanisms of 5'UTR and 3'UTR involved in transcript-specific control of translation regulation are discussed in more detail, based on former studies in this field.

1.2.1.2.2 Regulation translation by 5'UTR and its binding factors

The 5'UTR could regulate translation through binding with translational regulators. It could either enhance or repress translation. In the example of enhancing translation, a typical example is the 5'UTR of TMV. The 60-80 nucleotides sequence consists of a leader sequence (Ω) which enhances the expression of chimeric mRNAs (Gallie et al., 1987), possibly through enhancing recruitment of eEF4F rather than eEFiso4F (Gallie , 2002). An m^7G cap which stabilizes the mRNA and enhances the binding of 40S

ribosomal subunits to the 5'end usually exists at the 5' end of the leader sequence (Shatkin, 1976; Kozak, 1983). Removal of 5' cap affects ribosomal binding and translation. The cap binding protein complex is involved in melting of mRNA secondary structures and facilitating ribosome binding and migration. In terms of repression translation by the 5'UTR and its binding proteins, a prototypic example is that the IRE-binding protein binds to the IRE in the ferritin 5'UTR (Klausner et al., 1993). Studies have shown that the IRE-binding protein blocks the interaction of the 43S pre-initiation complex with the cap-binding complex eIF4F, and thus represses the translation initiation (Muckenthaler et al., 1998). In another study, the auto-regulation of PABP mRNA was shown to exhibit similarities with that of cap-distal Iron Repression protein-IRP complexes. PABP could bind to a cap-distal poly(A) tract in its own 5' UTR and represses translation (De-Melo-Neto et al., 1995). In another study, similar results was get for the analysis of PABP mRNA using sucrose gradients as compared with the model that PABP inhibits scanning of the 40S ribosomal subunit (Bag, 2001). All these studies showed that 5'UTR could regulate the mRNA expression either in a positive way by enhancing recruitment of translational initiation factors or in a negative way by inhibiting the 40S ribosome subunits to bind to mRNA.

1.2.1.2.3 Regulation of translation by 3'-UTR and its binding factors

The 3'UTRs of mRNAs have a diversity of translational regulatory mechanisms since they are near the termination codon and the poly(A) tail. They can harbor signals that regulate subcellular localization of transcripts (Jansen, 2001) and signal that regulate polyadenylation (an AU-rich element that regulates mRNA stability) (Mitchell and Tollervey, 2001). Also, they can regulate termination of translation and stabilize specific

transcripts by 3'UTR-binding proteins. For example, the 3'UTR of target transcripts could bind members of the PUF family to recruit deadenylase, which leads to shortening of the poly(A) tail (Wickens et al., 2002). The other example is that the binding of selenocysteine-binding protein (SBP)-2 to the selenocysteine insertion sequence of the phospholipid hydroperoxide glutathione peroxidase 3'UTR could lead to the translation of selenocysteine insertion instead of termination of translation (Copeland et al., 2000). Lastly, the sex determination gene tra-2 3'UTR could bind to *Caenorhabditis elegans* GLD (defective in germ-line development)-1, which causes rapid poly(A) shortening (Thompson et al., 2000). All these examples showed that the regulatory event happened by the protein–RNA interactions which are at the 3' terminus. There are studies that also identified several translational control mechanisms, in which the regulatory mRNA-binding protein does not bind near the mRNA 3' region that is responsible for regulation. One of the example is shown by Mendez and Richter in 2001, They found that the 3'UTR-binding proteins regulate the initiation of translation in the distant 5'region of the mRNA.

We can also gain some insights into the utilization of the 5'- and 3'-termini for controling of gene expression from a quantitative analysis of UTR length. A recent computational analysis of a large UTR database suggests that the average 3'UTR length in human transcripts is 500 nt, which is nearly four times longer than that of human 5'UTR-150 nt (Pesole et al., 2002). This extended UTR length might have its use. It might provide significant potential for transcript specific regulation originating at the 3'UTR. Also they did additional analysis for this database in term of its length of 3'UTR. Their data suggested that the length of 3'UTR increased with evolutionary age. By

contrast, their data showed that the 5'UTR length was remarkably consistent in organisms ranging from fungi and plants to invertebrates and vertebrates, including humans. This suggests that the 3'UTR-based translational regulation in higher vertebrates is much more important than their 5'UTR. At the same time, the length of 3'UTR might be important in the translational process.

Other than enhance translation, 3'UTRs of mRNAs could also negatively regulate, or repress translation without leading to degradation by harboring some elements (Decker and Parker, 1995). It is generally accepted by researchers that mechanistic analysis of translational regulation of 3'UTR is more difficult than that of 5'UTR. In recent years, there are several models which have been proposed to explain how complexes at the 3' end of the mRNA might affect translation (Gray and Wickens, 1998; Wickens et al.,1997; Preiss and Hentze, 1999).

1.2.1.2.4 Translational activation via poly(A) tail interaction with PABP

The poly(A) tail and m^7GpppG cap are located at opposite ends of the mRNA molecule, but they might act synergistically to stimulate translation (Gallie, 1998; Jacobson, 1996). Consequently, researchers usually focus on the factors that associated with mRNA termini to understand how 3' poly(A) tails might influence initiation at the 5' end. The mRNA termini might not be able to interact with each other directly. However, the mRNA might form end-to-end complexes through these binding factors. Many evidences suggested this phenomenon do exsit. For example, mRNAs have been visualized as circular structures by microscopy (Christensen et al., 1987; Wells et al., 1998). PABP plays an important role in the tranlstional regulation process (Jacobson, 1996). Also several other translation factors which could interact with PABP and play

important roles in mediating end to end complexes. In yeast, plants and vertebrates, the interaction between PABP and eIF4G was detected and studied extensively (Gray and Wickens, 1998; Gallie, 1998). Le and others also suggested the regulation of translation mechanism by PABP–eIF4G interaction which might involve the stabilization of poly(A)–PABP interactions (Le et al., 1997; 2000) and/or an increase in the affinity of eIF4F for the m^7GpppG cap (Wei et al., 1998; von Der Haar et al., 2000; Borman. et al.,2000). Enhancing translation by recruitment of 40S ribosomal subunits through eIF4G–eIF3 interaction could happen by stabilizing the end-to-end complex. Additional mechanisms has been studied in terms of poly(A)–PABP-mediated translation (Searfoss et al., 2001). Dever also showed that PABP could also interacte with eIF4B to aid the processivity of the eIF4A RNA helicase (Dever, 2002). Le first found this interaction in plants (et al., 1997). Then it has been suggested to enhance both poly(A)–PABP binding and eIF4A–eIF4B helicase activity (Le et al., 1997; Bi and Goss, 2000). The eIF4A–eIF4B helicase activity might promote removal of mRNAs 5'UTR secondary structure which usually exsit in mRNA 5'UTR. PABP also binds to eukaryotic release factor 3 (eRF3 or GSPT) through a series of studes (Hoshino et al., 1999; Uchida et al., 2002). Furthermore, Searfoss suggests that in yeast poly(A) tails might function indirectly by affecting the activity of eIF5B (Searfoss et al., 2001). eIF5B is an initiation factor involved in 60S-ribosomal-subunit joining. But it is still not clear if this putative links between eIF5B and poly(A) functions, and whether this effect involves PABP. To date, several PABP-interacting proteins have now been identified. These proteins function at multiple steps in the translational initiation pathway. However, which of these interactions are physiologically relevant remains to be determined. Also none of the

models adequately explain how changes in poly(A)-tail length alter translation. The increases in poly(A)-tail length might result in recruitment of additional PABP molecules is usually an accepted idea nowadays. Then the question is that how many interactions a single molecule of PABP can make, and whether the binding of different partners to PABP is sequentially or ramdomly.

The changes of cytoplasmic poly(A)-tail length often resulted in changes the translation of mRNAs: increases in length generally correlate with translational activation. It has been widely studied during early development in higher eukaryotes (Wickens et al., 1997), but has also been reported in somatic cells. For example, Jiang and Schuman reported that one dendritic mRNA was thought to be regulated by changes in poly(A)-tail length (Jiang and Schuman, 2002). However, the mechanism by which poly(A) tails control translation is still not fully understood.

1.2.1.3 Targeting of RNA to specific subcellular sites

Decker and others suggested that some mRNAs within eukaryotic cells had limited, specific subcellular distribution, and were not distributed uniformly throughout the cytoplasm (Decker and Parker, 1995; Gavis, 1997). For example, actin mRNAs in embryonic muscle cells, mRNAs that encode the proteins involved in establishing the positions of body segment boundaries in the developing insect embryo are such kind of mRNAs. Analysis showed that “zip-code” elements in the 3’UTR of these mRNAs are responsible for the specific localization of such mRNAs. Studies have shown that these elements can be functionally transplanted into heterologous mRNAs to direct the same specific localization. So these elements might presumably represent sites for the binding of proteins that are involved in the specific gathering of the mRNAs.

Localization of viral components is a strong theme in the amplification cycle of eukaryotic positive strand RNA viruses. Replication occurs in association with specific cellular membranes {chloroplasts for tymoviruses (Lesemann, 1977; Matthews, 1991), peroxisomes for most tombusviruses (Russo et al., 1983)). There might be "zip-code" elements in this viruses' 3'UTR which could tether the viral RNA to the specific locations for their replication. Furthermore, localization at one time to the plasmodesmata to permit cell-to-cell movement is a characteristic of plant viral genome. However, such localizations could be the result of protein-protein interactions involving viral protein(s) bound in some way to the RNA genome, possibly the "zip-code" element in their 3'UTR. Indeed, a region of the ORF1 product in tombusviruses is the likely determinant of the specific membrane tropism. It has been shown that a 6 kDa protein encoded by *tobacco etch virus* (TEV) interacts specifically with the endoplasmic reticulum to localize the virus (Schaad et al., 1997).

1.2.2 The translational regulation roles of viral 5' and 3'UTRs

The 5' and 3'UTR of plant viruses play important roles in translational regulation of viral protein expression. The cap is required for infectivity when RNA is used for plant inoculation (Dawson et al., 1986). During translation of replicase, the virion is stripped off the CP which is also called as 'co-translational disassembly'. At the 5' end the CP is loosely bound to the mRNA (Mundry et al., 1991) which facilitates this process. In the TMV 5'UTR, the Ω fragment enhances translation of free RNAs and neither the adjacent viral sequence nor the viral protein is required for its activity (Gallie et al., 1987). The 5' leader sequence contains AUU binding sites for a second ribosome upstream of 126 kDa start codon (Gallie et al., 1987), providing a putative second in-frame translation

initiation site (Tyc et al., 1984; Schmitz et al., 1996). Mutation of AUU to CUU had no effect on the enhancement effect given by the full length leader sequence of the Ω (Gallie et al., 1988). In the leaders of several TMV strains, two motifs, three copies of an eight-base direct repeat and a $(CAA)_n$, were found. Two copies of $(CAA)_n$ have been shown to be sufficient to enhance expression (Gallie and Walbot, 1992). The direct repeats also provide moderate enhancement effect. These two motifs are functionally redundant since both could have the translational enhancement effects. Further studies show that the TMV 5' UTR alone can act as a translational enhancer and it does not require the TMV 3'UTR for performing this function (Gallie et al., 1987). The TMV 5'UTR promotes translation through enhance recruitment of eIF4F (Gallie, 2002).

1.2.3 Other potential roles of viral UTRs

A study on *Tomato Mosaic Virus* (ToMV) has shown that the role of 5'UTR is important for viral replication (Takamatsu et al., 1991). In ToMV the deletion of nucleotides 2-8 in the leader sequence abolished any detectable viral replication. However, this mutant RNA is able to drive the expression of 130 kDa protein in rabbit reticulocyte lysate system. Studies on ToMV 3'UTR also show that it is important to viral replication. Several mutants with deletions in 3'UTR were tested in tobacco plant and protoplast systems. The deletion of double-helical segments II to V in central pseudoknot region D3 resulted in a reduction in viral replication, associated with loss of symptom development. Double-helical segment I upstream of the tRNA-like structure is indispensable for viral replication and double-helical segment VI is not essential for viral replication (Takamatsu at al., 1990). A further detailed analysis of ToMV 3'UTR regions using template dependent RdRP extracts has revealed that several double-helical regions,

that form the pseudoknot and stem-loop structures in domains D1, D2, and D3 and the central core, C, are necessary for high template efficiency. Domain D2 and central core C can bind to RNA polymerase with high affinity whereas domains D1 and D3 showed comparatively lesser affinity towards binding RNA polymerase. Mutation of 3' terminal CCCA identified that 3'-terminal CA was crucial for minus-strand synthesis. Maximum transcriptional efficiencies are achieved with termination of 3' end sequence with CCCA or GGCA (Osman et al., 2000).

1.2.4 Communication between the 5' and 3' end of mRNAs or viral RNAs enhancing translation

In mRNAs, the interaction between the 5' cap structure and the 3' poly(A) tail facilitates translation to the highest extent (Sachs et al., 1997; Tarun and Sachs, 1995). Reports have shown that translationally active mRNAs are circularized through a network of interactions mediated by RNA-binding proteins (Gallie, 1998; Jacobson, 1996; Sachs et al., 1997; Wells et al., 1998). Reports in some tissues also showed that polysomes are observed to be circular (Gallie, 1998; Jacobson, 1996). There are also several other physical interactions between the 5' and 3' termini which have been also observed. The dipeptidyl carboxypeptidase (Dcp1; the protein that removes the m^7GpppN cap) binds to the 5' terminus of the transcript. It also interacts with the transcripts 3' interacting PABP to form the circular complex (Vilela et al., 2000). The 3'UTR binding protein PUF-3 (a member of the PUF family) enhances 5' end decapping after stimulating deadenylation at the 3' terminus (Olivas and Parker, 2000). The presence of 5'cap stimulates a poly(A)-specific ribonuclease (PARN) (Dehlin et al., 2000). All these findings have led to the concept of a 'closed-loop' structure of mRNA. There is also

biochemical evidence supporting for this model. In yeast, poly(A)-bound PABP also interacts with the translation initiation factor eIF4G, which in turn interacts with the cap-binding protein eIF4E, thereby effectively circularizing mRNA via end-to-end complex formation (Tarun and Sachs, 1996). The circular polysomes have been detected in electron micrograph spreads occasionally (Warner et al., 1962). The histone mRNAs terminated with 3'-terminal stem–loop structure but not polyadenylated,, which is unique among all other mRNAs. Two proteins, namely stem–loop binding proteins (SLBP)-1 and -2, bind to the 3' terminal specific stem–loop structure of the histone mRNAs, mimicking PABP binding to the poly(A) tail and drive efficient initiation of translation by interacting with eIF4G and eIF3. This direct evidence shows that circularized mRNAs promotes translation (Ling et al., 2002). The *in vitro* reconstitution using purified components and the visualization by atomic force microscopy of filamentous loops closed by bulky complexes gives another direct evidence for this circularization model (Wells et al., 1998). Factors that bind the poly(A) tail stimulate both cap-dependent and cap-independent translation , presumably by circularizing the mRNA (Bergamini et al., 2000; Michel et al., 2001). In many mRNAs, the interaction of the 5'-bound eIF4G and the 3'-bound PABP could mediate this 5'-3' linkage either directly (Otero et al., 1999; Tarun and Sachs, 1996) or via the bridging protein, PABP-interacting protein (PAIP-1) (Craig et al., 1998). Through the use of RNA recognition motifs (RRM) within PABP, PABP may also interact specifically with ribosomal subunits, which allows it to bind directly to ribosomal RNA (Imataka et al., 1998).

In animal viral RNAs, several viral genomes lack the poly(A) tail as a translational enhancer, including members of the flaviviridae family and rotavirus (Reoviridae).

However, several mechanisms regarding the interaction of the 5' and 3' ends enhancing of translational efficiency has been demonstrated for these viruses (Chiu et al., 2005; Holden and Harris, 2004; Piron et al., 1998). For example, The flaviviruses, such as the dengue virus (DENV) and West Nile virus (WNV), are not polyadenylated. However their viral 3'UTRs contain conserved regions. This conserved regions include a terminal 100 nt which form a conserved stem loop termed the 3'SL (Brinton et al., 1986). Their structures are predicted to form pseudoknots (Shi et al., 1996). There is a 3' cyclization sequence (CS) which is complementary to a CS at the 5'end of the genome. This complementary is supposed to support the 5'-3' interaction enhancing through translation binding factors, but itis still not clear which factors facilitate the translation (Hahn et al., 1987). In other studies, the DENV 3'UTR has been reported to stimulate translation of reporter genes (Edgil et al., 2003; Holden and Harris, 2004), and the action of the 3'SL can attribute to half of this stimulation (Holden and Harris, 2004). Similar studies also reported that the 3'SL enhances translation significantly by the 3'UTR in DENV reporter constructs (Chiu et al., 2005). Conversely,studies using phosphorodiamidate morpholino oligomers (PMOs) directed to the top of the DENV 3'SL reduced approximately 50% in translation using DENV reporter constructs and DENV replicons containing the nonstructural protein genes in addition to a luciferase reporter (Holden et al., 2006). In WNV, an earlier study using WNV reporter constructs suggested that the WNV 3'SL in the absence of the rest of the viral 3'UTR could inhibit translation of reporter RNAs (Li and Brinton, 2001). While it is clear that the flavivirus 3'UTR plays a role in the modulation of translation efficiency, the mechanism of action is still not clear and possibly regulated by many factors, including the genomic context of the 3'SL. There are

conserved domains but not the 3'SL in the 3'UTR of flaviviruses which have been shown to regulate flavivirus translation. Regulation of viral RNA synthesis appear to be a more dramatic role of these domains (Alvarez et al., 2005a; Lo et al., 2003; Tilgner et al., 2005). Little effect on translation is observed when the entire 3'UTR is deleted from DENV or WNV reporter replicons (Alvarez et al., 2005a; Tilgner et al., 2005). This suggests that both positive and negative regulators of translation might exist within the flavivirus 3'UTR.

For the regulation of initiation by transcript circularization, several mechanisms have been proposed. Observation showed that eIF4G could form complex to mediate translation by interacting with poly(A)-tail (Gingras et al., 1999). This suggests that the eIF4G–PABP complex enhances ribosome recruitment, possibly by directed recycling of the 40S ribosomal subunit from the 3'UTR to the 5' terminus (Gingras et al., 1999). In this case, inhibit initiation of translation could happen when disruption of the 5'-3' interaction by intercepting the interaction of PABP either with the poly(A) tail or with eIF4G, which would be expected to block ribosome recycling, reduce ribosome availability . There are several experiments suggest that these and related mechanisms are likely to occur although specific examples of these inhibitory mechanisms have not been demonstrated with certainty.. For example, in the ORF of c-fos mRNA, there is an internal loop between poly(A)-bound PABP and a protein complex that binds to the major protein-coding region determinant of instability (mCRD). The c-fos mRNA degraded when the formation of this loop happens during the translation. It suggests that this internal loop interferes with the normal interaction between the 5'-cap and the poly(A) tail, thereby inhibiting initiation (Grosset et al., 2000). Using a different

mechanism to explain this, shortening of the poly(A) tail was caused by the sequences in the 3'UTR of c-mos and several cyclins and thus reduced efficiency of translation, possibly by inhibiting transcript circularization (Sheets et al., 1994). In maternal mRNA of *Xenopus,* whether to maintain in a dormant state in oocytes and to activate translation during maturation is controlled by the maskin protein with a different translational control mechanism (Stebbins-Boaz et al., 1999). The interaction of maskin with cytoplasmic polyadenylation element (CPE)-binding protein (CPEB) forms a closed loop. CPEB binds to the CPE sequence in the 3'UTR and to the cap-binding protein eIF4E. However, this interaction inhibits translation by competing with the eIF4E-eIF4G interaction, potentially blocking normal 5'- and 3'-interactions. All of these examples have a common theme: binding of a protein to the 3'UTR (or to a coding region near the 3' terminus) could inhibit initiation of translation by interfering the 5'-3' interactions that generate the translation-effective closed loop.

The exact mechanism has not been defined although it is clear that the circularization of cellular and viral mRNAs stimulates translation. It is thought that circularization serves to stabilize the mRNA and the translation complex in the 'closed-loop' model of mRNA translation. Furthermore, the translation may be ensured by the interaction of the UTRs, only when the RNAs is full-length containing both the 5' and 3' ends. However, under certain conditions and in cell-free system, the stimulation of translation of cellular mRNAs can be mediated by the poly(A) in *trans*. This suggests that it is not circularization of mRNAs, but the interaction of the ends with the translational machinery that prompts maximal translation efficiency (Borman et al., 2002). Alternatively, on the same strand of RNA circularization may promote efficient recycling of ribosomes and

rapid re-initiation of translation (Sachs, 2000). It would be particularly advantageous for viral RNAs to use this strategy to compete effectively with cellular messages for the limited translation factors and ribosomes.

1.2.5 Mechanism of viral IRES-driven translation and its interaction with 3'UTR

RNAs from a diverse group of viruses, which include members of the Caliciviridae, Picornaviridae, and Flaviviridae families (Michel et al., 2000; Bergamini et al., 2000) are able to bypass dependency upon an m^7G cap structure for translation initiation via various mechanisms. Initiation of protein synthesis through the use of an internal ribosome entry site (IRES) is such an mechanism. The IRES element directs translation in the absence or with a reduced number of cellular translation factors. Thus it avoids competition for scarce initiation factors, especially eIF4E. The availability of eIF4E is among the most highly regulated within the cell (Gingras et al., 1999).the cellular translation factors are used to direct ribosomal subunits to the translational start site in the absence of scanning once they have bound to IRES RNA secondary and tertiary structure. For the viral internal ribosome entry, there seems to be no universal mechanism. The same translation initiation factors as capped mRNAs are required for most of the picornavirus IRES elements, except for eIF4E, poly(A)-binding protein (PABP), and the N-terminal fragment of eIF4G (Lomakin et al., 2000; Ohlmann et al., 2002; Pestova et al., 1996). On the other hand, The HCV and pestivirus IRESescan bind and position the 40S ribosome subunit specifically and stably in the absence of any eIF, such that the ribosomal P site is placed immediately upstream of the initiator AUG (Pestova et al., 1998). However, they do require eIF3 for efficient translation initiation (Sizova et al., 1998; Kieft et al., 2001).

There is a marked translational synergy between the IRES near the uncapped 5' terminus and the poly(A) tail in picornavirus RNAs. This suggests that there is an IRES-mediated interaction between the termini. The interaction mechanism is not known yet. But *in vitro* studies indicate the participation of eIF4G and PABP in encephalomyocarditis virus translation (Michel et al., 2000). The 3' end of HCV genome is also not polyadenylated. Its IRES has been shown to interact *in vitro* with recombinant cellular factors such as PTB (Ali and Siddiqui, 1995) and La (Ali and Siddiqui, 1997). PTB can bind to both the X region at the 3' end of the RNA (Tsuchihara et al., 1997) and the IRES (Ali and Siddiqui, 1995). The HCV genome may be circularized by the multimerized PTB which binds to both ends of the RNA (Perez et al., 1997). Study showed that this interaction may not be critical for IRES-driven translation in transfected cell lines (Kong and Sarnow, 2002). However, its importance in the viral life cycle *in vivo* remains to be tested. In several studies, the functions of 3'UTRs of IRES-containing viral genomes are analyzed. They involved in the regulation of viral protein expression through the binding of cell-specific proteins required for IRES activity. For example, the replication of the picornavirus specifically in neuronal cells seems to involve in the sequences upstream of the poly(A) tail in the picornavirus 3'UTR (Brown et al., 2004; Dobrikova et al., 2003). In addition to stimulating translation via a poly(A)/PABP interaction, the IRES driven translation can be enhanced by sequences in the picornavirus 3'UTR upstream of the poly(A) tail alone(Lopez de Quinto et al., 2002). Study suggested that various cellular proteins might play a role in this process. For example, the cellular proteins eukaryotic elongation factor 1A (eEFIA), murine proliferation associated protein-1 (Mppl), poly-r(C)-binding protein (PCBP), La autoantigen (La), and

polypyrimidine tract binding protein (PTB) have been shown to bind the 5'UTR of picornaviruses and to enhance translation from picornavirus IRES elements (Blyn et al., 1996, 1997; Florez et al., 2005; Pilipenko et al., 2000), and some of these cellular proteins have also been observed to bind to the 3'UTR of the HCV genomic RNA (PTB) (Ito and Lai, 1999) andthe Norwalk calicivirus (La, PTB, and PABP) (Gutierrez-Escolano et al., 2003). Taken together, these observations suggest a potential means of communication between the viral UTRs wherein these cellular proteins interact with the viral RNA to functionally replace certain canonical translation factors.

1.3 Mechanisms of translation of positive strand viruses

Due to the complexity of protein synthesis, viruses cannot encode all the components necessary for translation. Therefore, the availability and activity of cellular translation factors are very important for them. During eukaryotic cap-dependent translation, initiation factors (eIF4F, the cap-binding complex), mediated by the cap-binding protein, eIF4E, recognize an m^7GpppN cap structure at the 5' end of mRNAs (Gingras et al., 1999). The eIF4F cap-binding complex consists of eIF4E, an adaptor protein (eIF4G), and a helicase (eIF4A) that functions in complex with the co-factor eIF4B. In the cell, the 40S ribosome associates with the initiator methionyl-tRNA/eIF2-GTP ternary complex, eIF3, and eIF1A to form the 43S pre-initiation complex (Pestova et al., 2001). Only when bound to the RNA cap structure can the eIF4F complex, mediated by eIF3, recruit the 43S ribosomal complex to the mRNA (Gingras et al., 1999). This forms the 48S complex, which scans the RNA until the AUG initiation codon is encountered, at which point GTP is hydrolyzed, the initiation factors are released, the 60S ribosomal subunit binds the pre-

initiation complex to form the 80S ribosome, and translation elongation begins (Pestova et al., 2001).

Two general mechanisms exist by which viruses initiate translation: cap-dependent and cap-independent. In mammalian viruses, genomes of members of the viral families Coronaviridae, Flaviviridae, Reoviridae, and Togaviridae contain an m^7GpppN-cap structure at the 5' end of mRNA and are presumed to initiate translation in a cap-dependent manner, which share similarities with the plant tobamovirus. Genome of HLSV also contains the cap structure and is presumed to initiate translation in the cap-dependent manner.

Members of the family Caliciviridae undergo cap-independent translation initiation through an entirely different mechanism. The naturally uncapped genomes of caliciviruses are covalently linked at their 5' ends to the viral protein VPg (Herbert et al., 1997). VPg has been found to interact directly with the translation initiation factors eIF4E and eIF3, promoting translation initiation from VPg-linked viral RNA while inhibiting the translation of capped mRNAs (Daughenbaugh et al., 2003; Goodfellow et al., 2005).

Translation of proteins from most eukaryotic mRNAs involves the binding of translation initiation factors to the 5' cap structure, followed by scanning of mRNA by 40S ribosomal subunit (pre-initiation complex) until it reaches an AUG codon. Subsequently, the larger 60S ribosomal subunit associates itself with the preinitiation complex to form 80S ribosome that deciphers the genetic code and translates it into a protein until it reaches the termination codon (Kozak, 1986; Kozak, 1989).

Favourable sequence context for the ribosome to initiate protein synthesis requires the presence of a purine (R) at -3 position and a G residue at position +4 (GCCRCCaugG)

(Kozak, 2002). If the first AUG codon resides in a weaker context lacking R in -3 position and G in +4 position, the 40S subunits may continue to scan further downstream and initiate when it encounters an AUG codon, which is also known as leaky scanning mechanism. Such a mechanism has been known to operate in rice tungro bacilliform virus (Futterer et al., 1997).

Termination-reinitiation is another mechanism by which ribosomes gain access to downstream AUGs after initiating in upstream ORFs (upORFs). The size of upORFs seems to be a limiting step for reinitiation to be operational. The size of upORFs could be from 10-12 codons (Kozak, 2001) and on some occasions re-initiation occurs following a 24 codon upORF (Luukkonen et al., 1995). Other variations in translation initiation include the utilization of a non-AUG codon (Sasaki and Nakashima, 2000) and 'shunting' mechanism (Futterer et al., 1993; Yueh and Schneider, 2000).

1.4 Methods used in the function analysis 5', 3'UTR of viruses

1.4.1 Nucleotides deletion or mutation of UTRs to analyze its function in the infection or translational process

Nucleotides deletion or mutation in the UTRs is a common method used to analyze their functions. The 3'UTR of *Alfalfa mosaic virus* (AMV) is found to fold into a series of stem-loops and bind with its coat protein with high affinity through mutation analyses of the regions (Olsthoorn et al., 1999). This binding plays a role in initiation of viral infection and has been though to substitute for TLS at the 3' termini of other plant viruses. As a model, the 3'UTR of TMV is analyzed intensively in terms of its influence on viral replication or act as translational enhancing elements (Leathers et al., 1993; Gallie and Walbot, 1990). Nucleotides deletion or mutations are introduced in all these

studies. In BYDV, the deletion of its 3'TE reduced the translation of the 5'-proximal open reading frames from uncapped mRNA by at least 3' folds (Wang and Miller, 1995). Through the deletion analyses, the 3'TE is found to mimic a 5'cap to facilitate the translation of uncapped mRNA (Wang et al., 1997).

1.4.2 Fusion with a reporter gene to analyze the UTRs as translational regulators

Since the mRNA or virus untranslated region is a short sequence (usually 20-200 nt in length), the method used to analyze this short sequence is critical. For analyzing these UTRs function as a translational enhancing element, the most commonly used method is to fuse these UTRs to a reporter ORF such as CAT, luciferase, β-Glucuronidase (GUS) (Lopez de Quinto et al., 2001; Gallie and Walbot, 1990; Wang and Miller, 1997). By comparing the activity of the reporter genes, it is easy to identify whether the UTRs have the function as translational enhancers (Gallie, 2002; Chiu et al., 2005). Studies on the Dengue virus genome have been used by this method to analyze the functions of its 5' and 3' UTRs (Chiu et al., 2005). Also in TYMV and TMV, the same methods have been used to analyze the functions of their UTRs in protoplasts (Matsuda et al., 2004; Gallie, 2002). *In vitro* translation is also an important method used for analyzing the function of UTRs (Gallie, 2002).

1.5 Objectives and significance of this study

Tobamoviruses are one of the most studied plant virus groups. In the study of TMV UTRs, the 5' and 3'UTRs were analyzed *in vitro* and *in vivo* extensively in recent years (Gallie et al., 1987; Gallie and Walbot, 1990). Owing to the newly discovered virus and unique 3'UTR feature, HLSV was selected as a study model and its UTRs were the main focus of this study. HLSV has two IRESs elements formerly identified (Srinivasan, 2003).

The 3'UTR may also influence this IRESs-driven translation.

In this study, the unique 3'UTR of HLSV which contains an internal poly(A) tract is characterized in terms of its influence of the expression of HLSV viral proteins. In addition, the interaction between the 5' and 3'UTRs regulating translation was examined. The 3'UTR regulating of IRES driven translation was also examined.

The aims of this project are:

1. To study the length of ploy(A) tract in its 3'UTR on the influence of expression HLSV coat protein and systemic movement in *N. benthamiana.*

2. To examine the effect of the putative polyadenylation signal sequence in the coat protein coding region on HLSV systemic movement in *N. benthamiana.*

3. To study the functions and interactions of 5'UTR and 3'UTR of HLSV in regulating mRNA translation *in vitro* and *in vivo,* respectively.

4. To examine the effects of 3'UTR on regulation of HLSV IRES-driven translation.

For most of the viral UTRs, the roles of them in the genome are still unknown. Through this study, it could give us a better understanding of the roles of HLSV UTRs, which could possibly apply to other related viruses. So it was significant that this study could broaden the knowledge on roles of the viral UTRs.

CHAPTER 2

MATERIALS AND METHODS

2.1 MATERIALS

2.1.1 Bacterial and agrobacterial strains

Escherichia coli cell strains XL1-Blue and DH5α were used for propagating plasmid clones. *Agrobacterium tumefacien* strain EHA 105 was used for transient GUS assays. Bacterial glycerol stocks were prepared by adding 150 µl of 100% glycerol to 850 µl of liquid culture, frozen in liquid nitrogen and stored at -80^{o}C. Fresh strains from frozen glycerol stocks were streaked onto stock plates and stored at 4^{o}C.

2.1.2 Cloning vectors

pBluescript II KS(+) (Stratagene, La Jolla, CA), pGEM ®-TEasy (Promega Corp., Madison, WI), pCAMBIA 1300, 1301 (Cambia Corp., Canberra, Australia) were used as cloning vectors.

2.1.3 Media

LB medium was prepared by 1% Bacto® - tryptone, 0.5% Bacto® - yeast extract, 0.5% NaCl, pH 7.5; LB agar medium was prepared by LB medium with 1.5% Bacto® - agar, pH 7.5;

SOC medium was prepared by 2% Bacto® - tryptone, 0.5% Bacto® - yeast extract, 10 mM NaCl, 2.5 mM KCl.

All medium was autoclaved at 121^{o}C for 20 min and cooled at room temperature. Filter sterilized $MgCl_2$ and $MgSO_4$ and glucose were added to SOC medium to final concentrations of 10 mM, 15 mM and 20 mM, respectively.

2.2 METHODS

2.2.1 HLSV purification

Virus was isolated from hibiscus leaves and was subsequently maintained in kenaf (*Hibiscus cannabinus* L.) plants. Mechanical inoculation was carried out by grinding the leaves in 0.2 M borate buffer (pH 8), with a mortar and a pestle. The extract was inoculated onto leaves dusted with Carborundum.

Virus was purified from fresh kenaf leaves by homogenizing the tissues in 3 volumes of 0.2 M borate buffer (pH 8), containing 0.2 mM diethyl dithiocarbamic acid. The homogenate was centrifuged at 12,000 x g for 15 min. The supernatant was clarified with an equal volume of butanol/chloroform (1:1), filtered and centrifuged at 35,000 x g for 2.5 hr. The pellet was resuspended overnight in 0.2 M borate buffer (pH 8), and subjected to centrifugation 9,000 x g for 15 min. The supernatant was dialysed against water for 9 hr and centrifuged in 30% CsCl at 40,000 x g for 16 hr at 20^{o}C. The centrifugation steps and overnight resuspension of the pellet were carried out at 4^{o}C. Virus band was collected and yield was quantified spectrophotometrically using an extinction coefficient of 3.3.

2.2.2 Isolation of viral RNA

To the purified viral suspension, equal volume of water saturated phenol pH 4.0, was added and vortexed vigorously for 2 min. The sample was centrifuged at 12,000 x g for 3 min. The upper aqueous layer was collected and re-extracted twice with an equal volume of water saturated phenol and chloroform. To the upper aqueous layer, 1/10 of the volume of 3 M sodium acetate pH 5.2 and either 2.5 volumes of 95% ethanol or 2 volumes of 100% ethanol were added. RNA was precipitated by incubating at -20^{o}C

overnight. The sample was centrifuged at 14,000 x g for 20 min at 4^{o}C to pellet the RNA. The resultant RNA pellet was washed with 200 µl of 70% ethanol (RNase free) and vacuum dried. The pellet was re-suspended in nuclease-free water and the concentration was measured at $A_{260/280\ nm}$.

2.2.3 cDNA synthesis

Using purified HLSV RNA as the template and a primer complementary to 3'end of the genome, first-strand cDNA was synthesized using Superscript II reverse transcriptase (Gibco-BRL) according to the manufacturer's instruction. Subsequent cDNA synthesis and cloning were done by the Gubler and Hoffman (1983)-based Gibco-BRL cDNA synthesis kit using gene-specific primers as per the manufacturer's instructions. The resultant double-stranded cDNA was cloned into pBluescript ^{TM} II KS (+) (Stratagene, La Jolla, CA).

2.2.4 Purification of PCR fragments

PCR fragments were purified directly if a single specific product was obtained using the Qiaquick gel extraction kit. In the event of several non-specific products being present in the PCR reaction, the fragments were electrophoresed on 1% agarose gels. The desired fragment was excised and purified using QIAquick gel extraction kit (Qiagen) according to the manufacturer's instructions.

2.2.5 Dephosphorylation of the vector

Restriction endonuclease digested DNA with compatible ends was dephosphorylated using 10 U of calf intestinal alkaline phosphatase (New England Biolabs) in 10 X CIAP buffer. The reaction was incubated at 37^{o}C for 1 hr. DNA was purified by phenol/chloroform extraction and ethanol precipitation.

2.2.6 End-filling of DNA fragments

Following restriction digestion, the DNA was purified and re-suspended in TE buffer pH 8.0. Typically a 50 µl reaction contained 2 µg of restriction enzyme-digested plasmid vector, 5 µl of 10 X Klenow buffer (Promega), 40 µm of dNTPs and 1µl (5U/µl) of Klenow enzyme. The reaction was incubated at 25^{o}C for 30 min. Subsequently, the end-filled DNA was recovered by phenol/chloroform extraction and ethanol precipitation.

2.2.7 Bacterial competent cell preparation and transformation

Escherichia coli competent cells were prepared according to Sambrook et al., (1989). A single bacterial colony was transferred to 2 ml LB medium and grown overnight in a 37^{o}C shaker-incubator at 250 rpm. Fresh LB medium (100 ml) was inoculated with 1ml overnight culture and grown at 37^{o}C, 250 rpm until the cell concentration reaches 0.3-0.5 $A_{600nm.}$ All subsequent manipulations were carried out at 4^{o}C. Cells were centrifuged at 2300 rpm for 5 min at 4^{o}C. The cell pellet was washed with 10 mM $CaCl_2$ once. The cell pellet was re-suspended in 2 ml of 50 mM $CaCl_2$ and 15% glycerol. Cells were aliquoted and frozen in liquid nitrogen and stored at -80^{o}C.

The frozen aliquots were thawed on ice and 5 µl of ligation mixture was added. The cells were subjected to heat shock (42^{o}C, 90 sec) and quick chilled on ice for 2 min. The cells were grown in 800 µl of LB medium for 1 hr, then plated onto LB agar containing appropriate selection antibiotics.

2.2.8 Construction of full length HLSV cDNA clones

The first-strand cDNA was synthesized using Superscript II reverse transcriptase (Gibco-BRL) according to the manufacturer's instruction. Primers complementary to 5' and 3' ends of HLSV genome were synthesized. The 5' end primer KpnI-T7 HLSV (+)

contained a Kpn I restriction site, T7 promoter sequence and a stretch of 22 nt of HLSV 5'end sequence. The 3' end primer, 3' MluI HLSV (-) has a MluI site and 23 nt region complementary to the 3' end of UTR sequence (nt 6474-6452). PCR was carried out to amplify the HLSV 5' (nt 1-3333, Primer T7-H5'-f and Mid-r) and 3' (nt 3334-6474, Primer Mid-f and H3'-r) fragments, respectively. The 3' fragment was inserted into pBluescript KSII (+) using XbaI/MluI, resulted in p3HLSV. The 5' fragment was inserted into pGEM®-T to generate p5HLSV which was then cut with KpnI/XbaI and inserted into p3HLSV, resulted in the HLSV full-length clone pHLSV. The full-length cDNA was confirmed by sequencing. Two different clones, one with a 85 nt poly(A), and another longer one with a 96 nt poly(A), were obtained. The resultant plasmid pHLSV was linearized with Mlu I and *in vitro* transcribed using Ambion mMessage mMachine® kit. The construction strategy was shown (Fig. 2.1A).

2.2.9 Construction of different poly(A) lengths and putative polyadenylation signal cDNA mutants

Primers were designed as listed in Table 2. 1. Using the 85 nt poly(A) full-length clone as a template, PCR amplifications were conducted with the relevant primers overlapping the poly(A) tract region. Then the overlapping PCR were conducted to amplify the relevant lengths of internal poly(A) tract. Using XbaI/NotI, the overlapped PCR product was cloned into pHLSV. For the mutation and deletion of putative polyadenylation signal clones, the same strategy was used (Fig. 2.1B). All constructs were confirmed by sequencing.

2.2.10 Construction of different clones fused with 5'UTR and 3'UTR

For the construction of these clones, primers were designed as listed in Table 2.2.

(A)

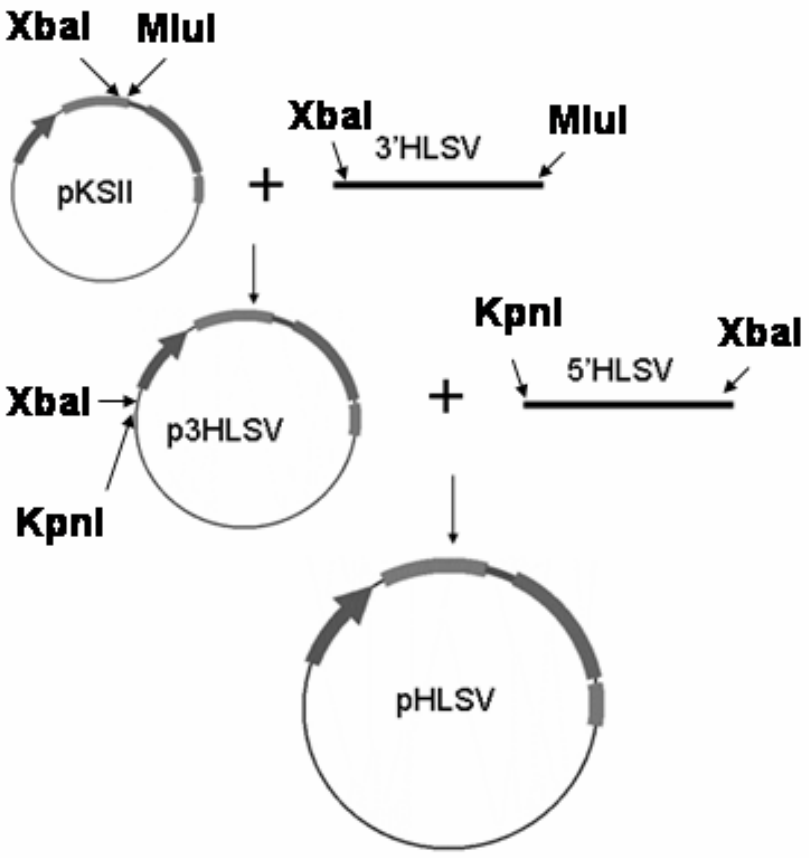
XbaI
MluI
pKSII
XbaI
3'HLSV
MluI
KpnI
XbaI
5'HLSV
XbaI
p3HLSV
KpnI
pHLSV

(B)

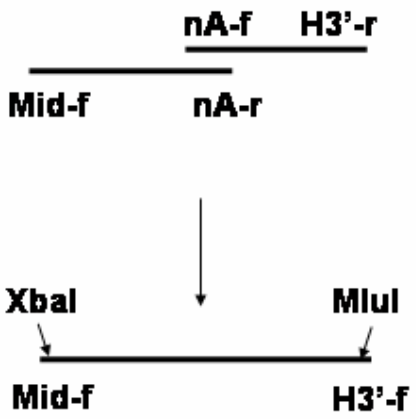

Fig. 2.1 (A) Strategy of construction of full-length HLSV cDNA constructs, RT-PCR product of 3'HLSV were digested by MluI and XbaI, ligated with same enzyme treated pKSII, resulted in p3HLSV; Subsequently RT-PCR product of 5'HLSV were cutted with KpnI and XbaI, ligated with same enzyme treated p3HLSV, resulted in pHLSV. (B) Strategy of construction of different length of Phlsv by over-lapping PCR. Different polyadenylation signal contructs were also using this strategy. First round two PCRs were set up with Mid-f and nA-r, nA-f and H3'-r primers respectively, using 85A pHLSV as template. Using first round PCR products as template, overlapping PCR were done using Mid-f and H3'-r to get relevance length of A products. Products were ligated back to pHLSV cut with XbaI and MluI.

Table 2. 1 Primers used for analyzing the different length of poly(A) tract and putative polyadenylation signals

Primers[a]	Nucleotide position[b]	Sequence(5' to 3')[c]	Objective construct
T_7-H5'-f	1 to19	ggggtacccctaatacgactcactataGTATGTTTTTAGTTTGAAC	pHLSV
H3'-r	6454 to 6474	aaggaaaaaagcggccgcTGGGCCCCAACCCGGGGTTA	pHLSV
Mid-f	3319 to 3346	ATTAGTTAGTTTATCTAGACATAAAAA	pHLSV
Mid-r	3319 to 3346	TTTTTATGTCTAGATAAACTAACTAAT	pHLSV
nA-f	6270 to 6390	ACAACGTCTACTACAACGTAA$(A)_n$GAGATGAGTCGAGGTATCGGGT	pHLSV-nA
nA-r	6270 to 6390	ACCCGATACCTCGACTCATCTC$(T)_n$TTACGTTGTAGTAGACGTTGT	pHLSV-nA
SS1-f	6162 to 6204	ATTCATAAAGAAATAGAT**AATAAA**TTACTATTATTACAGGGT	pHLSV-SS1
SS1-r	6162 to 6204	ACCCTGTAATAATAGTAA**TTTATT**ATCTATTTCTTTATGAAT	pHLSV-SS1
WS1-f	6162 to 6204	ATTCATAAAGAAATAGAT**AATAAG**TTACTATTATTACAGGGT	pHLSV-WS1
WS1-r	6162 to 6204	ACCCTGTAATAATAGTAA**CTTATT**ATCTATTTCTTTATGAAT	pHLSV-WS1
SS2-f	6162 to 6204	ATTCATAAAGAAATAGAT**ATTAAA**TTACTATTATTACAGGGT	pHLSV-SS2
SS2-r	6162 to 6204	ACCCTGTAATAATAGTAA**TTTAAT**ATCTATTTCTTTATGAAT	pHLSV-SS2
WS2-f	6162 to 6204	ATTCATAAAGAAATAGAT**AATAGA**TTACTATTATTACAGGGT	pHLSV-WS2
WS2-r	6162 to 6204	ACCCTGTAATAATAGTAA**TCTATT**ATCTATTTCTTTATGAAT	pHLSV-WS2
PS-f	6162 to 6204	ATTCATAAAGAAATAGAT**AATACA**TTACTATTATTACAGGGT	pHLSV-PS
PS-r	6162 to 6204	ACCCTGTAATAATAGTAA**TGTATT**ATCTATTTCTTTATGAAT	pHLSV-PS
MS-f	6162 to 6204	ATTCATAAAGAAATAGAT**AAGAAA**TTACTATTATTACAGGGT	pHLSV-MS
MS-r	6162 to 6204	ACCCTGTAATAATAGTAA**TTTCTT**ATCTATTTCTTTATGAAT	pHLSV-MS

[a] 'f' and 'r' indicate that the primer corresponds to or is complementary to HLSV genome RNA. n=0, 20, 40, 60, 70, 71, 72, 73, 74, 75, 76, 77 respectively; [b] Positions of the primers corresponding to HLSV genome are shown.

[c] Oligonucleotide sequences are shown in 5′ to 3′ direction. Putative polyadenylation signal sequences are indicated in bold. non-HLSV sequences are shown in lower case.

Table 2.2 Primers used for testing 5', 3'UTR interaction enhancing luciferase activity

Primers[a]	Nucleotide position[b]	Sequence(5' to 3')[c]	Objective construct
P1-f	6284-6313	GGCGGAAAGATCGCCGTGTA**AACGTAAAAAAAAAAAAAAAAAAAAA**	T7-luc-3'UTR
P2-r	6450-6474	**TGGGCCCCAACCCGGGGTTAGGGG**	T7-luc-3'UTR
P3-f		taatacgacgactcactatagggATGGAAGACGCCAAAAACATAA	T7-luc-3'UTR
P4-r	6284-6313	**TTTTTTTTTTTTTTTTTTTTTTTACGTT**TACACGGCGATCTTTCCGCC	T7-luc-3'UTR
P5-f	1-58	taatacgacgactcactatagggGTATGTTTTTAGTTTGAACATTTCAACAACATTCAACT**ACGAAACAGCAACAACAAAT**ATGGAAGACGCCAAAAACATAA	T7-5'UTR-luc-3'UTR
P6-r		TTACACGGCGATCTTTCCGCCC	T7-5'UTR-luc
P7-r	6346-6371	**CTCTTTTTTTTTTTTTTTTTTTT**	T7-5'UTR-luc-A_{77}
P8-f	1-39	taatacgacgactcactatagggGTATGTTTTTAGTTTGAACAAACATTCAACTACGAAAC**A**	T7-5'UTR-D-luc-3'UTR
P9-r	6426-6474	**TGGGCCCCAACCCGGGGTTAGGGGGGACAAACACCTCCCTCGGAAAGC**	T7-5'UTR-luc-3'UTR-S
P10-f	1-32	taatacgacgactcactatagggGTATGTTTTTAGTTTGAACATTTGAACAACAT	T7-5'UTR-M-luc-3'UTR
P11-f	6192-6214	GGGCGGAAAGATCGCCGTGTAA*GGTAGTCAAGATGCATAATAAA*	T7-luc-3'TMV
P12-r	6372-6395	GCGAGCTC*TGGGCCCCTACCGGGGGTAACGG*	T7-luc-3'TMV
P13-r	6192-6214	*TTTATTATGCATCTTGACTACC*TTACACGGCGATCTTTCCGCCC	T7-luc-3'TMV
P14-f	1-68	taatacgacgactcactatagggGTATTTTTACAACAATTACCAACAACAACAAACAACAAACAACA*TTACAATTACTATTTACAATTACA*ATGGAAGACGCCAAAAACATAA	T7-Ω-luc-3'TMV

[a] 'f' and 'r' indicate that the primer corresponds to or is complementary to HLSV (P1-10) or TMV-U1 (P11-14) genome RNA;

[b] Positions of the primers corresponding to HLSV (P1-10) or TMV-U1 (P11-14) genomes are shown;

[c] HLSV sequences are in BOLD. TMV-U1 sequences are in italic. Luc sequences are underlined. T7 promoter sequences are in lower case.

Using the full-length clone pHLSV, PCR product of HLSV 3'UTR was obtained with a forward primer P1 and a reverse primer P2. PCR product of T7-LUC was obtained with a forward primer P3 and a backward primer P4. Using both the PCR product of the HLSV 3'UTR and T7-LUC, the overlap PCR product of T7-LUC-3'UTR was obtained by P3 and P2. The PCR product of T7-5'UTR-LUC-3'UTR was obtained using a forward primer P5 and a reverse primer P2. Subsequently using T7-5'UTR-LUC-3'UTR as a template, the PCR products T7-5'UTR-LUC with forward primer P5 and reverse primer P6, T7-5'UTR-LUC-A77 with P5 and P7, T7-LUC-A77 with P3 and P7, T7-LUC with P3 and P6, T7-d5'UTR-LUC-3'UTR with P8 and P2, T7-5'UTR-LUC-d3'UTR with P5 and P9, T7-d5'UTR-LUC with P8 and P6, T7-d5'UTR-LUC-d3'UTR with P8 and P9, and T7-m5'UTR-LUC-3'UTR with P10 and P2, were obtained. The full-length TMV U1 infectious clone (kindly provided by Prof. Roger Beachy) was used as a template and a PCR product of the TMV 3'UTR was obtained with the forward primer P11 and the reverse primer P12. The PCR product of T7-LUC was obtained with P3 and P13. Using both PCR products of TMV 3'UTR and T7-LUC as templates, the overlap PCR product T7-LUC-3'TMV was obtained with P3 and P12. Subsequently, using T7-LUC-3'TMV as a template, the PCR product T7-Ω-LUC-3'TMV was obtained with P14 and P12, and the PCR product T7-Ω-LUC was obtained with P14 and P5. All the PCR products were cloned into the pGEMT-easy vector (Promega) and the sequences were confirmed by DNA sequencing (ABI 3000A).

To standardize the experiments, we choose all the screened constructs fused with the T7 polymerase promoter with the same orientation as the T7 promoter in pGEMT-easy. Before *in vitro* transcription, all these constructs were linearized by SacII/SpeI to release

the relevant fragments. The fragments ending with A_{77} have seven extra (AGAATCA) nucleotides at the 3' end and other fragments have four (ATCA) extra nucleotides at the 3' end.

2.2.11 Construction of bicistronic vectors for testing the 3'UTR on IRES-driven translation

2.2.11.1 Constructs for *in vitro* assays

T7 promoter-driven bicistronic constructs was assembled in construct hGFP-I-GUS. Two IRES-like elements were found in HLSV, namely HLSV IRES CP134 and IRES MP165 (Srinivasan, 2003). The bicistronic construct contains a hairpin loop at the 5' end immediately upstream of first ORF, and the green fluorescent protein (GFP) blocking the expression of GFP. This is followed by HLSV CP IRES134, MP165 (Icp, Imp) and then GUS ORF (Fig. 2.2). The HLSV 3'UTR was cloned into the SalI site after the GUS ORF. Subsequently the HLSV CP IRES-3'UTR construct (phGFP-Icp-GUS-3'UTR) and the HLSV MP IRES-3'UTR construct (phGFP-Imp-GUS-3'UTR) were linearized with XbaI, and translated in the TnT® coupled wheat germ extract systems (Promega) supplemented with biotinlyated-lysine and amino acid mixture minus lysine.

The translation products were separated by SDS-PAGE and detected by horseradish peroxidase(HRP). For GUS fluorimetric assays, the proteins were extracted and assayed for GUS activity. Targeted deletions within HLSV 3'UTR were generated by PCR. The PCR products were cloned into HindIII and NcoI sites of plasmid hGFP-I-GUS.

2.2.11.2 Constructs for *Agrobacterium* infiltration assays

Transient GUS assays can be performed by agro-infiltration using constructs harboring T-DNA borders. For this purpose, the GFP-IRES-GUS-3'UTR cassette was

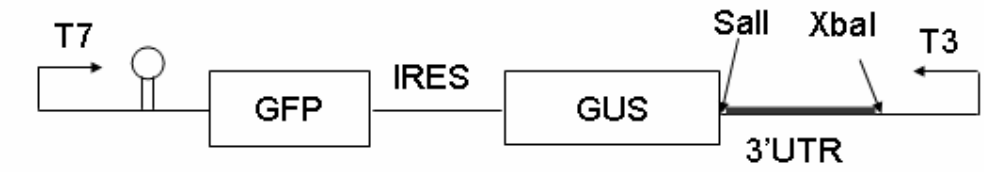

Fig. 2.2 Schematic diagram for construction of phGFP-I-GUS-3'UTR clones for *in vitro* translation assay.

cloned into pCAMBIA 1300 by XhoI sites. The pCAMBIA 1300 has XhoI sites flanking the hygromycin (R) gene which is conveniently located between the 35S promoter and the 35S terminator. The pCAMBIA 1300 was digested with XhoI, and the 7.8 kb fragment was purified using aQiaquick gel extraction column. The fragment was de-phosphorylated and used for cloning the HLSV IRES cassettes. Similarly, plasmids 35S-GFP-Icp-GUS-3'UTR, 35S-GFP- Imp-GUS-3'UTR were digested with XhoI. The resultant 2.7 kb fragments were ligated with the 7.8 kb XhoI-digested pCAMBIA 1300. The plasmids were named pCAM-GFP- Icp-GUS-3'UTR for CP IRES-3'UTR and pCAM-GFP-Imp-GUS-3'UTR for MP IRES respectively (Fig. 2. 3).

Background expression of GUS observed from *Agrobacterium* harbouring the IRES constructs during infiltration assays could interfere with quantifying the expression of GUS from infiltrated plant tissues. Insertion of a plant intron in the GUS gene can alleviate this problem (Ohta et al., 1990). A castor bean catalase intron derived from pCAMBIA 1301 was inserted into GUS ORF of the pCAM-GFP-Icp-GUS-3'UTR and the pCAM-GFP- Imp-GUS-3'UTR constructs. pCAMBIA1301 was digested with NcoI and BstBI which releases a 1.3 kb fragment containing the intron and a portion of GUS gene. This fragment was cloned into NcoI and BstBI digested pCAM-GFP-Icp-GUS-3'UTR and pCAM -GFP- Imp-GUS-3'UTR constructs, respectively.

2.2.12 Nucleotide sequencing

Nucleotide sequence was determined by automated sequencing using ABI PRISM^{TM} BigDye^{TM} Terminator Cycle Sequencing kit (Perkin Elmer). Fluorescence-based dideoxy sequencing reactions were performed using according to the manufacturer's instructions. One µg of DNA was added to 3.2 pmol of vector specific primer, 8 µl of terminator

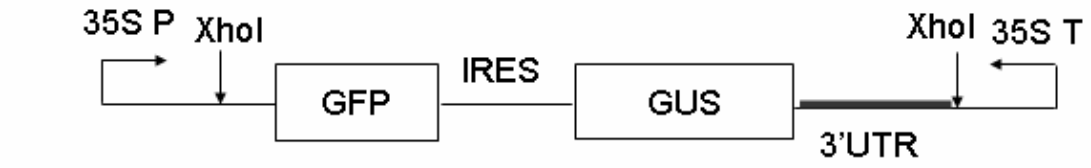

Fig. 2.3 Schematic diagram for construction of pCAM-GFP-Imp-GUS-3'UTR clones for in vivo GUS transient assay.

reaction mix and sterile water to 20 µl. The cycling conditions were 96°C for 10 s, 50 °C for 5s, 65 °C for 4 min for 25 cycles. The extension products were precipitated with 50 ml of 95% ethanol and 2 ml 3M NaOAc. The sample was centrifuged at maximum speed and resulting pellet was washed with 70% ethanol and vacuum dried. The pellet was resuspended and sequenced using an automated fluorescent DNA sequencing machine (ABI PRISM 377, Perkin Elmer, USA) following the manufacturer instruction. DNA sequences were determined on both strands of the cDNA clones.

2.2.13 RNA gel electrophoresis

Purified viral RNA or total RNA from plants or protoplasts was electrophoresed on a 1.2% agarose-formaldehyde denaturing gel and visualized by ethidium bromide staining using a modified protocol (Lehrach et al., 1977). A 1.2% (w/v) gel was prepared by melting 0.36 g of agarose in 20 ml of DEPC-treated water. Upon cooling 6 ml of 5X MOPS buffer (0.1 M (N-morphalino) propanesulfonic acid, 40mM NaOAc, 5 mM EDTA pH 7.0) and 5.5 ml of 37% formaldehyde were added. RNA samples (4.5 µl) were denatured in 2 µl 5 x MOPS, 3.5 µl 37% formaldehyde, 10 µl de-ionized formamide at 65°C for 15 minutes. The samples were mixed with 1 µl of loading dye and electrophoresed in 1X MOPS buffer at 50 volts for 2 hr.

2.2.14 Northern blot analyses

After electrophoresis, the gel was rinsed with DEPC-treated water and soaked in 0.05 N NaOH for 20 min. This step partially hydrolyzes RNA and helps the efficient transfer of larger RNAs. Subsequently, the gel was soaked in 20 X SSC for 45 min. Size fractionated RNAs were transferred to positively charged nylon membrane (Roche Diagnostics GmBH, Germany) by capillary action overnight (Sambrook et al., 1989) or

by using vacuum transfer (Vacugene XL, Pharmacia LKB) . The RNA was UV cross linked to the membrane using UVC 500, UV Crosslinker (Hoefer, USA) at energy setting of 120 mjoules / cm^2 according to manufacturer's instructions. After cross-linking, RNA was visualized by staining the membrane with 0.03% methylene blue in 0.03 M NaOAc. Hybridization of the cRNA probe and detection were performed using the DIG system (The DIG System User's Guide, Roche Diagnostics GmBH, Germany).

2.2.15 Generation of DIG-labeled cRNA probes

To generate a DIG-labeled probe, the HLSV genome 3'TLS fragment (nt 6368-6474) was subcloned into plasmid vector pGEM-T easy. To synthesize 'runoff' transcripts the plasmid was linearized with SpeI. The linearized template was *in vitro* transcribed with T7 polymerase to generate DIG-labelled antisense cRNA probes using DIG^{TM} RNA labeling kit (Roche Diagnostics GmBH, Germany). The labeling reaction was carried out as per the manufacturer's instructions. Hybridization was carried out with DIG-labelled antisense cRNA probe and signals were detected using colour substrate (NBT/BCIP), according to manufacturer's instructions (Roche Diagnostics GmBH, Germany).

2.2.16 Polyacrylamide gel electrophoresis and Western blotting

The CP of purified virus and proteins extracted from *in vivo* IRES assays were separated on 12% SDS-PAGE gels containing 0.4% sodium dodecyl sulfate (SDS-PAGE) according to Laemmli (1970). Protein bands were visualized by staining with coomassie brilliant blue or transferred onto polyvinylidine difluoride (PVDF) Western blotting membranes (Roche Diagnostics GmBH, Germany) using a mini trans-blot cell apparatus (Bio-Rad, USA). Proteins were transferred from SDS-PAGE gels to PVDF membrane in the presence of transfer buffer (10 mM Tris base pH 8.3, 96 mM glycine,

10% methanol). The membrane was incubated overnight at 4^0C in blocking buffer containing 5% nonfat milk dissolved in TBST (10 mM Tris pH 8.0, 150 mM NaCl, 0.1% Tween-20). The membrane was probed with protein-specific antibody e.g. polyclonal HLSV antibody (1 µl of crude antiserum dissolved in 10 ml of TBST) overnight at 4^0C with gentle shaking. Unbound antibodies were removed by washing the membrane three times in TBST buffer with each wash lasting up to 10 min. The membrane was probed with goat anti-rabbit IgG conjugated with alkaline phosphatase, as the secondary antibody (1 µl in 10 ml of TBST) for 1 hr. The unbound antibodies were washed with three changes of TBST buffer 10 min each. Bands were visualized using NBT/BCIP colour development substrate (Promega) in alkaline phosphatase buffer (100 mM Tris pH 9.5, 100 mM NaCl, 5 mM $MgCl_2$).

For analysis of *in vitro* translation reactions, the *in vitro* translation products (2 ul) were mixed with 2x SDS loading buffer and subjected to SDS-PAGE. Protein was transferred onto polyvinylidine difluoride (PVDF) Western blotting membranes (Roche Diagnostics GmBH, Germany) by using a semi-dry transfer apparatus (Bio-Rad), and the membrane were blocked at room temperature for 1 hr in blocking buffer in TBST (20 mM Tris-HCl (pH 7.4), 150 mM NaCl, 0.5% Tween 20). Then, streptavidin-HRP antibody was added diluted (1:10,000) in TBST and was incubated for 1 h at room temperature. After washing three times for 5 min each with TBST and three times for 5 min each with distilled water, the membrane was treated using a chemiluminescent detection kit (Promega) according to the manufacturer's protocol. As mentioned in the protocol, Wheat Germ Extract contains five major endogenous biotinated proteins: 200 kDa, 80 kDa, 34 kDa, and a doublet at 17 kDa. We used the 200 kDa and the 80 kDa

endogenous biotinlyated proteins as an internal control for the Western blot to analysis the luciferase expression level of different constructs.

2.2.17 *In vitro* transcription

Plasmid DNA was linearized with the appropriate restriction enzyme and cleaned up using a Qiaquick gel extraction column and 1 μg was used as template for RNA transcription reactions. The Ambion mMessage mMachine® kit was used for generating capped *in vitro* transcripts.

Components	Amount
2 x NTP/CAP	10 μl
10 x Reaction buffer	2 μl
Linearized DNA template	1 μg
Enzyme mix (T7 polymerase)	2 μl
Nuclease free water	to 20 μl

Ambion MEGAsript® T7 kit was used for generating uncapped *in vitro* transcripts.

Components	Amount
2 x ATP, UTP, GTP, CTP	2 μl each
10 x Reaction buffer	2 μl
Linearized DNA template	1 μg
Enzyme mix (T7 polymerase)	2 μl
Nuclease free water	to 20 μl

The reaction mixtures were mixed thoroughly and incubated at 37°C for 2 hr. The integrity of both capped and uncapped *in vitro* transcripts was checked by agarose gel electrophoresis.

2.2.18 *In vitro* translation

In a 25 µl reaction, 12.5 µl wheat germ extract (Promega) and 1 µg *in vitro* transcribed capped mRNA were mixed together with a complete non-radioactive amino acid mixture, containg biotinylated lysine tRNA, and were incubated.

Components	Amount
Wheat germ extract	12.5 µl
In vitro transcribed RNA	0.5 µg
Amino acid mixture, minus lysine	1 µl
Biotinylated-tRNA lysine	1µl
Nuclease free water	to 25 µl

The reaction was incubated at 30^{o}C for 2 h. The amount of translation product was determined by densitometry.

2.2.19 Coupled *in vitro* transcription and translation

Proteins obtained from linearized plasmid DNA templates were expressed using TnT® Coupled Wheat Germ Extract Systems (Promega) according to the manufacturer's instructions. Typically, a 50 µl reaction mix contained 1 µg of linearized plasmid DNA template, 25 µl TnT wheat germ extract, 2 µl TnT reaction buffer, 1 µl T7 RNA polymerase, 1 µl biotylated-tRNA lysine, 2 µl amino acid mixture minus lysine (1 mM), 1µl RNasin® (40U/µl), and nuclease free water up to the total volume 50 µl. The reaction was incubated at 30^{o}C for 2 hr. Template concentrations were optimized for different constructs independently. The translation products were resolved by SDS-PAGE and were detected by HRP. Translation reaction supplemented with unlabeled amino acids was used for assaying GUS activity by a fluorimetric assay.

2.2.20 Isolation of protoplasts

Kenaf cultivar, Everglade-41 leaf material was used for isolating protoplasts. Seeds of kenaf cultivars were kindly provided by Dr. B. S. Baldwin, Mississippi State University, USA. Kenaf seedlings were grown at 25^{o}C, 16/8 hr, light/dark cycle. One month old kenaf seedlings at 4- 6 leaf stage were used for protoplast isolation. The method followed for isolating protoplasts were according to previously published work (Liang et al., 2002). Leaves were surface sterilized for 10 min with 0.8% Clorox® containing active ingredient 0.04% sodium hypochlorite. Following that, the leaves were rinsed three times with sterile distilled water, each wash lasting up to 5 min. Leaves were sliced into thin 1 mm strips and incubated in filter sterilized enzyme solution. The enzyme mixture contained 0.2 mM KH_2PO_4, 1 mM KNO_3, 1 mM $MgSO_4$, 1 µM KI, 0.01 µM $CuSO_4$, pH 5.6, 0.6 M mannitol, 10 mM $CaCl_2$, 0.8% cellulase Onozuka R-10 (Yakult Honsa Co. Ltd), 0.25% macerase R-10 (Yakult Honsa Co. Ltd). Digestions were carried out at 25^{o}C in dark with shaking 10 x g/ min (Heidolph Rotamax 120, Germany) for 16 hr. Protoplasts were gently pipetted using a Pasteur pipette and released. The protoplast containing solution was passed through 70 µm nylon cell strainer (Becton Dickinson, Franklin Lakes, NJ) to remove the cell debris. The filtrate was later transferred to 50 ml centrifuge tubes and centrifuged at 100 x g for 5 min at 4^{o}C. Pellets were washed in wash solution containing 0.6M mannitol and 10 mM $CaCl_2$, (pH 5.6), three times. Protoplast yields were calculated using haemocytometer slide (Marienfield, Germany) and protoplast viability was determined by fluorescein diacetate (FDA) staining (Widholm, 1972).

2.2.21 PEG inoculation of protoplasts

Concentrated kenaf protoplasts (4x 10^5 cells) were mixed with 20 µg (30 µl) of *in vitro* transcript (capped or uncapped) of different constructs and 200 µl of 40% PEG 3000 in 3 mM $CaCl_2$ for 15 sec. Then protoplast/RNA mixture was diluted with 1.5 ml of wash solution and left on ice for 2 min. The protoplast/RNA mixture was diluted twice with 1.5 ml of wash solution and incubated on ice for another 15 min. The mixture was washed once with 2 ml of wash solution. The protoplast concentration was adjusted to 1x 10^5 cells per ml with MS medium (Murashige and Skoog, 1962) containing 0.6 M mannitol and 10 mm $CaCl_2$. Transfected protoplasts were collected by centrifugation at 100 x *g* for 10 min at 6 h post inoculation (h. p. i.). The pellets were resuspended in luciferase assay lysis buffer (Promega) and subjected to luciferase activity assay. Each construct was assayed at least three times with duplicates and the mean values were calculated. Relative luciferase activity was used to avoid differences from different experiments due to significant variability (50%) (Qu and Morris, 2000).

2.2.22 Luciferase assay

To test the *in vitro* translation products, aliquots of translation samples (2 µl) were added to luciferase assay reagent. To assay the protoplast luciferase activity, the protein was extracted by the lysis buffer supplied from the kit (Promega E1500). Luciferase activity was assayed according to the supplied protocol. Typically, protoplast extract or wheat germ lysate were assayed for luciferase activity by injection of 0.5 M luciferin using LS50B Luminescence Spectrometer (Perkin-Elmer) in 96 wells plate.

2.2.23 Preparation of electro-competent *Agrobacterium* cells

Agrobacterium EHA 105 (Hood et al., 1993) competent cells were prepared by inoculating a single colony to 5 ml of LB medium supplemented with 50 µg/ml

rifampicin and incubated in a shaker incubator at 28°C. The overnight grown bacterial culture was transferred to 100 ml LB medium containing 50 µg/ml rifampicin. Cells were harvested when they reached a density of 0.5 at $A_{600\ nm}$. Cells were centrifuged at 10,000 x g for 10 min at 4°C. The pellet was washed with 40 ml of 1 mM HEPES buffer pH (7.0). The cells were washed again with 40 ml of 1mM HEPES buffer pH (7.0) containing 10% glycerol. Finally the bacterial pellet was resuspended in 2 ml of 1mM HEPES buffer pH (7.0) containing 10% glycerol. Bacterial cells were transferred as 100 µl aliquots, frozen in liquid nitrogen and stored at -80°C.

2.2.24 Electroporation of *Agrobacterium*

After thawing the *Agrobacterium* competent cells, 0.5 µl miniprep DNA was added and incubated on ice for 10 min. The contents were transferred to a pre-chilled, Gene Pulser® electroporation cuvette (BIO-RAD, 2 mm gap). The electroporation parameters were set as 25 µF capacitance, 400 Ω resistance and 2.5 KV pulse with an 8-9 sec delay. A BIO-RAD GENE PULSER II was used for electroporation. After pulsing the cells, 1 ml of LB medium was added immediately to the DNA/competent cell mixture and chilled on ice for 2 min. The contents were transferred to a sterile tube and the cells were grown at 28°C for 2 hr to allow recovery and marker expression. The bacterial cells (30 µl) were plated onto LB agar supplemented with appropriate selection antibiotics (kanamycin 50 µg/ ml, rifampicin 10 µg/ ml). Cells were grown for 2 days at 28°C.

2.2.25 β-Glucuronidase (GUS) fluorimetric assay and leave staining assay

To test the IRES activity, a GUS fluorimetric assay (Jefferson, 1987) was used. The fluorimetric assay involved quantifying the rate of β-glucuronidase activity in hydrolyzing 4-methylumbelliferyl β-D-glucuronide, (4-MUG, SIGMA # 5664) substrate,

to give the breakdown product, 4-methylumbelliferone (4-MU).

Translation samples (20 µl) were diluted with 80 µl of GUS extraction buffer (50 mM sodium phosphate buffer (pH 7.0) containing 10 mM β- mercaptoethanol, 10 mM Na-EDTA, 0.1% (v/v) Triton x-100). From the diluted samples 40 µl was taken to which 70 µl of GUS extraction buffer was added. To the diluted samples, 1 µl of 10 mM 4-MUG solution was added and the mixture was incubated at 37^{o}C for 1 hr. To stop the reaction and to enhance fluorescence, 1 ml of 0.2 M Na_2CO_3 was added. The rate of accumulation of 4-MU was assayed using excitation and emission wavelengths of 365 nm and 455 nm, respectively.

For assaying *in vivo* GUS activity from *N. benthamiana* leaves, infiltrated areas were excised 72 hr after inoculation, homogenized in 10 volumes (w/v) GUS-extraction buffer. The sample was centrifuged to pellet the debris and to the supernatant (100 µl), 1 µl of 10mM 4-MUG solution was added. The reaction mix was incubated at 37^{o}C for 1 hr. To stop the reaction and to enhance fluorescence, 1 ml of 0.2 M Na_2CO_3 was added. GUS activity was determined using excitation and emission wavelengths of 365nm and 455nm, respectively.

For calculating protein content, 5 µl of leaf extract was diluted with 155 µl of GUS buffer. 40 µl of Bradford reagent was subsequently added. Absorbance at 595 nm was measured and the protein concentration was compared against BSA standard curve (Bradford, 1976).

For GUS staining the *N. benthamiana* leaves, the infiltrated leaves were cut and soaked in GUS staining solution (80 mM sodium phosphate buffer [pH 7.0], 0.4 mM potassium ferricyanide, 0.4 mM potassium ferrocyanide, 8 mM EDTA, 0.05% Triton X-

100, 0.8 mg/mL 5-bromo-4-chloro-3-indolyl-β-D-glucuronide) for 24 hrs, then destaining the leaves with 100%EtOH for 48hrs (changed the EtOH 4-5 times during the destain). Picture were taken after the destain process.

2.2.26 RNA secondary structure prediction

The RNA secondary structure was predicted with version 2.3 M-fold from web server of M. Zucker (http://www.bioinfo.rpi.edu/applications/mfold/). Predictions were performed at 25°C in order to mimic the conditions of the natural environment for the plant virus RNAs.

2.2.27 RT-PCR analysis

Total RNA extracted from *N. benthamiana* leaves was used as the template. Two primers complementary to the HLSV CP coding region were chosen and RT-PCR was carried out according to the Titan® RT-PCR kit (Roche Diagnostics GmBH, Germany) protocol. The condition for RT-PCR was as following: 42C 30min; 94C 30sec, 50C 45sec, 68C 45 sec for 35 cycles; 68C for 10min; 16C in the end. The products were separated in 0.8% agarose gel and photo was taken under UV light.

2.2.28 Observation of leave symptoms

One-month old *N. benthamiana* were inoculated with different transcripts. Photographs from uninoculated upper or inoculated leaves were taken 15 days after inoculation.

CHAPTER 3

THE LENGTH OF INTERNAL POLY(A) TRACT AND MODIFICATION OF THE PUTATIVE POLYADENYLATION SIGNAL SEQUENCE INFLUENCE HLSV CP EXPRESSION AND SYSTEMIC MOVEMENT IN *N. BENTHAMIANA*

3.1 Introduction

The HLSV 5'UTR contains 58 nucleotide and is predicted to be a stem-loop structure and its 3'UTR contains a 77-96 nt internal poly(A) tract, followed by a TLS at the 3' terminus, ending with CCA as a putative replication initiation site (Singh and Dreher, 1998). The unique 3'UTR feature of HLSV is different from all other tobamoviruses in that it possesses an internal poly(A) tract, which is variable in length. The HLSV internal poly(A) tract seems functionally similar to that of TMV UPD since they both located upstream TLS. Through sequencing the full-length cDNA clones, the length of the internal poly(A) tract is determined to be variable, from 77 nt to 96 nt. In eukaryotic mRNAs, the 3'UTRs contain regulatory elements affecting mRNA translation, stability, and transport. Mature 3'UTRs are formed by polyadenylation of the pre-mRNA, a coupled reaction involving endonucleolytic cleavage followed by poly(A) synthesis. A significant fraction of mRNAs display multiple polyadenylation sites (Gautheret et al. 1998). In HLSV, there is a putative polyadenylation site (AAUAUA) 105 nt upstream the poly(A) tract. It is located in the CP and encoded two amino acids (NI), which may regulate the formation of HLSV 3'UTR.

Different polyadenylation signals have been described (Beaudoing et al., 2000) and the efficiency of these signals were different, which is shown as Fig. 3.5A (The HLSV putative polyadenylation signal is indicated as WT). The choice of polyadenylation

signals may influence the stability, translation efficiency, or localization of an mRNA in a tissue- or disease-specific manner (Edwalds-Gilbert et al., 1997). In the mammalian system, effective polyadenylation requires two main sequence components: a highly conserved AAUAAA signal located 10-30 nt 5' to the cleavage site and a more variable GU-rich element, 20-40 nt 3' of the polyadynelation site (Colgan and Manley, 1997). Although the AAUAAA signal is often considered to be present in 90% of the mRNAs and replaced by a AUUAAA variant in the other 10% (Wahle and Keller, 1996), alternate signals are certainly present in a significant fraction of the 3' ends of mRNA (Claverie, 1997; Gautheret et al., 1998; Tabaska and Zhang, 1999; Graber et al., 1999).

Since tobamoviruses are well characterized, they have been used as a useful system for understanding the basic processes of virus replication and evolution. In this study, the effects of different lengths of poly(A) tract and modification of the sequence of the putative polyadenylation signal on HLSV CP expression and systemic movement in *N. benthamiana* were analyzed in detail.

3.2 Transcripts derived from three full-length cDNA clones with different lengths of poly(A) tract are able to infect and move systemically in *N. benthamiana*

The length of the internal poly(A) tract of HLSV is variable *in vivo*. To characterize whether transcripts with different lengths of poly(A) tract could infect *N. benthamiana*, full-length cDNA clones were constructed with different lengths of poly(A) tract. Three clones were obtained, with poly(A) tract lengths of 77 nt, 85 nt and 96 nt, respectively (Fig. 3. 1A). These transcripts were able to infect *N. benthamiana* and were able to replicate in both the inoculated and upper leaves since viral gRNA and sgRNAs were detected in both leaves (Fig. 3.2B, 2C). Also both Western blot detection of the HLSV

A.

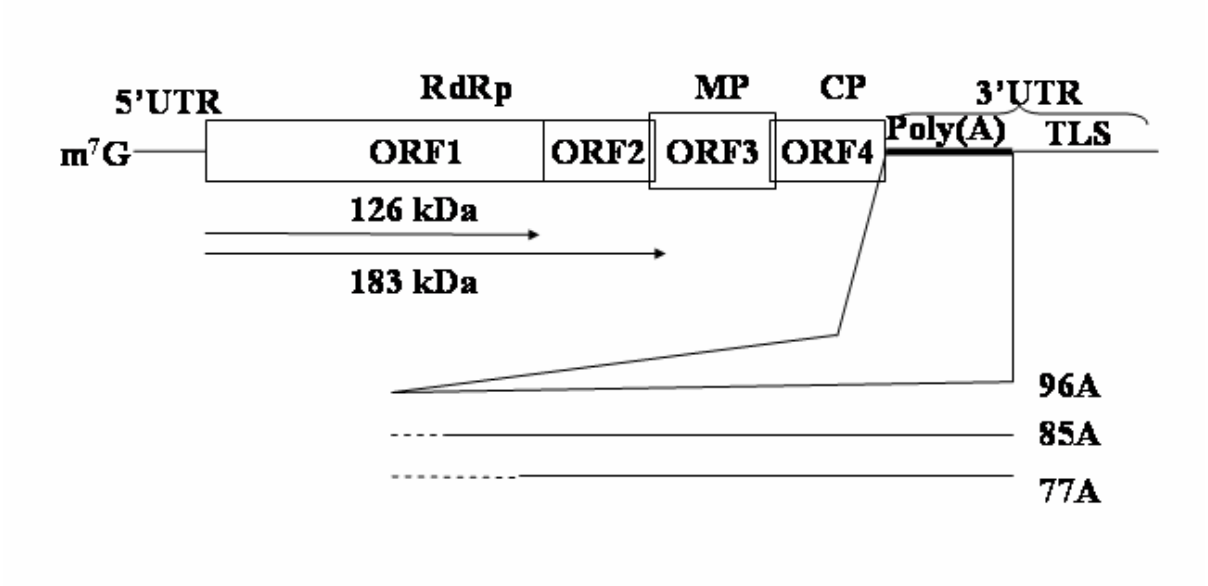
5'UTR
RdRp
MP
CP
3'UTR
m7G
ORF1
ORF2
ORF3
ORF4
Poly(A)
TLS
126 kDa
183 kDa
96A
85A
77A

B.

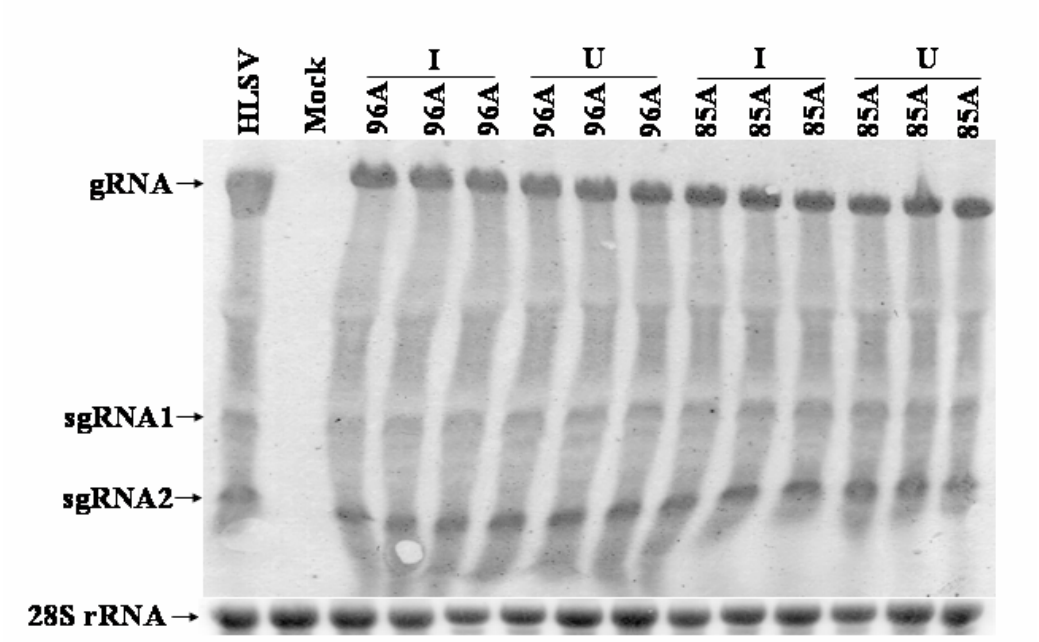
HLSV
Mock
I
U
I
U
96A
96A
96A
96A
96A
96A
85A
85A
85A
85A
85A
85A
gRNA
sgRNA1
sgRNA2
28S rRNA

C.

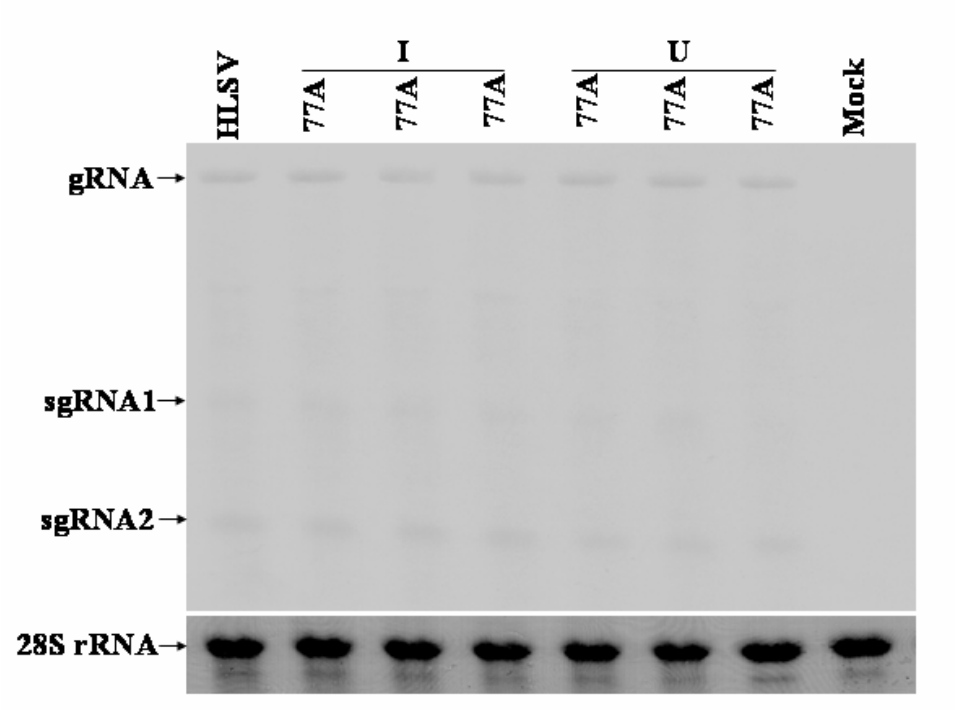

Fig. 3.1 Infectivity and systemic movement in *N. benthamiana* by transcripts with 77 nt, 85 nt and 96 nt poly(A) tract. (A) Diagram of 77 nt, 85 nt and 96 nt length of poly(A) tract HLSV cDNA clones; (B) Northern blot can detect viral gRNA and sgRNAs inoculated with transcripts from 96 nt and 85 nt poly(A) clone on both inoculated and upper leaves; i, inoculated leaves; u, upper leaves; (C) Northern blot detection of viral gRNA and sgRNAs inoculated with transcripts from 77 nt poly(A) clone on both inoculated and upper leaves; I, inoculated leaves; U, upper leaves.

CP and RT-PCR of the region which encodes the HLSV CP were positive (Fig. 3.2).

3.3 Difference of CP expression in upper leaves inoculated with transcripts with less than 77 nt poly(A) tract in *N. benthamiana*

In order to further analyze the function of poly(A) tract in the 3'UTR of the virus, clones containing different lengths of poly(A) were obtained. The 3'UTR of tobamoviruses played an important role in viral infection cycle. The HLSV internal poly(A) tract in the 3'UTR maybe a translational regulator which influence the viral CP expression. Subsequently viral systemic movement in plants was affected due to low CP expression. However, the mechanism of the poly(A) tract in regulating translation is not clear till now. Experiments were conducted on the lengths of the poly(A) tract (Fig. 3. 2A) and the results showed that the length of poly(A) tract was important for viral CP expression. Furthermore, viral systemic movement in *N. benthamiana* was affected (Fig. 3. 2B). Without the poly(A) tract (Fig. 3.4B, 0A), the transcripts were biologically inactive. No viral RNA accumulation in the upper systemic leaves was detected when the poly(A) tract was less than 77 nt. Western blot or RT-PCR also could not detect any CP expression or viral cDNA, respectively (Fig. 3. 2C, 2D). Transcripts with less than 77 nt poly(A) tract were not able to move systemically in *N. benthamiana*. However, further characterization of the transcripts on inoculated leaves is needed to determine the importance of the poly(A) tract in local infection. From the results, it is suggested that there is a minimum poly(A) length for transcripts to be able to move systemically in *N. benthamiana*.

A.

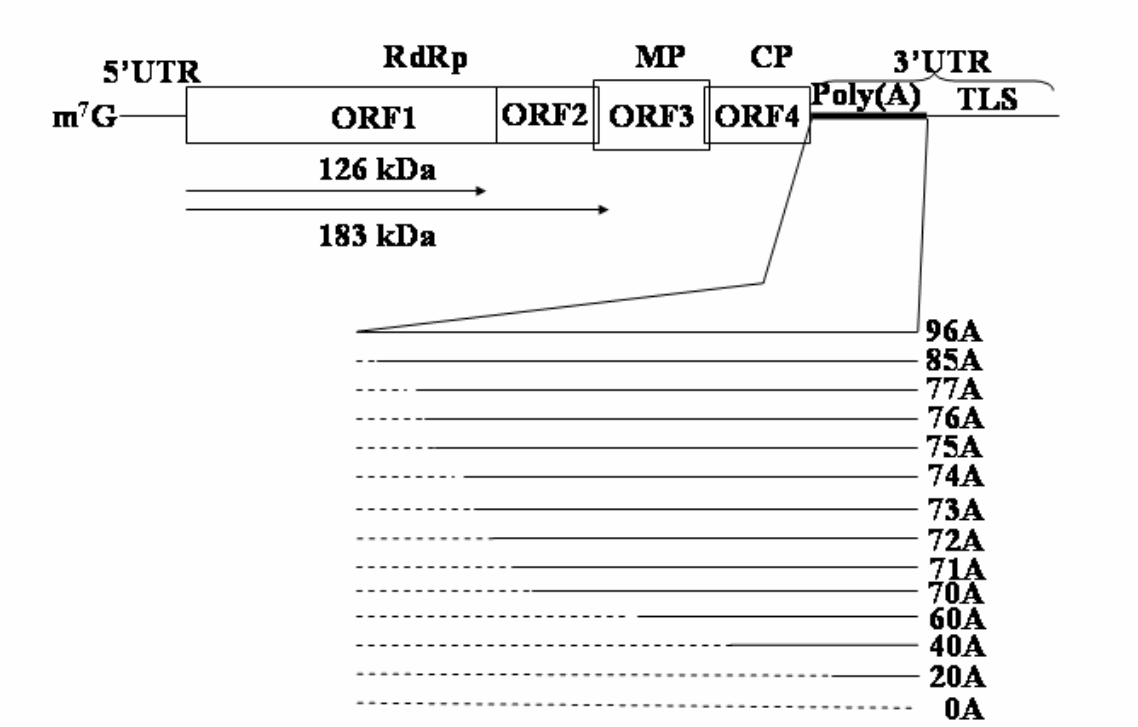
5'UTR
RdRp
MP
CP
3'UTR
m7G
ORF1
ORF2
ORF3
ORF4
Poly(A)
TLS
126 kDa
183 kDa
96A
85A
77A
76A
75A
74A
73A
72A
71A
70A
60A
40A
20A
0A

B.

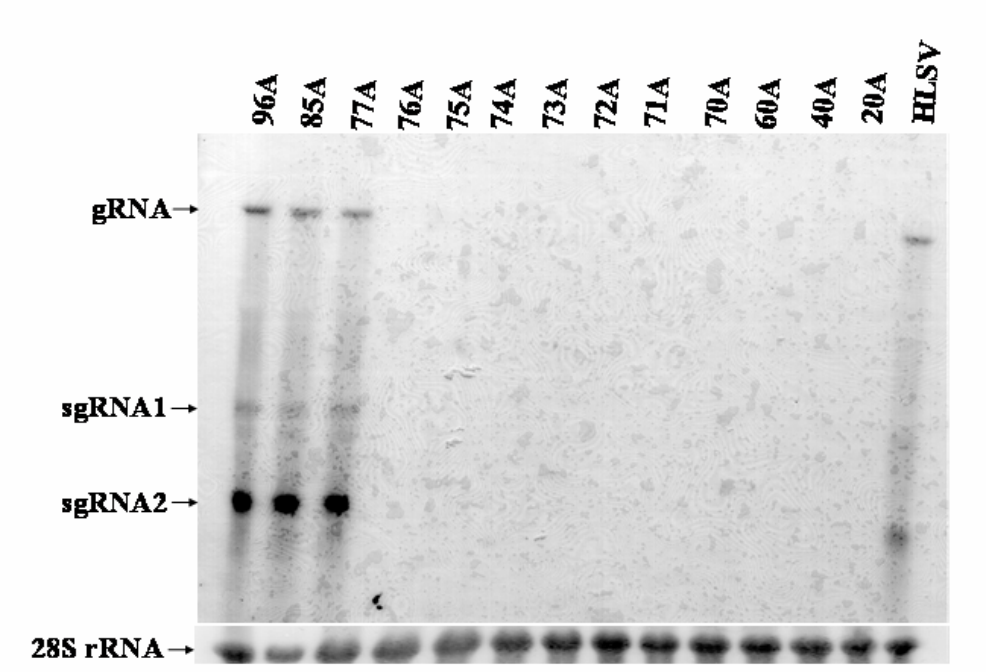
96A
85A
77A
76A
75A
74A
73A
72A
71A
70A
60A
40A
20A
HLSV
gRNA
sgRNA1
sgRNA2
28S rRNA

C.

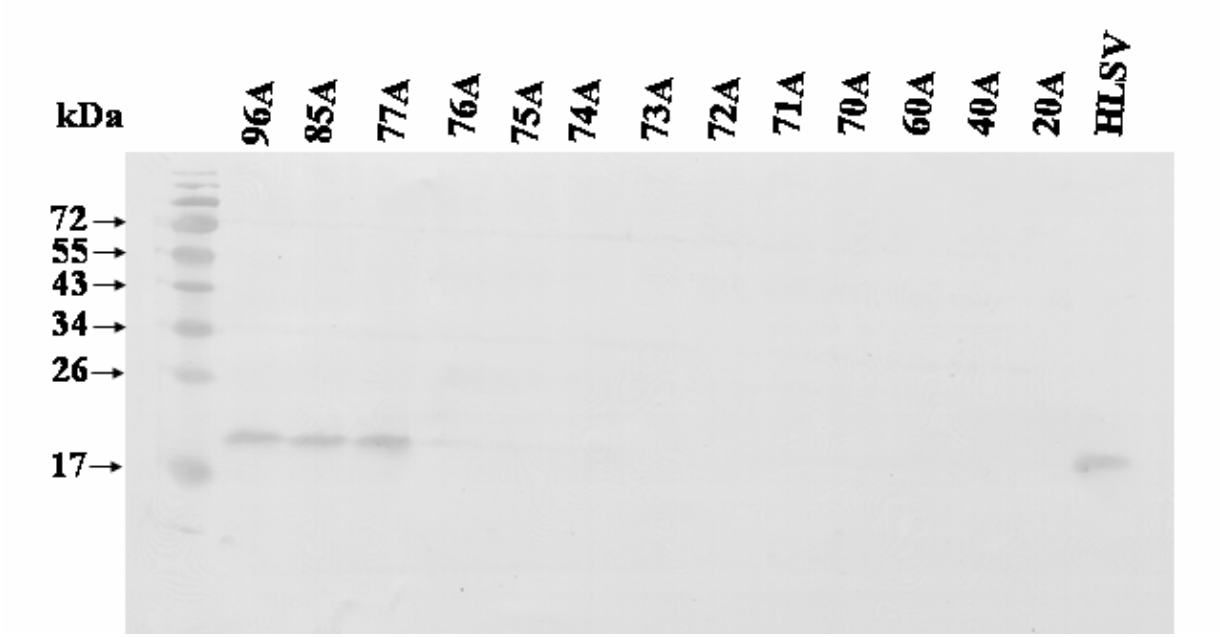
kDa
96A
85A
77A
76A
75A
74A
73A
72A
71A
70A
60A
40A
20A
HLSV
72
55
43
34
26
17

D.

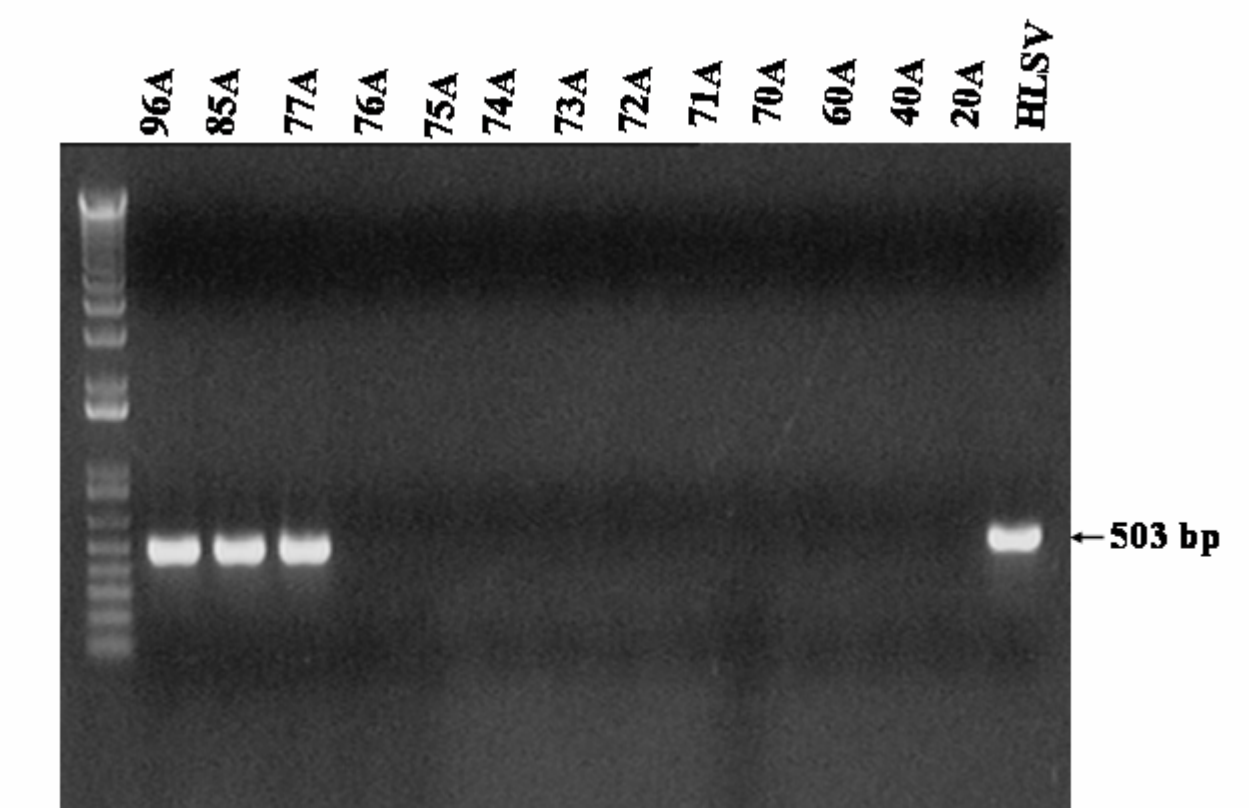

Fig. 3.2 The minimum poly(A) length for HLSV transcripts to infect *N. benthamiana* is 77 nt. (A) Diagram of different lengths of polyA tract cDNA clones; (B) Northern blot detection of the viral gRNA and sgRNAs from the systemic leave of *N. benthamiana*; *N. benthamiana* was inoculated with transcripts of different length of poly(A) tract; (C) Western blot detection of CP with anti-HLSV CP antiserum from the upper leave of *N. benthamiana*; (D) RT-PCR detection of CP coding region using specific primers and total RNA from different upper leaves.

3.4 Symptoms on upper leaves of *N. benthamiana* inoculated with transcripts of different internal poly(A) lengths

HLSV could infect *N. benthamiana* and caused a curly leaf symptom (Srinivasan et. al., 2005). To further supplement the previous molecular analysis results, photographs of the upper leaves of test plants were taken (Fig. 3. 3). The results showed that the symptoms were apparent when plants were infected. However, no symptoms were detected on leaves inoculated with transcripts that were not infectious. Here the symptoms derived from the transcripts containing 77 nt, 85 nt and 96 nt internal poly(A)(Fig. 3.3, M-O) were indistinguishable to those from leaves infected with virus (positive control, Fig. 3.4, P). These distinct curly leaves were also different from those that did not show symptoms (Fig. 3.3, A-L). Combined with the results from Northern (Fig. 3.2 B), Western blots (Fig. 3.2 C) and RT-PCR (Fig. 3.2 D), it is suggested that the length of the poly(A) tract in the HLSV transcripts could affect HLSV CP expression and systemic movement in *N. benthamiana*. There might have a minimum poly(A) length required for HLSV transcripts to move systemically in *N. benthamiana.* CP expression may also be enhanced by the length of poly(A).

3.5 The putative polyadenylation signal sequence is important for infectivity of transcripts

Polyadenylation signal is an important signal to generate the poly(A) tail in mRNA. In HLSV, the putative polyadenylation signal is located in the CP region of the virus. Seven different cDNA mutants corresponding to the signal strengths reported in the literature and a deletion variant were constructed (Fig. 3.4A). One was mutated from the wild type (WT) signal to plus signal (PS), which possesses slightly higher

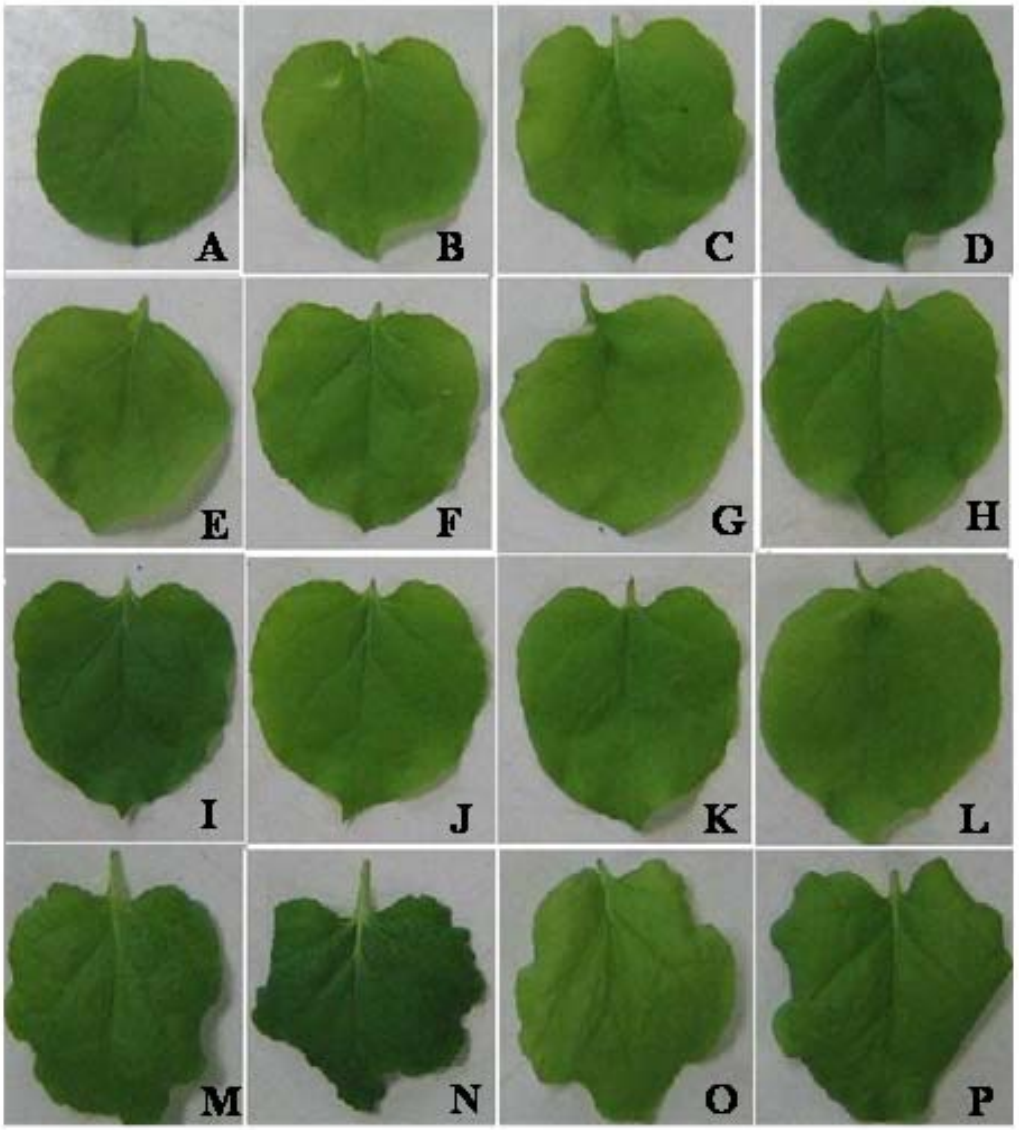

Fig. 3.3 Obvious curly top disease symptom of upper leaves of *N. benthamiana* inoculated with transcripts of 77 nt, 85 nt and 96 nt length of poly(A), same as the symptom of the virus infected leaves; while no symptom inoculated with the transcript less than 77 nt, which is the same as Mock. (A) Mock; (B) 0A; (C) 20A; (D) 40A; (E) 60A; (F) 70A; (G) 71A; (H) 72A; (I) 73A; (J) 74A; (K) 75A; (L) 76A; (M) 77A; (N) 85A; (O) 96A; (P) HLSV.

A.

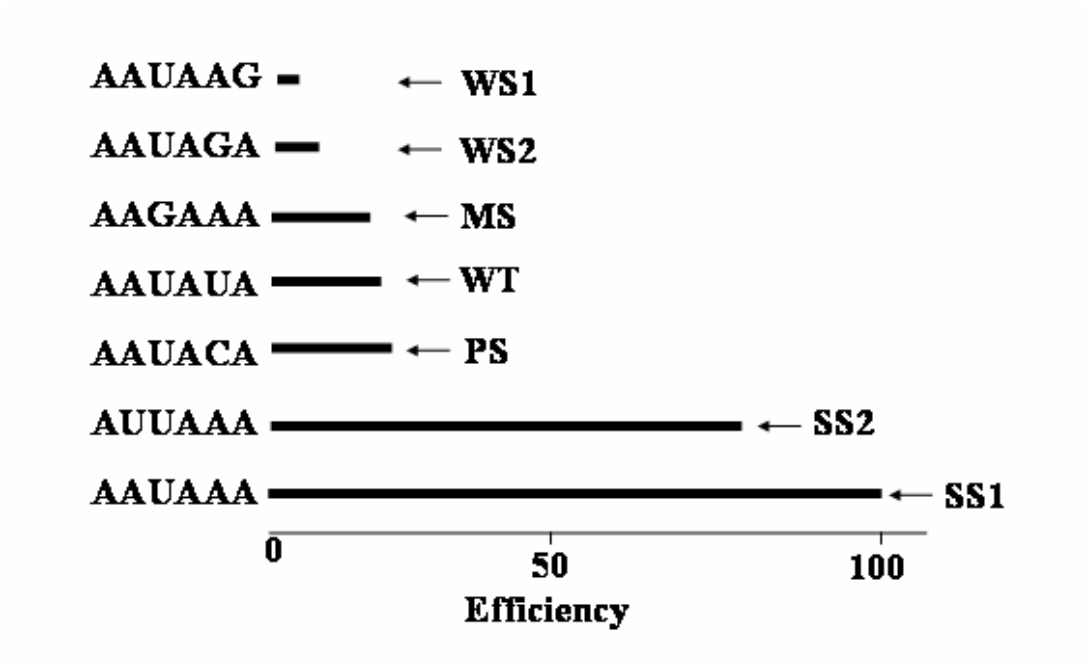
AAUAAG
WS1
AAUAGA
WS2
AAGAAA
MS
AAUAUA
WT
AAUACA
PS
AUUAAA
SS2
AAUAAA
SS1
0
50
100
Efficiency

B.

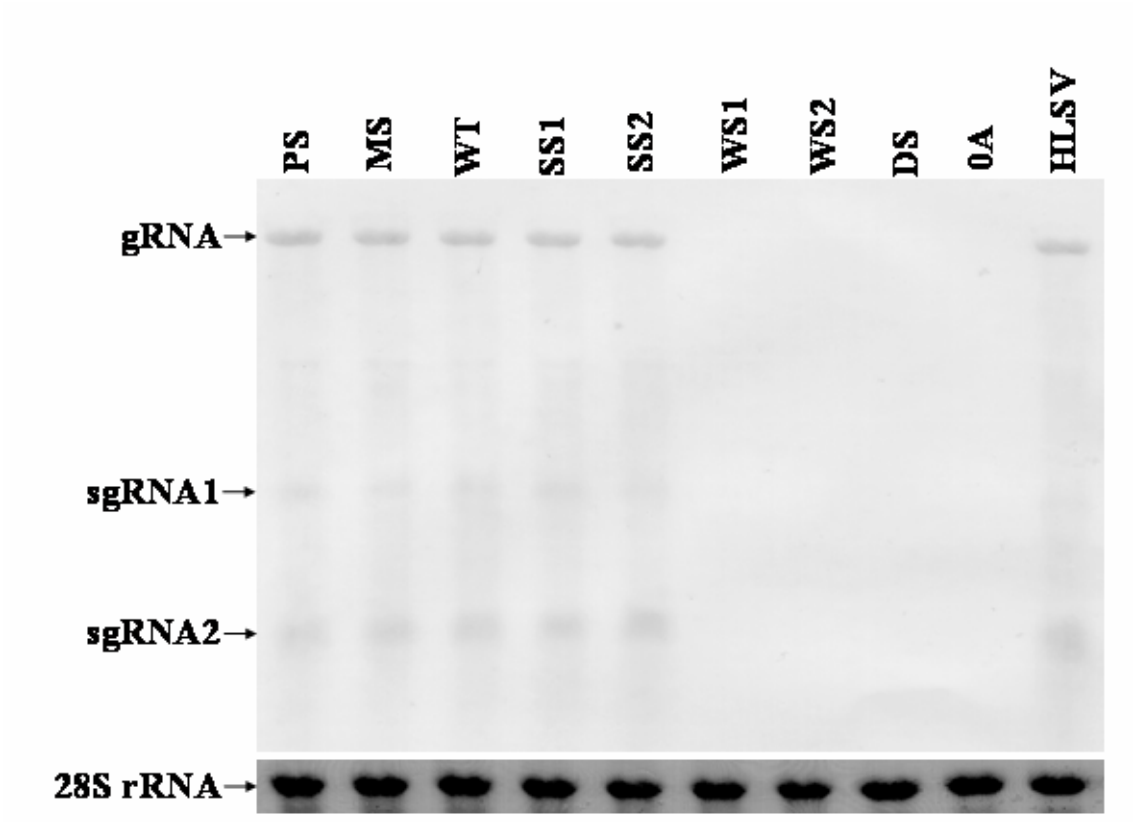
PS
MS
WT
SS1
SS2
WS1
WS2
DS
0A
HLSV
gRNA
sgRNA1
sgRNA2
28S rRNA

C.

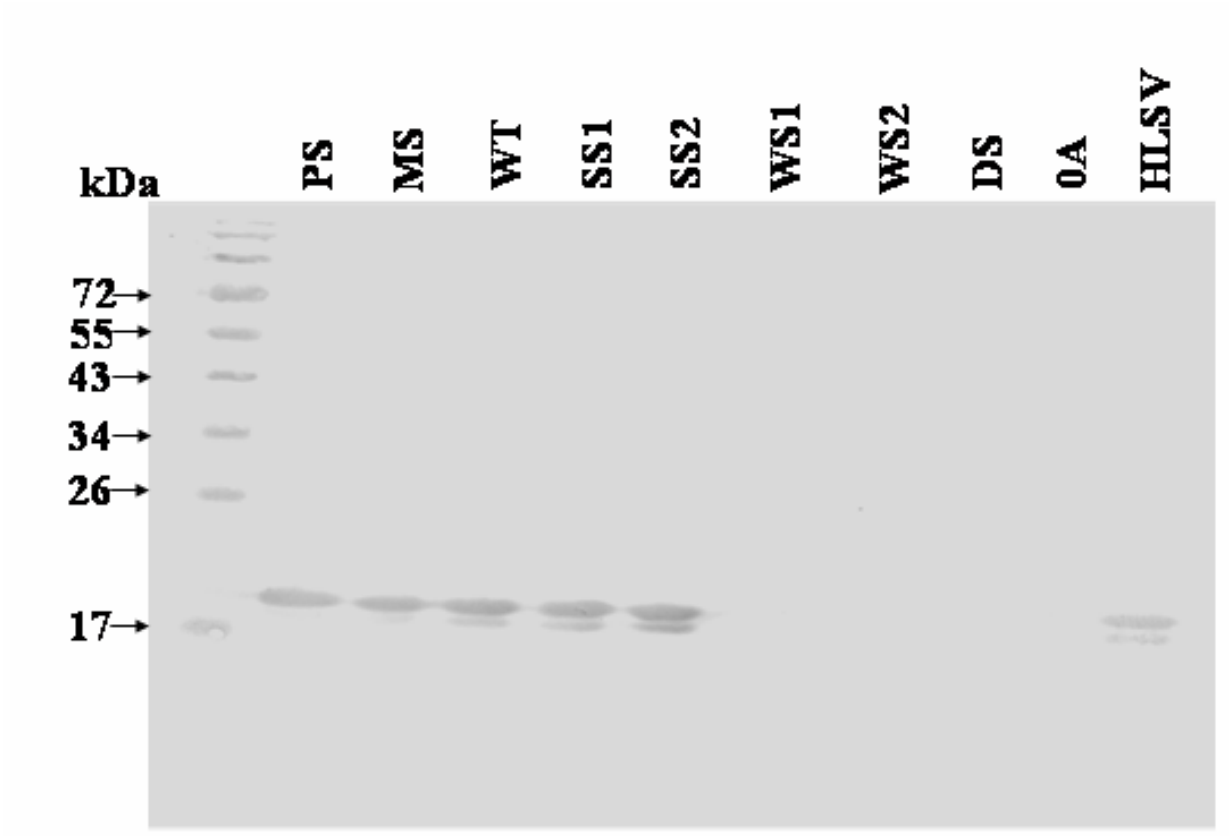

D.

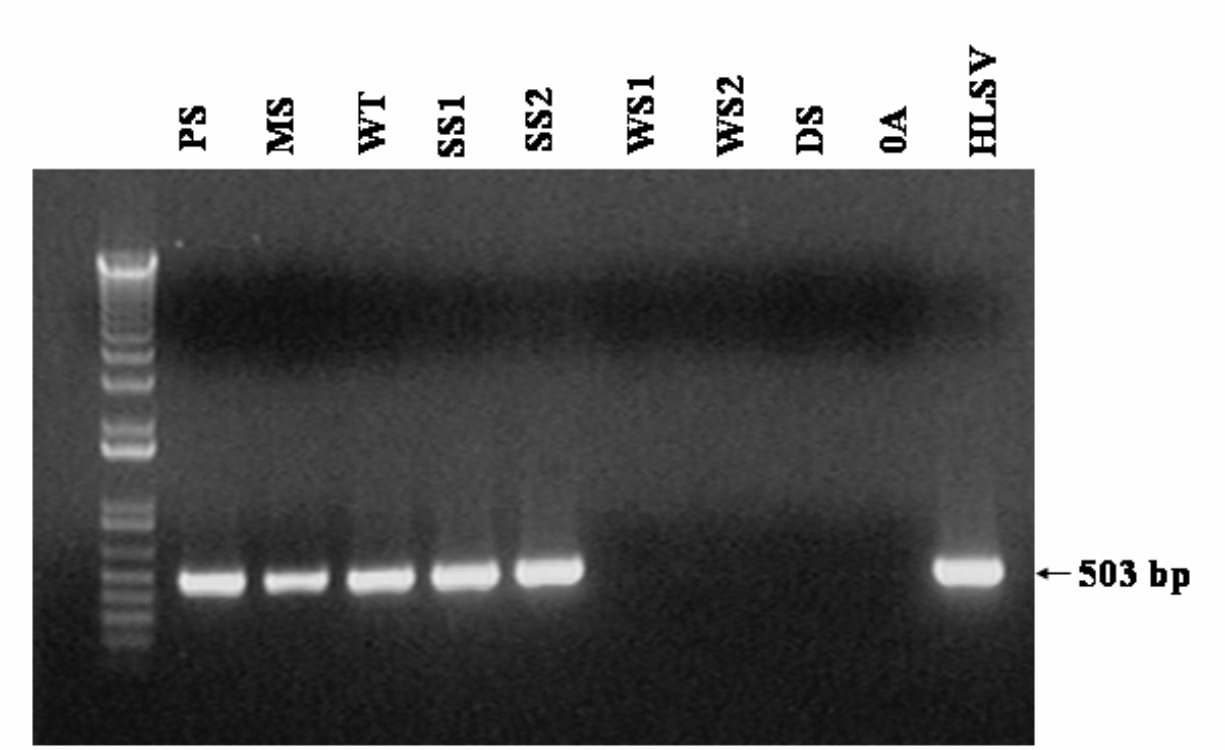

Fig. 3.4 The significance of the putative polyadenylation signal for HLSV transcripts to infect *N. benthamiana.* (A) Diagram of polyadenylation activity of different putative signals; WT showed the HLSV original signal sequence; (B) Northern blot detection of viral gRNA and sgRNAs from the upper leaves of different transcripts inoculated; DS-deletion of signal. (C) Western blot detection of different upper leaves; (D) RT-PCR detection of HLSV CP coding region of different upper leaves.

polyadenylation activity than the WT. One was mutated to minus signal (MS), which has slightly lower polyadenylation activity than the WT. Two were mutated to the weakest signals (WS1, WS2), two were mutated to the strongest signals (SS1, SS2), and one was generated with signal sequence totally deleted (DS) in its CP region. The results showed that the transcripts from the PS, MS, SS1 and SS2 clones remained infectious as the WT transcripts (Fig. 3.4 B, C, D; lanes PS, MS, SS1, SS2 and WT). If the sequence of the putative polyadenylation signal was deleted (DS), it led to two CP amino acids (NI) being deleted and an incomplete CP sequence. The results showed that transcripts from the mutant DS were not able to move systemically in *N. benthamiana,* which suggested that the sequence was important (Fig. 3.4 B, C, D, lane DS). In the DS mutants, two amino acids in the CP were deleted, which may introduce nonfunctional CP and impede the viral systemic movement in *N. benthamiana*. With the change of WT to WS1 or WS2, the transcripts also were unable to move systemically in *N. benthamiana* (Fig. 3.4 B, C, D, lanes WS1 and WS2). This further demonstrated the significance of the sequence on viral systemic movement in *N. benthamiana*. This result suggests that the two amino acids in the HLSV CP region sequence are essential sequence which may affect the viral systemic movement in plants.

3.6 Symptoms on the upper leaves inoculated with mutants containing different putative polyadenylation signals

We also examined the symptoms of the upper leaves of those plants inoculated with transcripts from the putative polyadenylation signal mutants (Fig. 3.5). The results coincided with the Northern blots (Fig. 3.4 B), Western blots (Fig. 3.4 C), and RT-PCR data (Fig. 3.4 D).

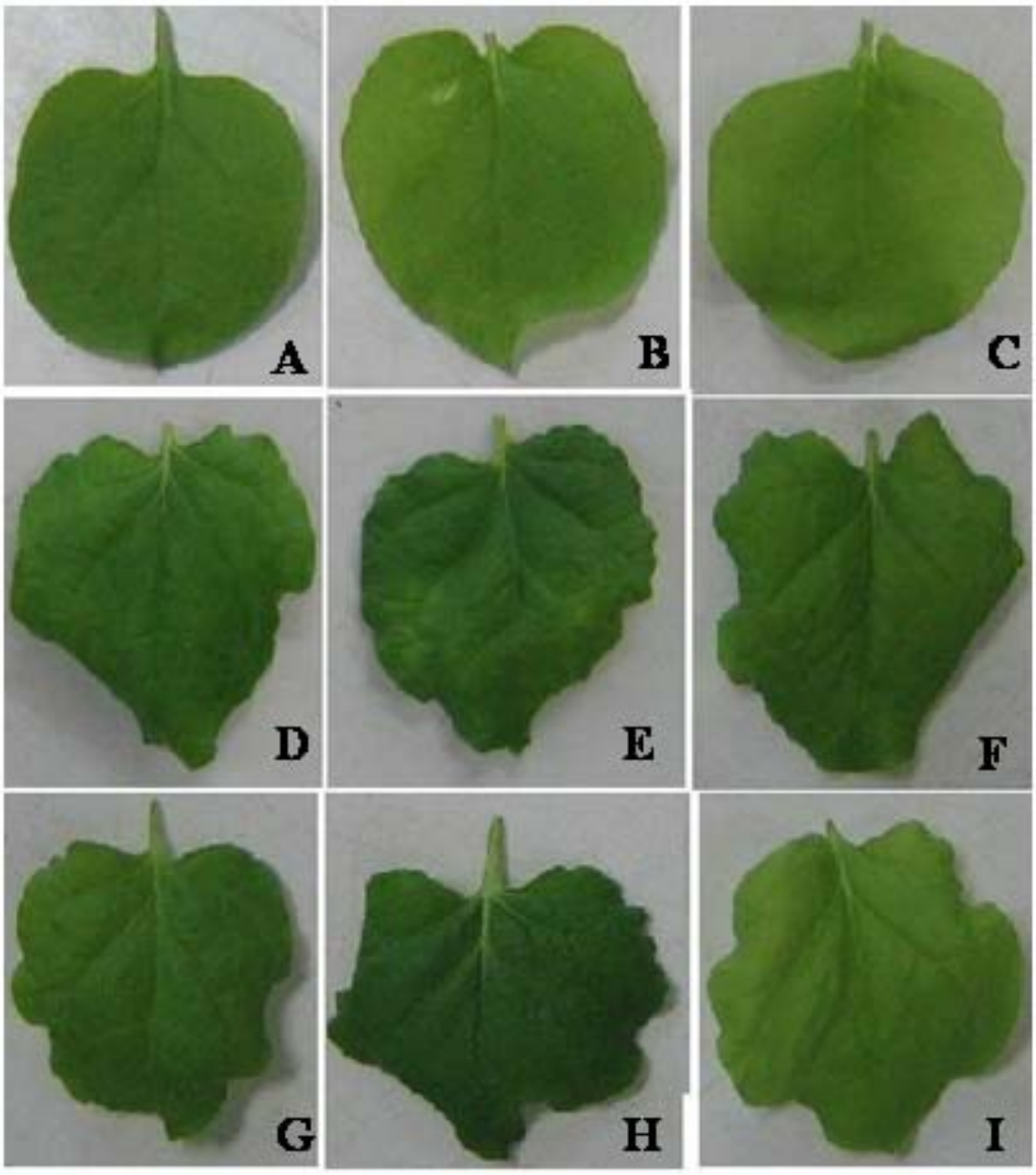

Fig. 3.5 Obvious curly top disease symptom of upper leaves of *N. benthamiana* inoculated with transcripts of PS, MS, WT, SS1, SS2 infected plants, same as the disease symptom of HLSV infected leaves (D-I); while no disease symptom inoculated with the transcript of WS1, WS2, DS (A-C). (A) WS1; (B) WS2; (C) DS; (D) PS; (E) MS; (F) WT; (G) SS1; (H) SS2; (I) HLSV.

The symptoms on these leaves were obvious in those plants inoculated with transcripts containing 77 nt, 85 nt and 96 nt poly(A) length mutants as compared to virus infected leaves. Transcripts from PS, MS, SS1 or SS2 clones also caused the upper leaves to exhibit curly and mild mosaic symptoms. However, the transcripts from the deletion of mutant containing the putative polyadenylation signal (DS) or expressing the weakest signal (WS1 or WS2) did not produce symptoms, as in the mock inoculated leaves. The results indicated that the putative polyadenylation signal was essential to the viral systemic movement in *N. benthamiana*. In this report, change of the original putative polyadenylation signal sequence to a stronger signal did not affect the viral systemic movement in plants. However, when changed to the weakest signal, the transcripts could not move systemically.

3.7 Viral RNA accumulates but CP is not detected in the inoculated leaves with defect transcripts

With shorter poly(A) or some of the mutated putative polyadenylation signal sequences, the systemic movement of the mutant virus has been abolished. It is believed that the amount of CP for viron assembly could influence systemic movement of the virus. To further examine whether these systemic movement defective mutant virus could still accumulate viral RNA in *N. benthamiana* inoculated leaves, experiments were carried out on the inoculated leaves (Fig. 3.6). The results showed that all these long distance defected transcripts could accumulate viral RNA in the inoculated leaves with more than 60As, which suggested that the transcripts still could replicate in the inoculated leaves (Fig. 3.6A). But with less than 60As, the transcripts could not accumulate viral RNA. There is no viral RNA accumulation in the inoculated leaves with transcripts of 40A, 20A

A.

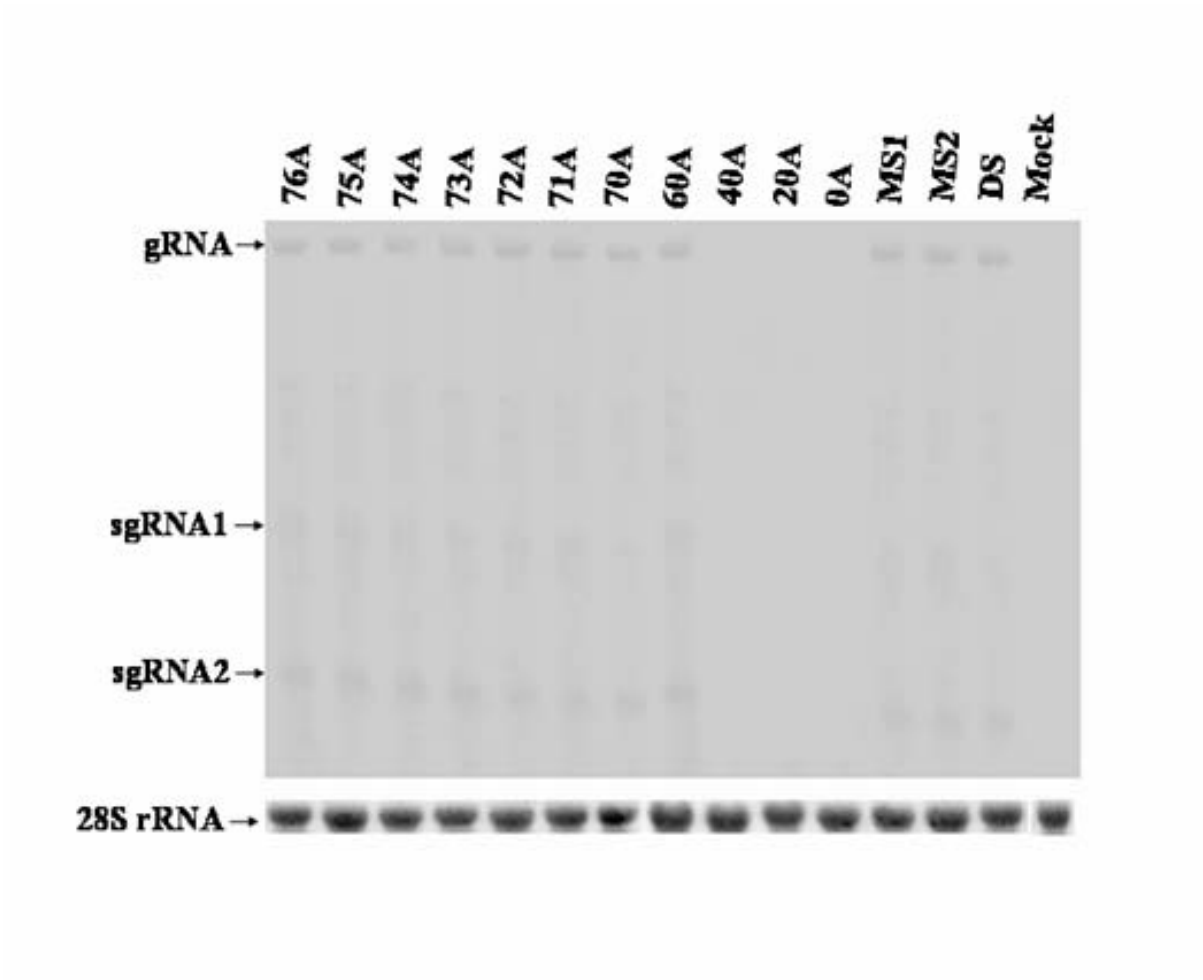
76A
75A
74A
73A
72A
71A
70A
60A
40A
20A
0A
MS1
MS2
DS
Mock
gRNA
sgRNA1
sgRNA2
28S rRNA

B.

Fig. 3.6 Accumulation of viral RNA while no coat protein expression in the inoculated leaves with defect transcripts. (A) Northern blot detection of viral gRNA and sgRNAs from the inoculated leaves of different transcripts inoculated; (B) Western blot detection of different inoculated leaves.

or 0A, which shows the same pattern as mock inoculated leaves. However, when examining coat protein expression of these inoculated leaves, there are not protein detected on all the leaves with less than 77A transcripts, which means that these transcripts might not able to assembly virions and thus mutant virus could not move systemically in the plants (Fig. 3.6B).

3.8 Discussion

In this study, a full-length clone of HLSV was generated using PCR and overlapping primers. This clone was infectious to *N. benthamiana* and progeny virus from the transcripts infected plants was transmissible. HLSV could induce curly leaves and mild mosaic symptoms in *N. benthamiana*, which could be used as a detection method to examine whether the plants have been infected by the *in vitro* transcripts. This finding is consistent with an infectious clone of an isolate of *Beet mild curly top virus* which is associated with an outbreak of curly top disease symptom in pepper and tomato crops (Soto et al., 2005).

Since the 3'UTR of tobamoviruses plays an important role in viral replication process, and the poly(A) tract is a part of HLSV 3'UTR, its function was examined in this study. However, instead of a poly(A) tail at the 3' end or an internal poly(A) tract, other tobamoviruses have an UPD followed by a 3'TLS in their 3'UTR which plays several roles in viral protein expression.

It was 204 base pairs in length with a TLS at the 3' extremity and a stretch of 3 consecutive pseudoknots upstream of it (van Belkum et al., 1985). Also many other tobamoviral 3'UTRs were found to contain the pseudoknots and TLSs (Pleij et al., 1987; Garcia-Arenal, 1988; Isomura et al., 1991). The 3'UTR can be folded into a TLS

consisting of a 3' pseudoknotted domain (D1) which acts as a tRNA acceptor branch ending in an unpaired CCA sequence and a domain (D2) which looks similar to a tRNA anticodon branch (Felden et al., 1994; van Belkum et al., 1985). Upstream of the TLS is domain D3, containing three pseudoknots, each of which contains two double-helical segments. Domains D1, D2, and D3 are connected by a central pseudoknotted structure C. The TLSs are excellent substrates for aminoacylation (Mans et al., 1991) and can be catalyzed by specific aminoacyl-tRNA synthetases. In tobamoviruses it can accept histidine in general, except for *Sunn hemp mosaic virus* which is valylated (Oberg and Philipson, 1972). Several functions have been proposed for plant viral 3'UTRs and TLSs (Haenni et al., 1982; Florentz et al., 1984). To study the functions of 3'UTR region, several ToMV mutants with deletions in 3'UTR region were tested in both plant and protoplast systems of tobacco. Deletion of double-helical segments II to V in central pseudoknot region D3 resulted in a reduction in viral replication, associated with loss of symptom development. Double-helical segment I upstream of the TLS is indispensable for viral replication and double-helical segment VI is not essential for viral replication (Takamatsu at al., 1990). Further detailed analysis of 3'UTR regions of ToMV using template dependent RdRP extracts revealed several double-helical regions that form the pseudoknot and stem-loop structures in domains D1, D2, and D3 and the central core C, are necessary for high template efficiency. Domain D2 and central core C can bind to RNA polymerase with high affinity whereas domains D1 and D3 showed comparatively lesser affinity towards binding RNA polymerase. Mutation of 3' terminal CCCA identified that 3'-terminal CA was crucial for minus-strand synthesis. Maximum transcriptional efficiencies are achieved with termination of 3' end sequence with CCCA

or GGCA (Osman et al., 2000). TMV has 3 pseudoknots immediately downstream of the CP gene, while HLSV has the poly(A) tract. TMV 3'UTR when fused with a chimeric mRNA enhanced the expression levels to several fold and increased the stability of chimeric mRNA (Gallie et al., 1991). Enhanced expression of 5'-capped RNAs has been attributed to improved translational efficiency, which is due to the synergistic interaction between 3'UTR and 5'cap and to a smaller extent due to increased mRNA stability (Leathers et al., 1993; Gallie and Kobayashi, 1994). Translational enhancement by the TMV 3'UTR is primarily due to the pseudoknot structure that is upstream of the TLS. The TLS has been shown to enhance mRNA stability (Gallie and Walbot, 1990).

A study (Beaudoing et al., 2000) provided evidence for the existence of 10 variant putative polyadenylation signals that may be responsible for up to 14.9% of the mRNA 3' ends. They analyzed the distribution of noncanonical signals in UTRs with alternate poly(A) sites and assessed the processing efficiency of polyadenylation signals in function of their sequence and their position in the UTR. Significant biases were observed, with interesting consequences for the regulation of mRNA 3' end formation (Graber et al., 1999). In this study, seven different putative polyadenylation signals sequences including HLSV signal sequence were examined for its significance of the viral systemic movement in plants. Since those studies showed that the sequence of putative polyadenylation signal is important, in HLSV it could influence viral systemic movement in plants. Results suggested that the putative polyadenylation signal is of significant in the viral systemic movement process, since deletion or alteration to the weakest putative polyadenylation signal (WS1 or WS2) resulted in no systemic movement in the plants. The changes of other signals such as SS1, SS2, PS or MS did not affect the virus

movement. Taken together, the experimental results suggest that the length of poly(A) tract are able to influence the viral coat protein expression and its systemic movement in the plant. It is not clear whether the lack of systemic movement is due to changes of nucleotide sequence in the putative polyadenylation signal or due to the changes of two amino acids in the coat protein.

However, this study has its limitations. First of all, the work was done on the *N. benthamiana* whole plant which is not the usual way to analyze the plant virus transcripts. The *Kenaf* protoplasts are well-established system in our lab. I've tried several times by testing the HLSV transcripts in *Kenaf* protoplasts. Unfortunately the transcripts were not infectious in the protoplasts. It hard to explain why it's not infectious in this protoplast' system while the viral RNA can have very faint gRNA and sgRNA bands by Northern-blotting. My interpretation is that the viral RNA was also not infectious in this protoplast system. What i detected the gRNA and sgRNA bands was still the inoculum (viral RNA) to the cells. Another problem I've encountered is that I also tried several times of *N. benthamiana* protoplasts and I failed to get enough good cells for the inoculation of transcripts. When I extracted the total RNA from these protoplasts, most of the RNA are either degraded or no RNA at all. Since this protoplast system is not very well established in our lab, I did not try any more of *N. benthamiana* protoplasts but rather test all these transcripts in the whole plants. So there might be some flaw in terms of its infectivity or systemic movement of the virus. Secondly, to test the transcripts of different length poly(A) mutants infectivity in plant, it is necessary to test the progenys the length of poly(A) of different mutants. But in this study, I did not test the progeny of the different mutants, it's hard to say whether the transcripts infectivity is due to the reversion of the

length of poly(A). So this might be another limitation of this study.

CHAPTER 4

THE 5', 3' UTR-UTR INTERACTION FACILITATES BOTH POLY(A) TAIL-DEPENDENT AND POLY(A) TAIL-INDEPENDENT TRANSLATION OF HIBISCUS LATENT SINGAPORE VIRUS

4.1 Introduction

HLSV 3'UTR is believed to possess poly(A) tract consisting of at least 77 nt followed by a TLS at the 3' terminus, ended with a CCA trinucleotides. The genome organization of HLSV is shown as Fig. 4.1A. Genomic RNA (gRNA) and subgenomic RNAs (sgRNAs) could be identified by using anti-TLS and oligo-dT probes (Fig. 4.1B). The 5'UTR contains 58 nucleotide and is predicted to possess a stem-loop structure (Fig. 4.1C) by the M-fold RNA structure prediction program with a ΔG= -11.8 kcal/mol. The unique feature of the 3'UTR which is different from all other tobamoviruses is the presence of an internal poly(A) tract. The 5'UTR of plant viruses could enhance translation. An example is the TMV Ω sequence, which promotes translation through enhancing recruitment of eukaryotic initiation factor 4F (eIF4F) (Gallie et al., 1987; Gallie, 2002). Capped mRNA could enhance translational efficiency several folds higher than uncapped mRNA and these viruses possess cap structure at their 5' end of the gRNA (Matsuda et al., 2004; Gallie, 1991). As a result, a combination of the cap, 5'UTR and 3'UTR will enhance translation to the greatest extent.

A.

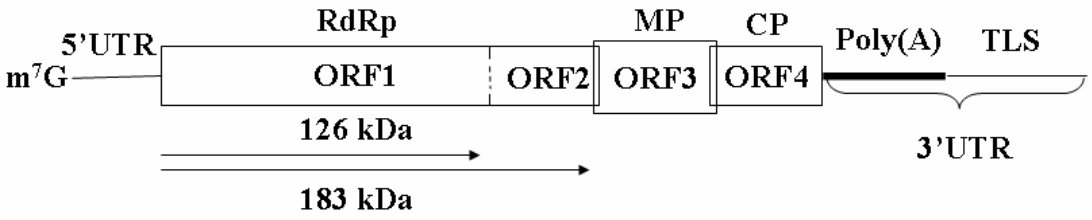
RdRp
MP
CP
5'UTR
Poly(A)
TLS
m7G
ORF1
ORF2
ORF3
ORF4
126 kDa
3'UTR
183 kDa

B.

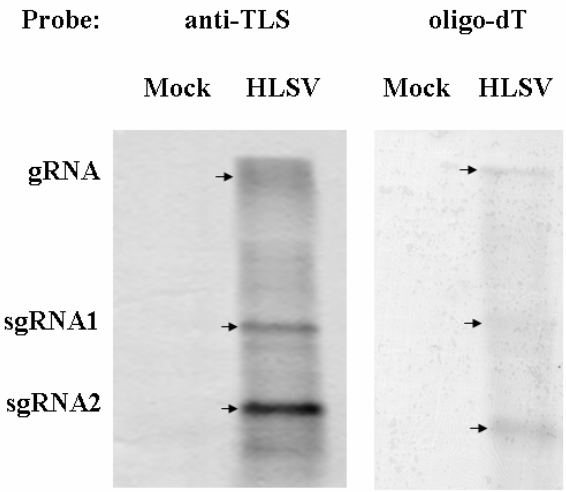
Probe:
anti-TLS
oligo-dT
Mock
HLSV
Mock
HLSV
gRNA
sgRNA1
sgRNA2

C.

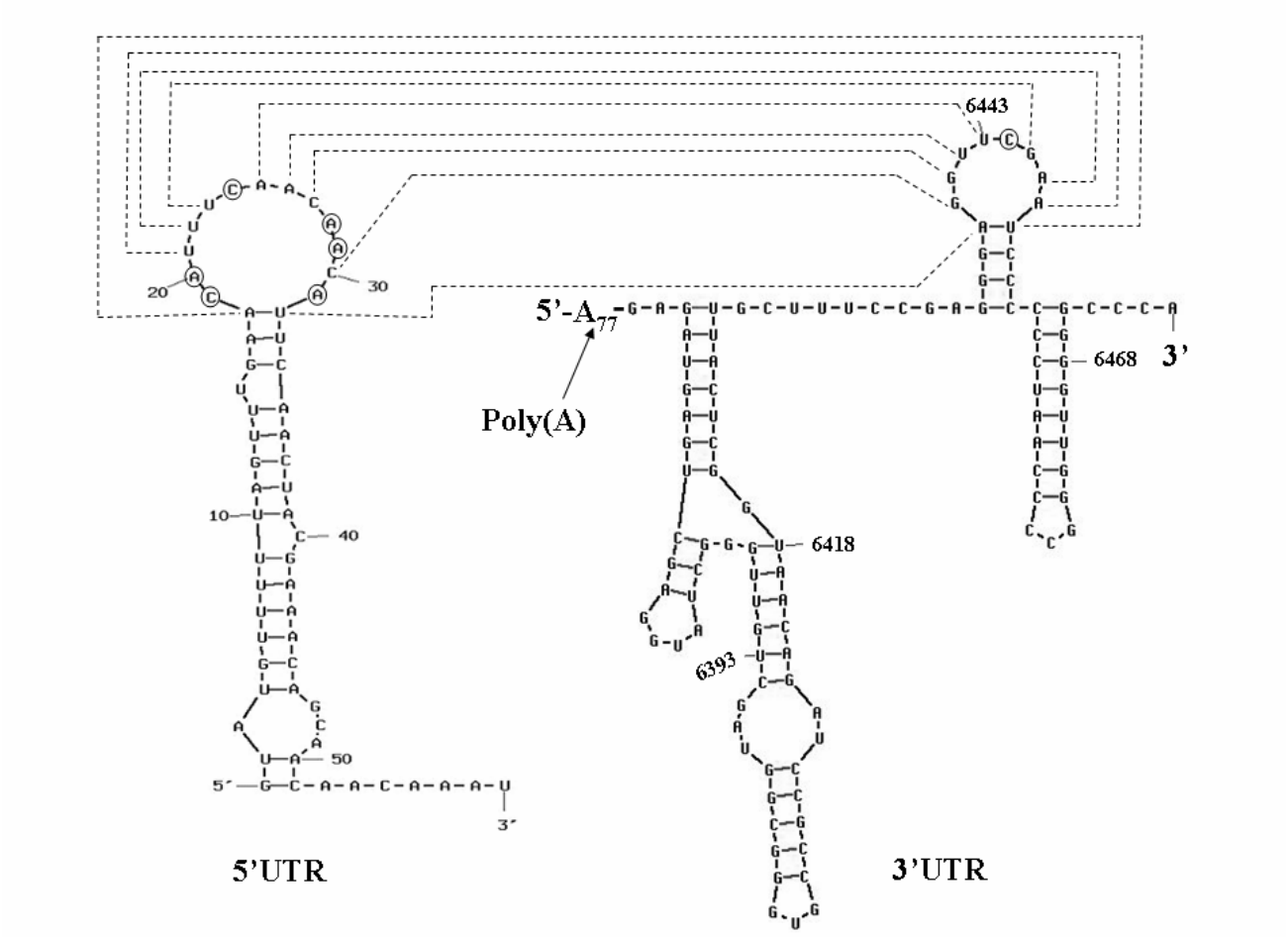
6443
20
30
5'-A77
Poly(A)
6468
3'
10
40
6418
6393
50
5'
3'
5'UTR
3'UTR

D.

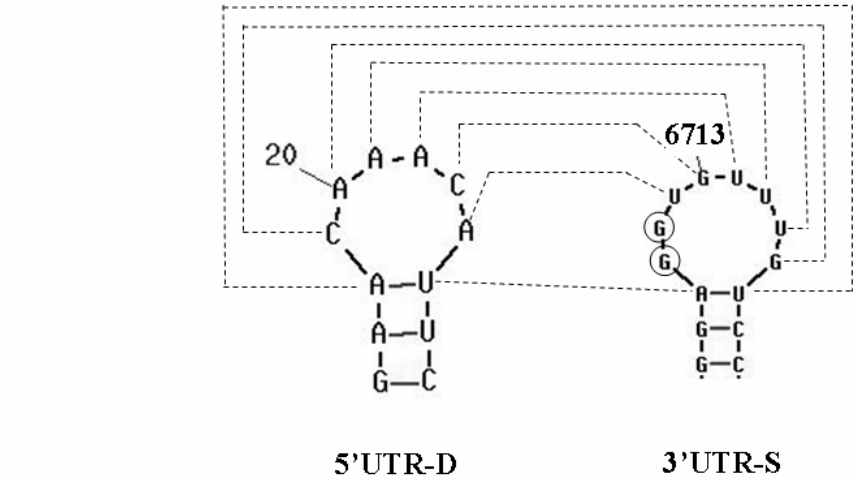
20
6713
5'UTR-D
3'UTR-S

E.

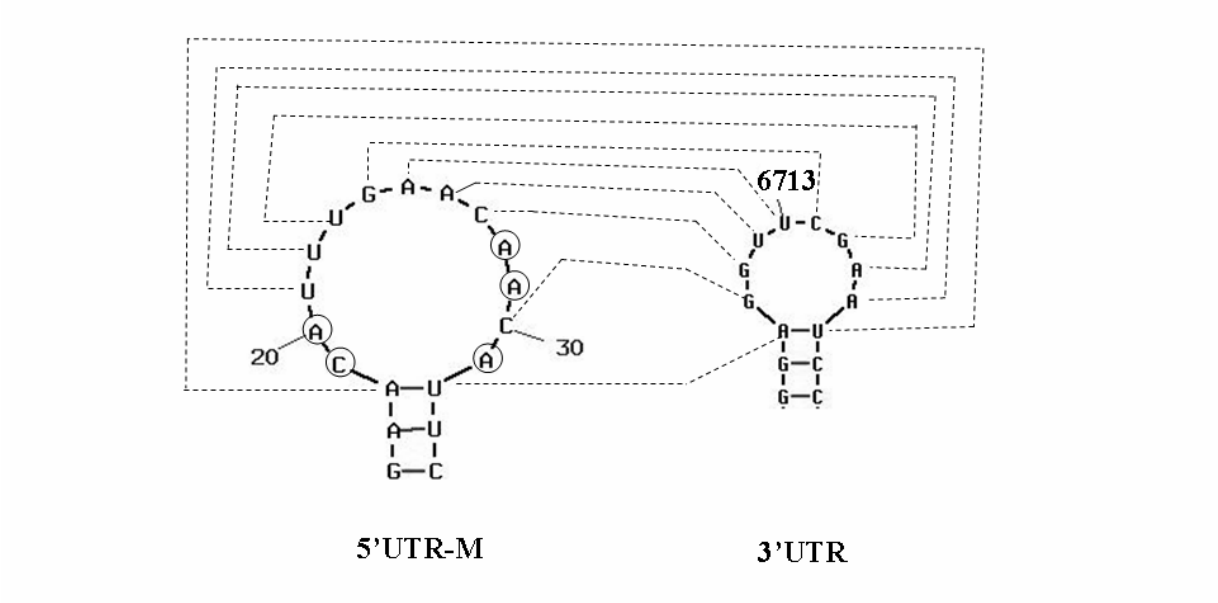

Fig. 4.1 Genome organization of HLSV and characterization of its 5'UTR and 3'UTR. (A) Genome organization of HLSV. (B) Detection of HLSV genome and subgenome RNAs by anti-TLS or Oligo-dT probe. (C) Predicted secondary structure of full-length HLSV 5'UTR and 3'UTR by M-Fold program, http://www.bioinfo.rpi.edu/applications/mfold/. Nucleotide base-pairing between loops were shown in details and those without base-pairing were circled. (D) HLSV 5'UTR-D (deletion mutant of 5'UTR $U^{21}UUCAAC^{27}$) and 3'UTR-S (substitution mutant of 3'UTR $U^{6443}CGAA^{6447}$ with $G^{6443}UUUG^{6447}$), while maintaining base-paring. Only the loop region was shown in details and the rest remained unchanged. Circles denote nucleotides that are not base-pairing. (E) HLSV 5'UTR-M (mutation of 5'UTR C^{24} to G^{24}), which added one more nucleotide for base-pairing between 5'UTR-M and 3'UTR as compared 5'UTR and 3'UTR. Details were shown between the loops and the rest remained unchanged. Circles denote nucleotides that are not base-paired.

In this study, however, we show that the cap, the 5'UTR and the 3'UTR of HLSV are all involved in contributing to total translation of the virus, but there was no synergistic enhancement in translation.

Stem-loop "kissing" interaction of 5'UTR and 3'UTR of plant viruses is another way of enhancing translation through evolution. In BYDV, a cap-independent translational element functions in either the 5' or the 3'UTR (Wang and Miller, 1995; Wang et al., 1997) and base-pairing between the two UTRs could enhance cap-independent translation (Guo et al., 2001). In TBSV, 5', 3' RNA-RNA interaction could facilitate cap- and poly(A)-independent translation (Fabian and White, 2004). In STNV, the 5' and 3' extremities translational enhancer domains contribute differentially to stimulate translation (van Lipzig et al., 2002). In TNV, base-pairing elements between 5' and 3' end cooperate synergistically to enhance cap-independent translation (Shen et al., 2004; Meulewaeter et al., 2004). In HLSV, the predicted stem-loops between the 5' and 3' UTRs could form nine nucleotide base-pairing which possibly served as an element of translational enhancer. These translational regulating elements, which included the cap structure, 5'UTR, 3'UTR (internal poly(A) tract and TLS), was analyzed in wheat germ extract and in kenaf protoplasts respectively. Also two models for the 5'UTR and 3'UTR which are involved in poly(A)-dependent and poly(A)-indepdendent translation of HLSV mRNA were proposed from the results of the study.

4.2 HLSV 5'UTR enhances translation

To analysis whether HLSV 5'UTR could enhance translation of capped mRNA, constructs (Fig. 4.2A) were designed and tested both in wheat germ extracts and in kenaf protoplasts. In wheat germ extracts, translation product of Ω-luc was set as l00.0% using densitometry estimation. Luciferase from the Western blot showed that 5'UTR-luc was 63.3%, while luc was

A.

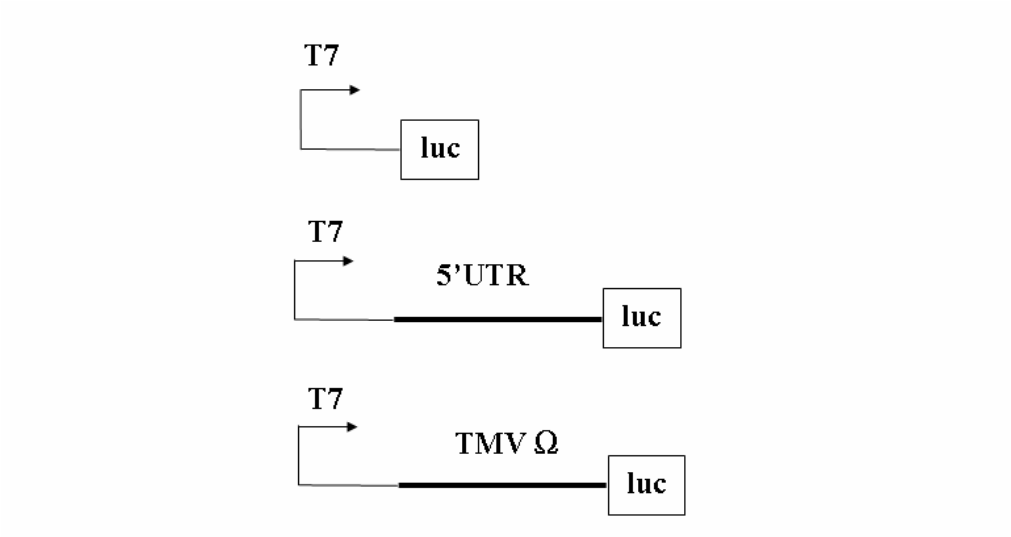
T7
luc
T7
5'UTR
luc
T7
TMV Ω
luc

B.

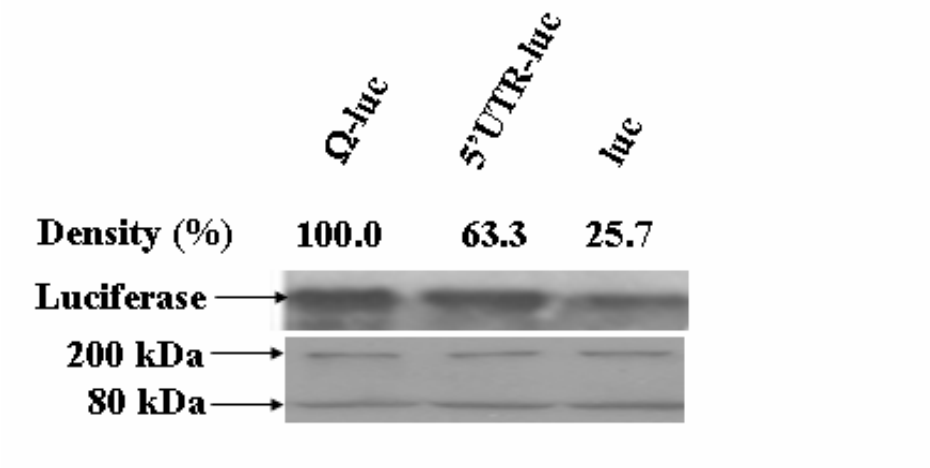
Ω-luc
5'UTR-luc
luc
Density (%)
100.0
63.3
25.7
Luciferase
200 kDa
80 kDa

C.

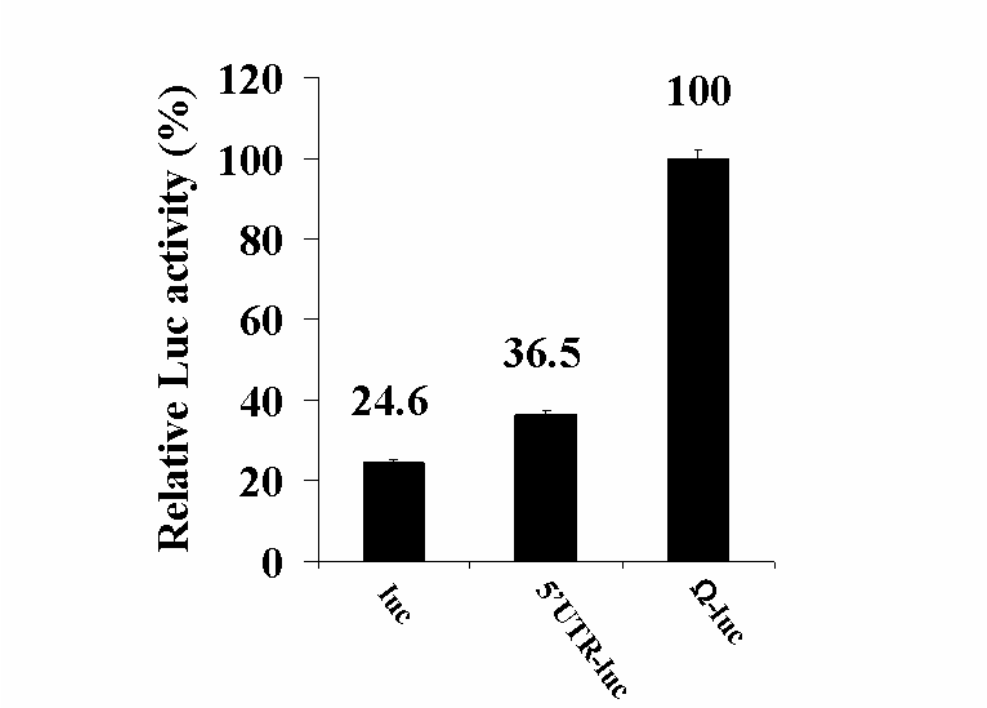

Fig. 4. 2 Marginal enhancement of translation by HLSV 5'UTR. (A) Schematic of constructs of luc, 5'UTR-luc and Ω-luc. (B) Western blot analysis of *in vitro* translation products of luc, 5'UTR-luc and Ω-luc. Density of each translation products was estimated and the percentage was indicated above each constructs. (C) Relative luciferase activity of luc, 5'UTR-luc and Ω-luc constructs measured in kenaf protoplasts. Each construct was assayed at least three times with duplicates and the mean values represent the relative luciferase activity.

25.7% (Fig. 4.2B). In kenaf protoplasts, we also set the relative luciferase activity from Ω-luc as 100.0%, and the relative luciferase activity of 5'UTR-luc was 36.5%, while the luc was 24.6% (Fig. 4. 2C). The results showed that 5'UTR enhanced translation efficiency slightly *in vivo*, but less than the *in vitro* experiments.

4.3 HLSV 3'UTR enhances translation better than the 5'UTR

The HLSV 3'UTR contains an internal 77 nt poly(A) tract and a TLS at its 3'end (Fig. 4.1A). To assay its translational efficiency, constructs were designed (Fig. 4.3). The 3'TMV was used as a positive control for its well-known translational enhancer effect (Leathers et al., 1993; Gallie, 1991). In the wheat germ extract, luciferase intensity of luc-3'TMV was set at 100.0%. Densitometry estimation of a Western blot showed that the band intensity derived from luc-3'UTR was 91.3% and the luc-A_{77} and the luc constructs yielded 45.7% and 8.8%, respectively. In kenaf protoplasts, the relative luciferase activity of luc-3'TMV was set at 100.0%. The relative luciferase activity of luc-3'UTR and luc-A_{77} reached 88.3% and 40.5%, respectively. The luc construct showed relatively lower activity of 6.9%. Both *in vitro* and *in vivo* results suggested that the 3'UTR of HLSV is a strong translational enhancer, comparable to that of the 3'UTR of TMV.

4.4 Cap, 5'UTR, 3'UTR of HLSV enhance translation to the highest level

Since both 5'UTR and 3'UTR of HLSV could enhance translational efficiency individually, would the translational enhancement reach a higher level when both UTRs operate together, or would they operate synergistically? With this supposition, constructs (Fig. 4. 4A) were designed and tested in the wheat germ extract and in kenaf protoplasts. In the wheat germ extract, the luciferase band intensity of capped 5'UTR-luc-3'UTR was set at 100.0%. The band intensity of luc was 9.9% and 5'UTR-luc was 20.2%. The luc-A_{77}, 5'UTR-luc-A_{77} and luc-3'UTR were

A.

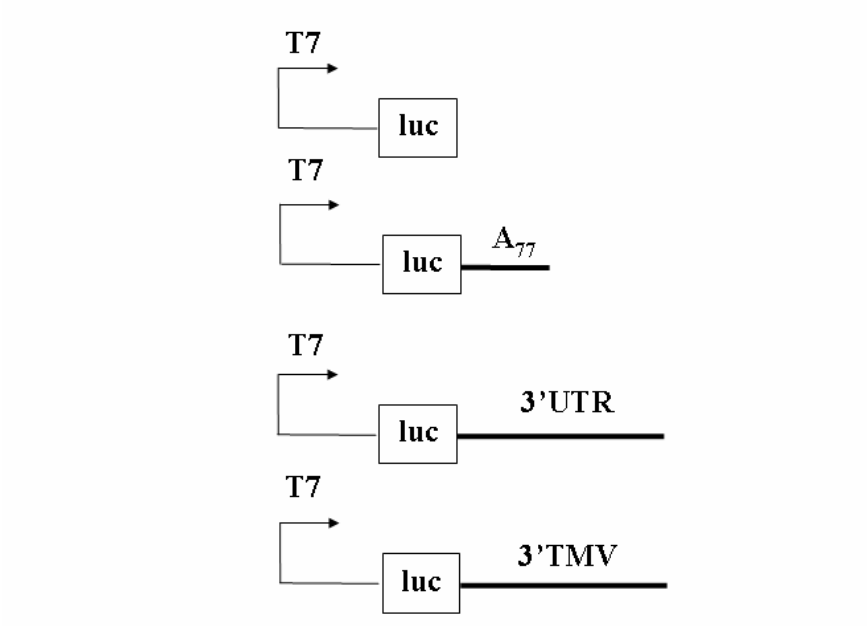
T7
luc
T7
luc
A_{77}
T7
luc
3'UTR
T7
luc
3'TMV

B.

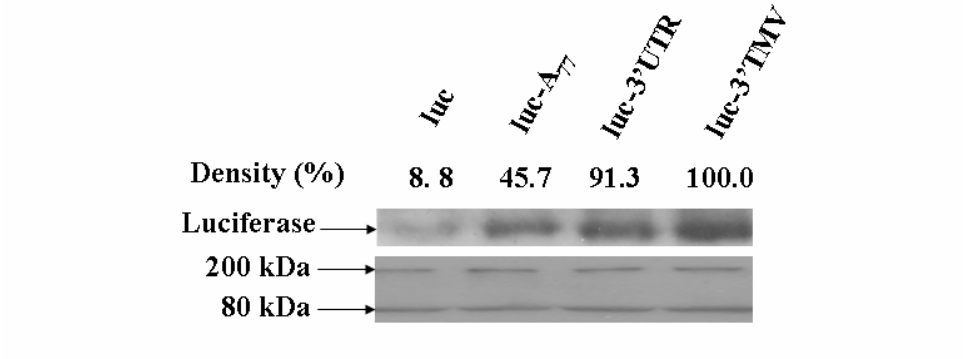
luc
luc-A_{77}
luc-3'UTR
luc-3'TMV
Density (%)
8. 8
45.7
91.3
100.0
Luciferase
200 kDa
80 kDa

C.

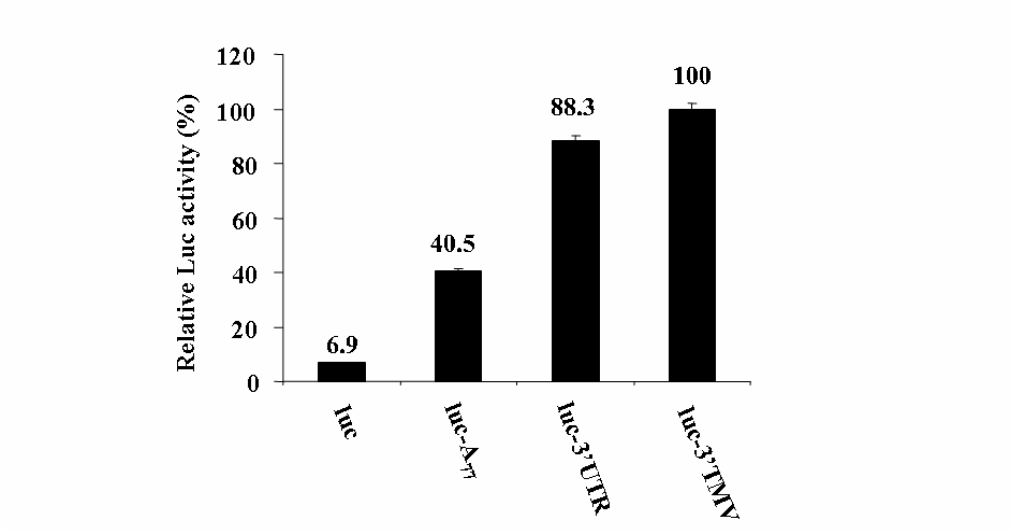

Fig. 4.3 The enhancement of translation by HLSV 3'UTR is greater than its 5'UTR. **(**A**)** Schematic of constructs of luc, luc-A_{77}, luc-3'UTR, luc-3'TMV. (B) Western blot analysis of *in vitro* translation products of luc, luc-A_{77}, luc-3'UTR, luc-3'TMV. The density of each translation product was estimated and the percentage is indicated above each construct. (C) Relative luciferase activity of luc, luc-A_{77}, luc-3'UTR and luc-3'TMV constructs measured in kenaf protoplasts. Each construct was assayed at least three times with duplicates and the mean values represent the relative luciferase activity.

A.

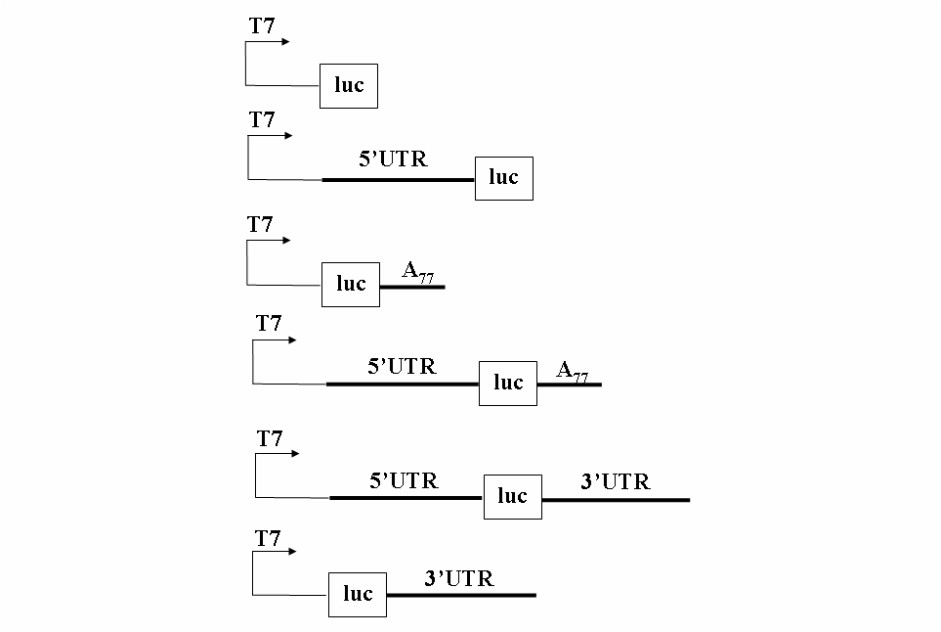
T7
luc
T7
5'UTR
luc
T7
luc
A77
T7
5'UTR
luc
A77
T7
5'UTR
luc
3'UTR
T7
luc
3'UTR

B.

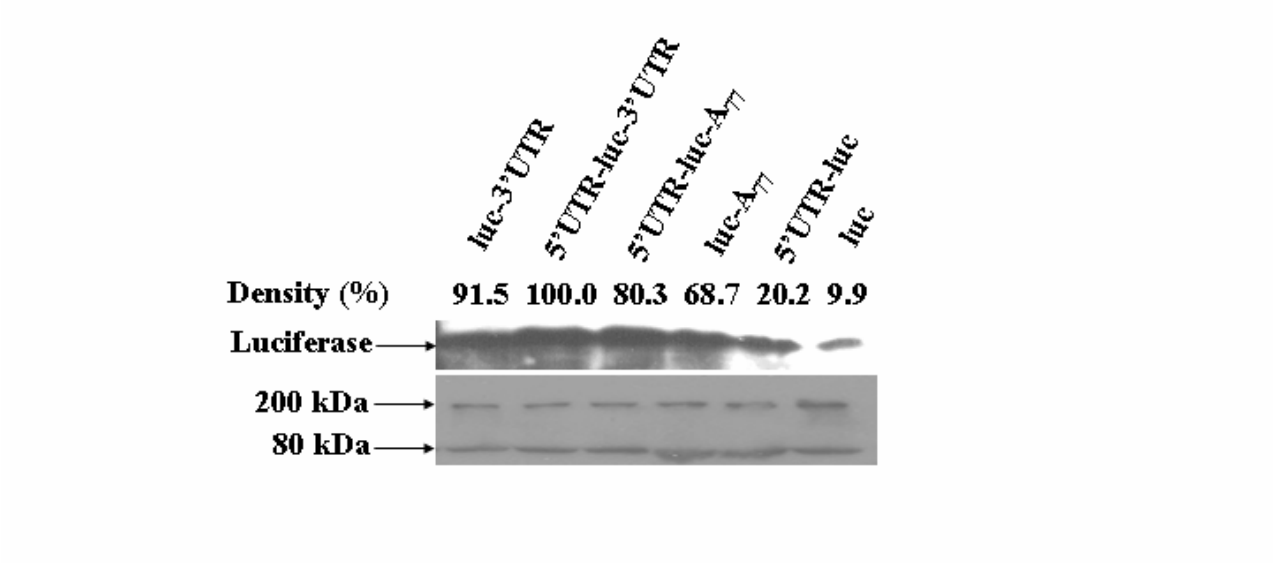
luc-3'UTR
5'UTR-luc-3'UTR
5'UTR-luc-A77
luc-A77
5'UTR-luc
luc
Density (%)
91.5 100.0 80.3 68.7 20.2 9.9
Luciferase
200 kDa
80 kDa

C.

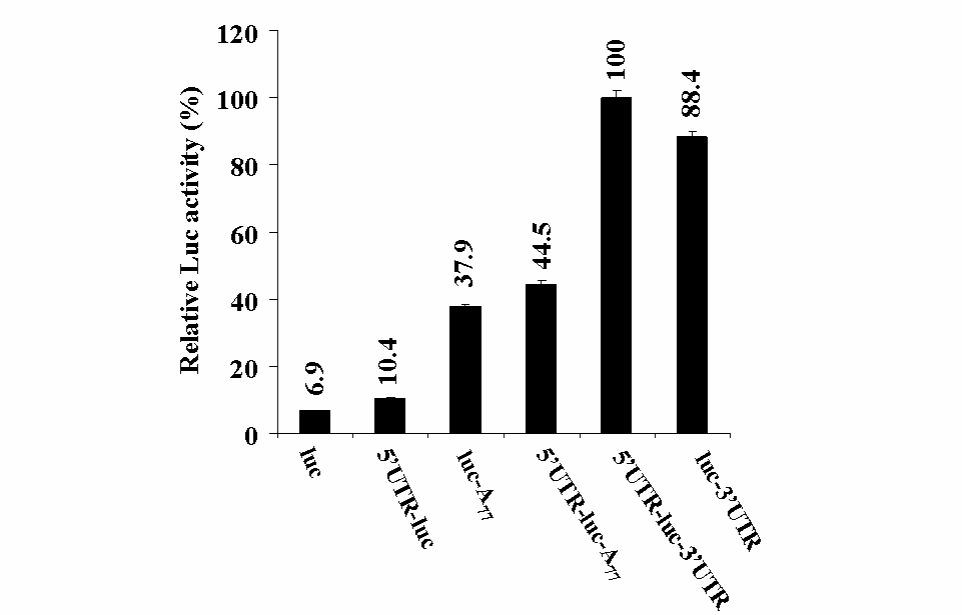

Fig. 4.4 The enhancement of translational efficiency by Cap, 5'UTR, 3'UTR of HLSV is the highest. (A) Schematic of constructs of luc, 5'UTR-luc, luc-A_{77}, 5'UTR-luc-A_{77}, 5'UTR-luc-3'UTR, luc-3'UTR. (B) Western blot analysis of *in vitro* translation products of luc, 5'UTR-luc, luc-A_{77}, 5'UTR-luc-A_{77}, 5'UTR-luc-3'UTR, luc-3'UTR. The density of each translation products was estimated and the percentage was indicated above each constructs. (C) Relative luciferase activity of luc, 5'UTR-luc, luc-A_{77}, 5'UTR-luc-A_{77}, 5'UTR-luc-3'UTR, luc-3'UTR constructs measured in kenaf protoplasts. Each construct was assayed at least three times with duplicates and the mean values represent the relative luciferase activity.

68.7%, 80.3% and 91.5%, respectively. In kenaf protoplasts, the relative luciferase activity of 5'UTR-luc-3'UTR was set at 100.0%. The relative luciferase activity of luc and 5'UTR-luc was 6.9% and 10.4%, respectively. And the relative luciferase activity of luc-A_{77}, 5'UTR-luc-A_{77} and luc-3'UTR were 37.9%, 44.5% and 88.4%, respectively. *In vitro* and *in vivo* results showed that 5'UTR-luc-3'UTR reached the highest level of translational enhancement. There was no synergistic contribution by the both 5'UTR and 3'UTR, while the 3'UTR appeared to be the major contributor. The results from luc-A_{77} and 5'UTR-luc-A_{77} were very similar and it is speculated that A_{77} does not interact with 5'UTR but may interact with the 5'cap to form a circularized mRNA which could be translated more efficiently. These results speculated some functional overlap of cap, 5'UTR and 3'UTR for translational enhancement. However, the cap, 5'UTR and 3'UTR could further enhance the luciferase activity to the highest level both *in vitro* and *in vivo.*

4.5 Disruption of base-pairing between 5'UTR and 3'UTR decreases translation efficiency

Base-pairing between 5'UTR and 3'UTR could enhance translation (Guo et al., 2001; Meulewaeter et al., 2004). The secondary structure prediction showed that a loop region in the 5'UTR of HLSV could base-pair 9-nt with a loop in its 3'UTR (Fig. 4. 1C). Reports on TBSV (Fabian and White, 2004), BYDV (Guo et al., 2001), *Turnip crinkle virus* (TCV) (Qu and Morris, 2000), TNV (Shen and Miller, 2004; Meulewaeter et al., 2004) and STNV (Lipzig et al., 2002) showed that base-pairing between the 5'UTR and 3'UTR of these viruses could enhance translation. A 5-nt base-pairing in the 5'UTR and 3'UTR of BYDV could enhance translation *in vitro* and *in vivo*. The stability of the base-pairing interaction could possibly be strengthened by host proteins or possibly by the "kissing" stem loops which are more kinetically and thermodynamically favored, as compared to equivalent base-pairing of linear RNAs (Guo et al.,

2001). In TNV, 5-nt loop-loop base-pairing between the 5'UTR and 3'UTR also enhanced luciferase activity (Meulewaeter et al., 2004). To further characterize whether the predicted 9-nt loop-loop base-pairing in HLSV could affect the translational enhancement, disruption of base-pairing experiments were conducted (Fig. 4.5). As showed in Fig. 4.1C, & 1D, base pairing between 5'UTR-D and 3'UTR, as well as 5'UTR and 3'UTR-S, were disrupted. In kenaf protoplasts, the results showed that different constructs (Fig. 4.5A) enhanced translation differentially. The relative luciferase activity of 5'UTR-luc-3'UTR was set at 100.0%. The relative luciferase activity of 5'UTR-D-luc-3'UTR, 5'UTR-luc-3'UTR-S, 5'UTR-D-luc, 5'UTR-luc and luc were 89.2%, 81.6%, 8.4%, 10.4% and 6.9%, respectively. The results showed that disruption of base-pairing (both 5'UTR-D-luc-3'UTR and 5'UTR-luc-3'UTR-S) decreased the luciferase activity slightly. This may be due to partial deletion of 5'UTR-D or 3'UTR-S which caused disruption of base-pairing. The major enhancing effect of the poly(A) tract remained strong. The 5'UTR-D or 3'UTR-S also did not change in their secondary structures as compared with the 5'UTR or the 3'UTR. These UTRs mainly contributed to translational enhancement. The disruption of base-pairing affects translational efficiency. This suggests that base-pairing between the 5'UTR and 3'UTR of HLSV might be an element in enhancing translation. However, the mutations per se of the loops might also affect the translation efficiency.

4.6 Restored base-pairing between 5'UTR-D and 3'UTR-S enhance translation to the wild-type levels

To further analyze the base-pairing effects on translation, restored base-pairing and additional base-pairing experiments were conducted. As seen in Fig. 4.1C, 1D, 1E, base-pairing between 5'UTR-D and 3'UTR-S was restored, which formed a 8-nt base-pairing; The 5'UTR-M and 3'UTR could form a 10-nt base-pairing, with one additional base-pairing as compared to the

A.

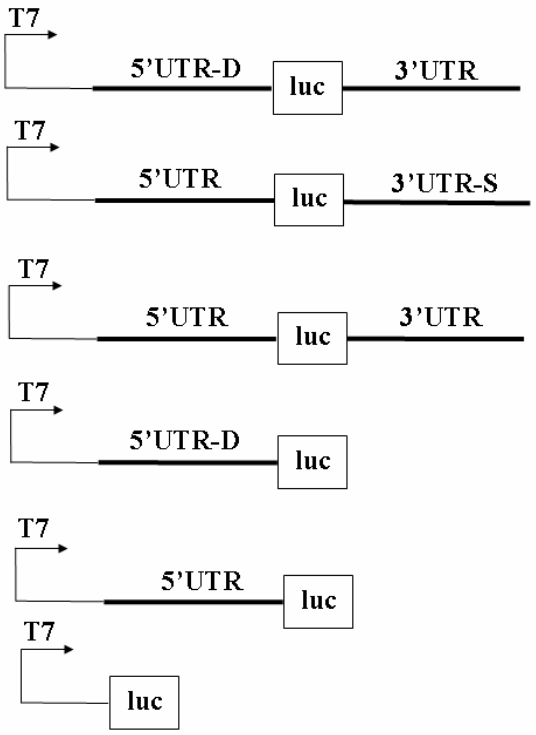
T7
5'UTR-D
luc
3'UTR
T7
5'UTR
luc
3'UTR-S
T7
5'UTR
luc
3'UTR
T7
5'UTR-D
luc
T7
5'UTR
luc
T7
luc

B.

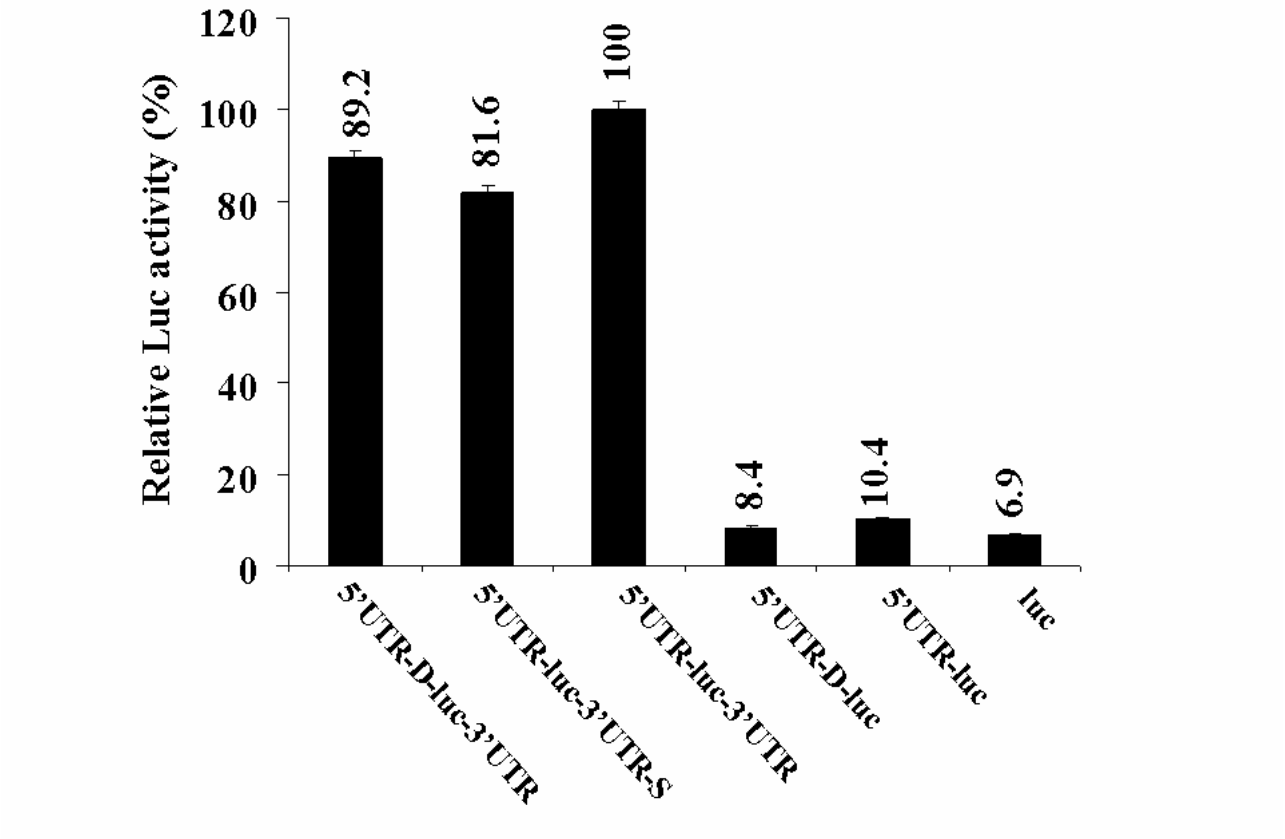

Fig. 4.5 Decrement of luciferase activity by disruption of base-pairing. (A) Schematic of constructs of 5'UTR-D-luc-3'UTR, 5'UTR-luc-3'UTR-S, 5'UTR-luc-3'UTR, 5'UTR-D-luc, 5'UTR-luc, luc. (B) Relative luciferase activity of 5'UTR-D-luc-3'UTR, 5'UTR-luc-3'UTR-S, 5'UTR-luc-3'UTR, 5'UTR-D-luc, 5'UTR-luc, luc constructs measured in kenaf protoplasts. Each construct was assayed at least three times with duplicates and the mean values represent the relative luciferase activity.

wild-type. Constructs (Fig. 4.6A) were tested in kenaf protoplasts. After restoring the base-pairing, the relative luciferase activity of 5'UTR-D-luc-3'UTR-S was higher than that of either 5'UTR-D-luc-3'UTR or 5'UTR-luc-3'UTR-S. In addition, the relative luciferase activity from 5'UTR-M-luc-3'UTR was the highest as compared with the others. The construct of 5'UTR-M-luc-3'UTR which had 10 nt base-pairing had higher luciferase activity than that of 5'UTR-luc-3'UTR, which had 9 nt base-pairing. Therefore, it is apparent that the base-pairing effect on enhancing translation does exist. This kind of translational enhancement is poly(A)-independent.

4.7 Different combinations of 5'UTR and 3'UTR or mutants enhance translation differentially

To analyze translational enhancement of test constructs (Fig. 4.7A), the luciferase expression levels were examined both *in vitro* and *in vivo*. In the wheat germ extract, the intensity of luciferase bands in the Western blot were examined (Fig. 4.7B). The band intensity of either 5'UTR-luc-3'UTR-S or 5'UTR-D-luc-3'UTR was slightly less than that of 5'UTR-luc-3'UTR, which resulted from disruption of the base-pairing. When the base-pairing was restored, the band intensity of 5'UTR-D-luc-3'UTR-S was comparable with that of 5'UTR-luc-3'UTR. The band intensity of 5'UTR-M-luc-3'UTR was higher than that of 5'UTR-luc-3'UTR, which further confirmed the base-pairing effect. Other constructs also were measured (Fig. 4.7B). The results suggest that 5'UTR and 3'UTR were able to enhance translation to a different level. After deleting part of the sequence of 5'UTR, translational enhancement was reduced. It suggests that the original 5'UTR is important for translation enhancement. The A_{77} translation enhancement was less than that of the 3'UTR of HLSV. This indicates that the original 3'UTR is of greater importance than mRNA poly(A) tail in regulating translation. Since both the luc-A_{77} and the 5'UTR-luc-A_{77} could enhance translation to a comparable level, the A_{77} was assumed to be able

A.

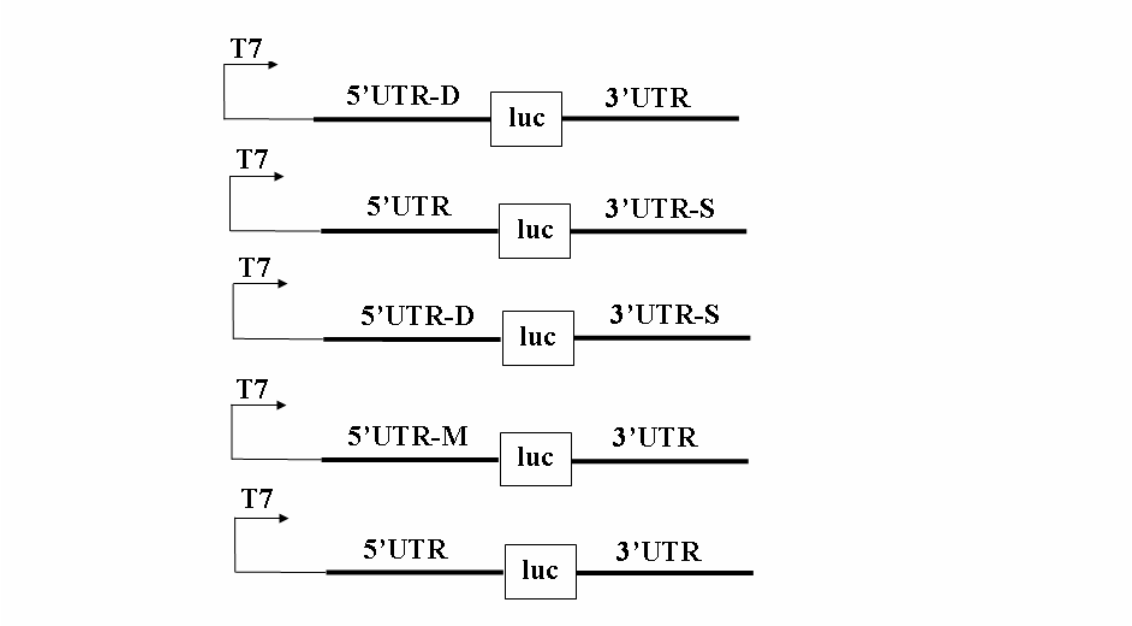
T7
5'UTR-D
luc
3'UTR
T7
5'UTR
luc
3'UTR-S
T7
5'UTR-D
luc
3'UTR-S
T7
5'UTR-M
luc
3'UTR
T7
5'UTR
luc
3'UTR

B.

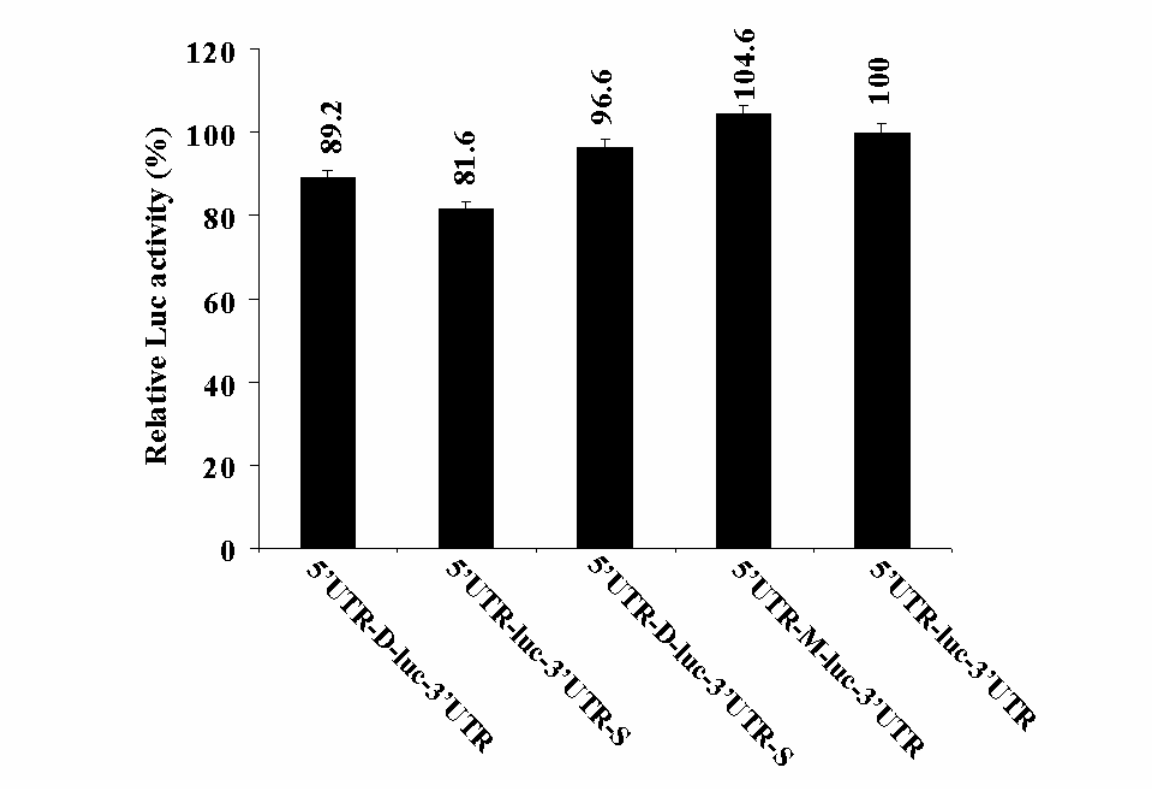

Fig. 4.6 Increase of translational efficiency by restoring base-pairing. (A) Schematic of constructs of 5'UTR-D-luc-3'UTR, 5'UTR-luc-3'UTR-S, 5'UTR-D-luc-3'UTR-S, 5'UTR-M-luc-3'UTR, 5'UTR-luc-3'UTR. (B) Relative luciferase activity of 5'UTR-D-luc-3'UTR, 5'UTR-luc-3'UTR-S, 5'UTR-D-luc-3'UTR-S, 5'UTR-M-luc-3'UTR, 5'UTR-luc-3'UTR constructs measured in kenaf protoplasts. Each construct was assayed at least three times with duplicates and the mean values represent the relative luciferase activity.

A.

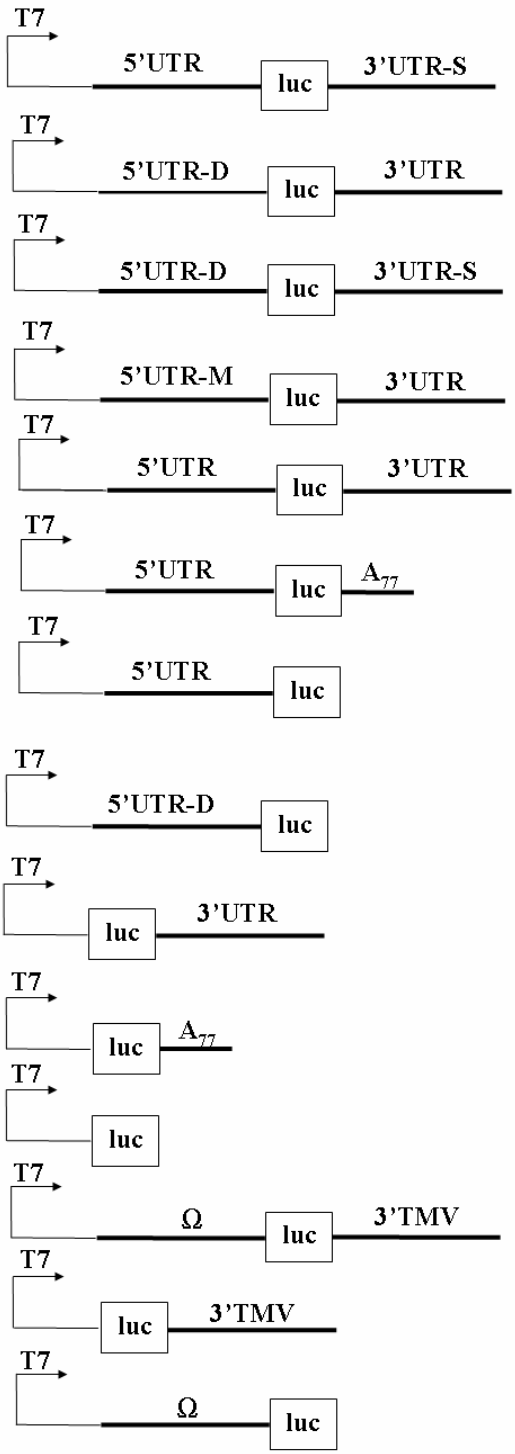
T7
5'UTR
luc
3'UTR-S
T7
5'UTR-D
luc
3'UTR
T7
5'UTR-D
luc
3'UTR-S
T7
5'UTR-M
luc
3'UTR
T7
5'UTR
luc
3'UTR
T7
5'UTR
luc
A77
T7
5'UTR
luc
T7
5'UTR-D
luc
T7
luc
3'UTR
T7
luc
A77
T7
luc
T7
Ω
luc
3'TMV
T7
luc
3'TMV
T7
Ω
luc

B

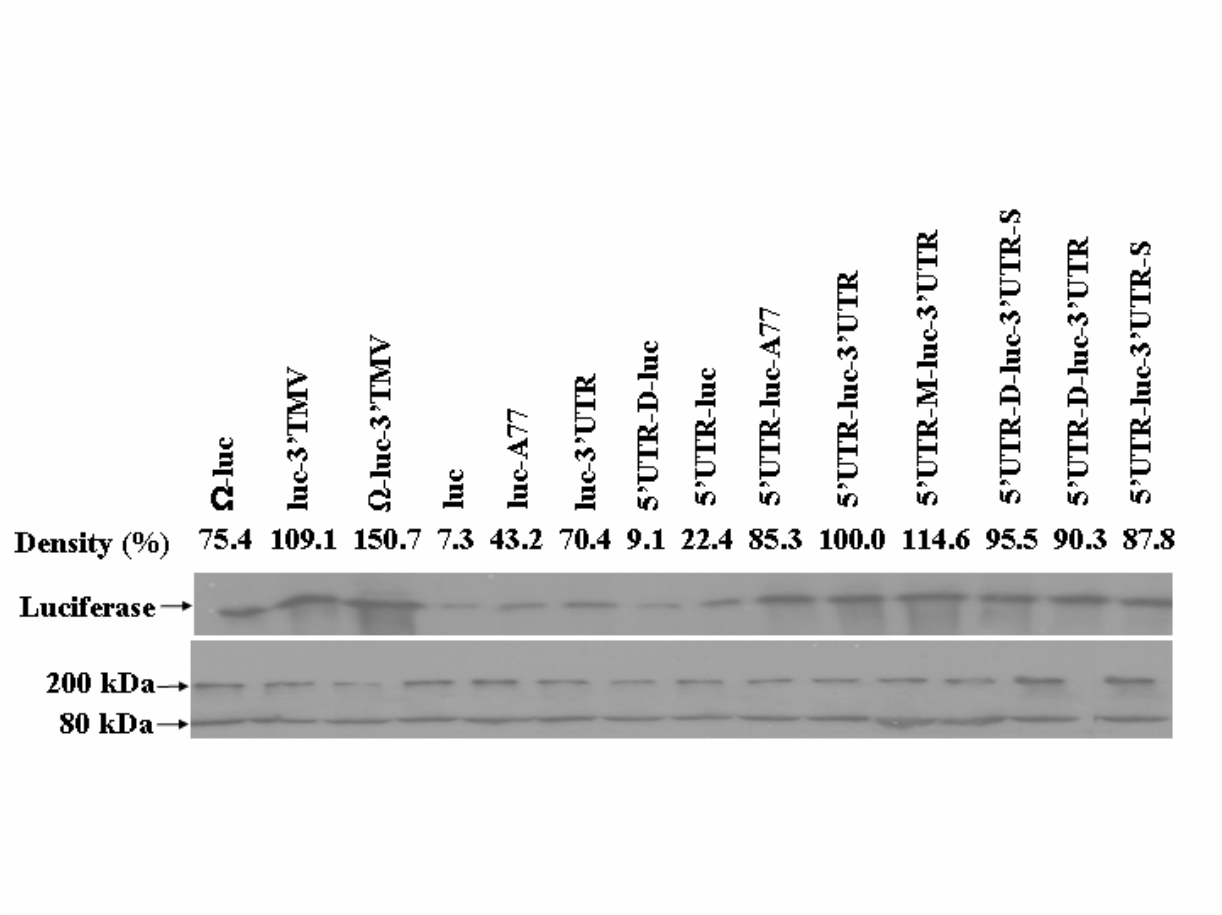
Ω-luc
luc-3'TMV
Ω-luc-3'TMV
luc
luc-A77
luc-3'UTR
5'UTR-D-luc
5'UTR-luc
5'UTR-luc-A77
5'UTR-luc-3'UTR
5'UTR-M-luc-3'UTR
5'UTR-D-luc-3'UTR-S
5'UTR-D-luc-3'UTR
5'UTR-luc-3'UTR-S
Density (%) 75.4 109.1 150.7 7.3 43.2 70.4 9.1 22.4 85.3 100.0 114.6 95.5 90.3 87.8
Luciferase
200 kDa
80 kDa

C.

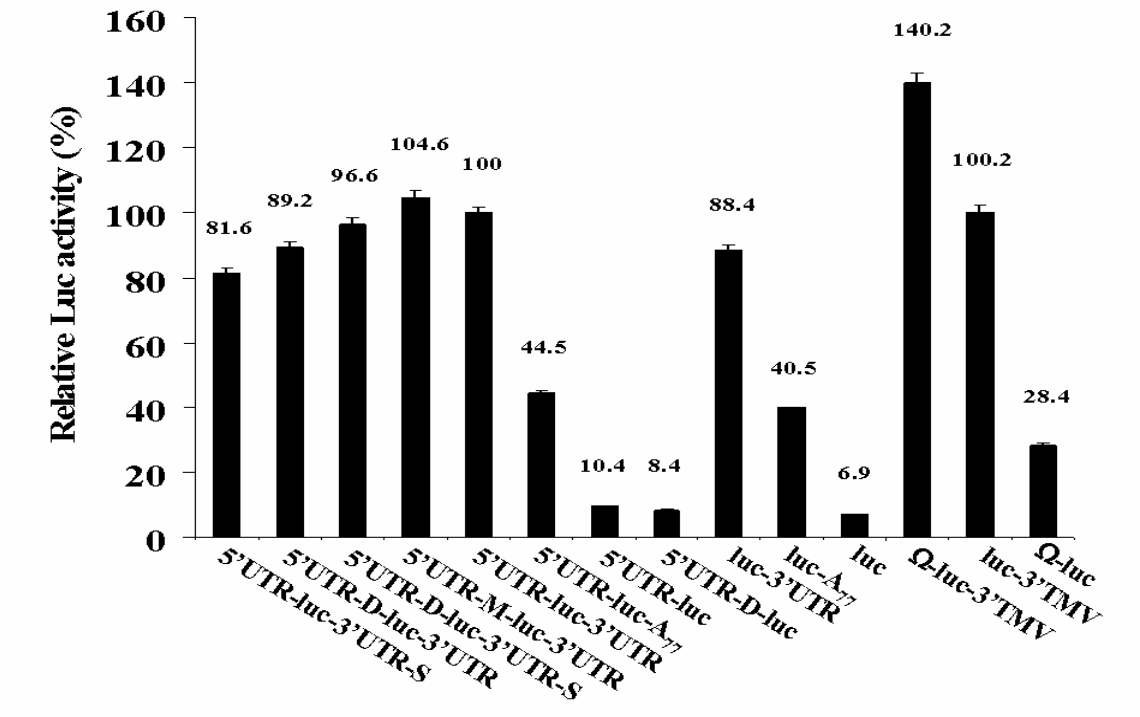

Fig. 4.7 Increment of translation differentially of different constructs. (A**)** Schematic of constructs of 5'UTR-luc-3'UTR-S, 5'UTR-D-luc-3'UTR, 5'UTR-D-luc-3'UTR-S, 5'UTR-M-luc-3'UTR, 5'UTR-luc-3'UTR, 5'UTR-luc-A_{77}, 5'UTR-luc, 5'UTR-D-luc, luc-3'UTR, luc-A_{77}, luc, Ω-luc-3'TMV, luc-3'TMV, Ω-luc. (B) Western blot analysis of *in vitro* translation products of 5'UTR-luc-3'UTR-S, 5'UTR-D-luc-3'UTR, 5'UTR-D-luc-3'UTR-S, 5'UTR-M-luc-3'UTR, 5'UTR-luc-3'UTR, 5'UTR-luc-A_{77}, 5'UTR-luc, 5'UTR-D-luc, luc-3'UTR, luc-A_{77}, luc, Ω-luc-3'TMV, luc-3'TMV, Ω-luc. The density of each translation products was estimated and the percentage was indicated above each constructs. (C) The relative luciferase activity of 5'UTR-luc-3'UTR-S, 5'UTR-D-luc-3'UTR, 5'UTR-D-luc-3'UTR-S, 5'UTR-M-luc-3'UTR, 5'UTR-luc-3'UTR. 5'UTR-luc-A_{77}, 5'UTR-luc, 5'UTR-D-luc, luc-3'UTR, luc-A_{77}, luc, Ω-luc-3'TMV, luc-3'TMV, Ω-luc constructs measured in kenaf protoplasts. Each construct was assayed at least three times with duplicates and the mean values represent the relative luciferase activity.

to bind to the 5'-cap, but not the 5'UTR. In kenaf protoplasts, the relative luciferase activity of different constructs was also compared. The relative luciferase activity of 5'UTR-luc-3'UTR-S or 5'UTR-D-luc-3'UTR was less than that of 5'UTR-luc-3'UTR, which suggested disruption of base-pairing affecting translational efficiency. On the other hand, the activity of 5'UTR-D-luc-3'UTR-S was increased as compared with that of 5'UTR-luc-3'UTR-S or 5'UTR-D-luc-3'UTR, which suggested that restoring the base-pairing could restore the highly translational efficiency. The activity of 5'UTR-M-luc-3'UTR was even higher than that of 5'UTR-luc-3'UTR. We observed similar trends with different constructs in translational enhancement *in vitro* and *in vivo* experiments. However, there is percentage difference of each construct in enhanced translation *in vitro* versus *in vivo.* Here we showed all the tested constructs could have different levels of translational enhancement as compared to luc construct both *in vitro* and *in vivo*. The translational enhancing effect of the 3'UTR is higher than that of the 5'UTR, which suggests that 3'UTR is more important in regulating translation of viral proteins. In addition, the translational enhancement of poly(A) tract in the 3'UTR was explored. It showed a lower enhancing effect compared with the 3'UTR, which indicated that there was interaction other than poly(A)-cap interaction.

4.8 Both 5'UTR and 3'UTR of HLSV translational enhancements are cap-dependent

All the above results were obtained based on capped transcripts used in the experiments. To test whether the translational enhancement of 5'UTR and 3'UTR is cap-dependent or cap-independent, we tested luciferase activity of capped and uncapped RNA in kenaf protoplasts (Fig. 4.8). The results showed that all capped transcripts had at least 48-folds translational enhancement than all corresponding uncapped transcripts. The effect of a cap had 50 fold

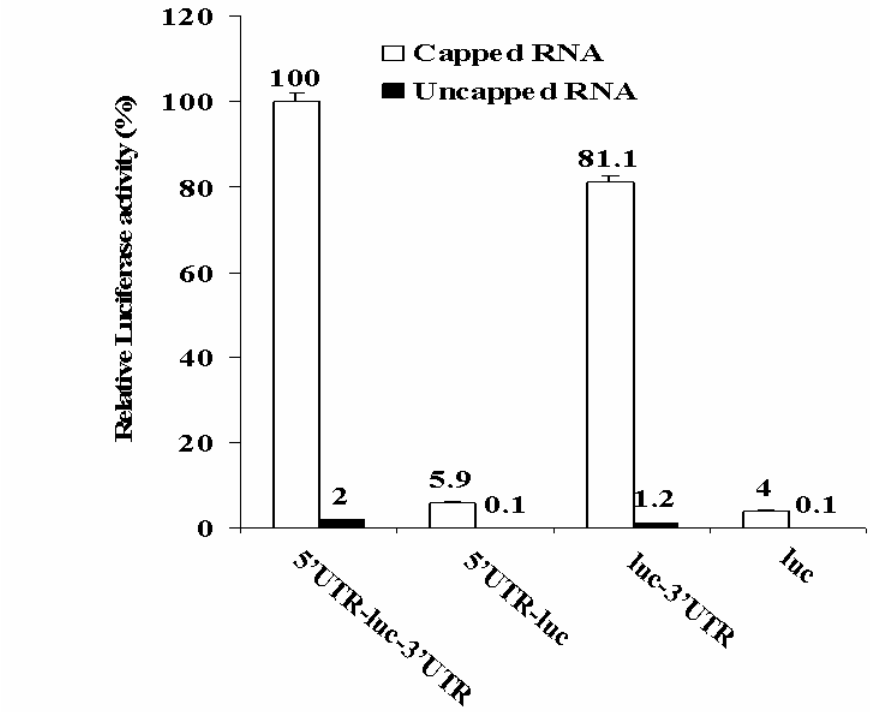

Fig. 4.8 The 5'UTR and 3'UTR translational enhancement of HLSV is both cap-dependent. Capped and uncapped RNA transcripts of 5'UTR-luc-3'UTR, 5'UTR-luc, luc-3'UTR, luc were made. RNAs were transfected to kenaf protoplasts and translational efficiency of these RNAs were assayed. The relative luciferase activity was shown individually. Each construct was assayed at least three times with duplicates and the mean values represent the relative luciferase activity.

enhancement for 5'UTR-luc-3'UTR transcripts; and 48 fold enhancement for 5'UTR-luc transcripts; 69 fold enhancement for luc-3'UTR transcripts; 48 fold enhancement for luc transcripts. A cap greatly enhances translation similar to previous studies reported in cowpea protoplasts for TYMV (Matsuda et al., 2004) and in carrot protoplast for TMV (Galie, 2002). These results suggest that translational enhancement by both 5'UTR and 3'UTR of HLSV are cap-dependent.

4.9 Discussion and Conclusion

4.9.1 5'UTRs as translational enhancers

HLSV 5'UTR is a (CAA)-rich sequence which is similar to the TMV Ω sequence. Its secondary structure was predicted to be a stem loop with a free energy of -11.8kcal/mol. A comparison showed that HLSV 5'UTR has 6 (CAA) while TMV Ω has 11 (CAA). The poly(CAA) rich region of TMV Ω sequence could recruit heat shock protein 101 which functions as a specific translational regulatory protein (Galie, 2002; Wells et al., 1998). The CA-rich elements also were found in or near its 5'UTR of viral gRNA or subgenomic RNA (sgRNA) of TCV, TBSV, TNV, TEV, and *Potato virus X* (PVX), although their roles in translational enhancement have not been well defined (Qu and Morris, 2000). The HSP101 could enhance the recruitment of eIF4F and translation was promoted (Galie, 2002). The functions of the two homologies eIF4G and eIFiso4G are different. The eIF4G could promote internal translation, cap-independent translation and translation of structured mRNAs, while its homologue eIFiso4G could not (Gallie and Browning, 2001). HLSV 5'UTR was predicted to possess a 5'-proximal structured mRNA (Fig. 4.1C) and it could slightly enhance translation *in vitro* and *in vivo* (Fig. 4.2). This translational enhancement could be attributed to the enhanced recruitment of HSP101 and subsequent enhanced recruitment of eIF4F which promotes the translation of an mRNA

containing a 5'-proximal secondary structure (Gallie and Browning, 2001). Studies on *Cauliflower mosaic virus* (CaMV) leader sequence showed 40S ribosome shunt-mediated translation (Pooggin et al., 2000, 2001). There are a growing number of reports describing the ribosome shunt or related processes operating at the level of viral RNAs (Futterer et al., 1996; Latorre et al., 1998; Remm et al., 1999; Yueh et al., 2000) and cellular mRNA (Yueh et al., 2000), suggesting that shunting is a general translation mechanism reflecting an intrinsic property of the eukaryotic ribosome. In addition, human heat shock protein 70 (HSP70) has been shown to promote ribosome shunting (Yueh et al., 2000). Based on the evidence that the poly(CAA) sequence could enhance recruitment of heat shock protein while in turn promotes ribosome shunting, it is possible that the same mechanisms may be operating in HLSV, since a stem-loop structure between the cap and the start AUG codon prevents translation (Kozak, 1991). However, from the proposed secondary structure of the HLSV 5'UTR (Fig. 4.1C), the 40S ribosome may bind to the cap, bypassing the stem-loop structure and initiate scanning of the linear sequence which contains two CAA sequences and enhances recruitment of heat shock protein. Translation is believed to be enhanced through this ribosome shunting mechanism.

4.9.2 3'UTRs as translational enhancers

The HLSV 3'UTR is a unique sequence which contains an internal poly(A) tract upstream of its 3'TLS. Plant viruses possessing a poly(A) tail downstream of its 3'UTR include both rubi- and tymo-lineages (Dreher, 1999). Different plant viruses whose genomes terminate in poly(A) tails include poty-, potex-, como-, capillo-, carla-, and *Beet necrotic yellow vein virus* (Dreher, 1999), but rarely with an internal poly(A) tract upstream of its 3'TLS. The only known example among plant viruses is BSMV which contains a short internal poly(A) tract in its 3'UTR (Gustafson and Armour, 1986). However, its function in enhancing translation has not been

reported. Studies on different viruses showed that the 3'UTRs could act as translational enhancers. In HCRSV, a 6-nt segment in its 3'UTR plays an important role in translational enhancement (Koh et al., 2002). Synergism between HCRSV 3'UTR and its IRES was found to enhance its CP synthesis (Koh et al., 2003). The 3'UTR and the terminal 3' stem loop domain of DENV were found to enhance virus translation (Holden and Harris, 2004). In AMV, the 3'UTR was a competitive determinant for enhancing its CP mRNA translation (Hann et al., 1997). In *Red clover necrotic mosaic virus* (RCNMV) (Mizumoto et al., 2003), TBSV (Fabian and White, 2004), TNV (Shen and Miller, 2004; Meulewaeter et al., 2004), BYDV (Guo et al., 2001), STNV (Lipzig et al., 2002), and TCV (Qu and Morris, 2000), the presence of translational enhancing elements in its 3'UTR were also reported. In HLSV, the poly(A) tract upstream of the TLS exists instead of a UPD region. Experiments showed that this sequence could enhance translation *in vitro* and *in vivo* (Fig. 4.7). This translational enhancement was probably contributed together by the poly(A) tract and the TLS region at its 3'end, since the enhancement from 3'UTR was greater than the A_{77} alone. This suggests that TLS could also complement the poly(A) tract for translational enhancement. However, in TMV, the TLS alone could not enhance translation (Gallie, 1991). The entire TMV 3'UTR, including the UPD region, is required to maximize translational efficiency (Gallie, 1991). In HLSV, the A_{77} alone could enhance translation efficiency to a relatively high level (Fig. 4.7) and it may bind to the 5'cap to establish a "circular form" to enhance translation (Fig. 4.8A). Interestingly, the results provided direct evidence that poly(A) acts as a 3' translational enhancer which confirms the notion that UPD functions as a substitute for poly(A) in TMV (Gallie and Walbot, 1990). The results showed that the full-length 3'UTR of HLSV enhanced translation efficiency to a similar level as compared to the 3'UTR of TMV. Since the HLSV 3'UTR could enhance translational efficiency to a higher level than the

poly(A) tract alone, it indicates that the HLSV 3'UTR is more efficient in enhancing its protein synthesis than host mRNAs. Studies on RCNMV RNA1 showed that deletion of its 3'UTR resulted in reduced level of translation (Mizumoto et al., 2003). These results indicate that an intact 3'UTR is important for viral gene expression. From the results, the 3'UTR of HLSV was shown to be a strong translational enhancer which could enhance translation efficiency more significantly as compared to its 5'UTR. This is the first study demonstrating that a plant virus that possesses an internal poly(A) tract that can function as a translational enhancer. Similarities between the 3'UTR of HLSV and 3'UTR of TMV suggest that the poly(A) tract or UPD region may be important for recruitment of host factors for protein synthesis, while the TLS could cooperate to enhance translation.

4.9.3 Poly(A)-dependent translation

A concept concerning mRNA or viral RNA has been developed and states that the poly(A) tail can interact with the 5'cap on the same RNA to form a "closed loop" to enhance translation (Dreher, 1999). Among *Encephalomyocarditis virus* (EMCV), *Hepatitis A virus* (HAV) or poliovirus, the presence of poly(A) significantly stimulated translation (Michel et al., 2001). Disruption of eIF4G and Poly(A) binding protein (PABP) interaction or cleavage of eIF4G abolished or severely reduced the poly(A)-mediated stimulation of picornavirus IRES-driven translation (Michel et al., 2001). In *Foot and mouth disease virus* (FMDV), the IRES-driven translation was stimulated separately by the 3'UTR and poly(A) sequence and it is suggested that host factors such as eIF4G, PABP, eIF4B and eIF3 play import roles in the translational enhancement (Lopez de Quinto et al., 2002). In mammalian cells, mRNA could formed a "closed loop" between its cap and poly(A) by the interaction of PABP and eIF4G. PABP is a canonical translational initiation factor (Kahvejian et al., 2005). To initiate translation, many factors are

involved in the formation of the “closed-loop” mRNA, including PABP, eIF4F (comprised of 4E, 4G and 4A), eIF3, eIF1A and eIF2-GTP-Met-tRNA; For IRES-driven translation, there could be additional trans-acting factors involved (Komar and Hatzoglou, 2005). In the rabbit reticulocyte lysate, the eIF4G-PABP interaction increased the functional affinity of the eIF4E for the 5’capped mRNA and translation was enhanced through this cap-poly(A) synergy (Borman et al., 2000). In eukaryotes, the PABP and the 3'-poly(A) interact synergistically with the 5' cap to promote translation initiation and increase translation efficiency by forming the "closed-loop" initiation complex (Sachs et al., 1997). PABP is also found to bind eukaryotic release factor 3 (eRF3) and this interaction supports a proposed model that the poly(A) tail promotes recycling of terminating ribosome from the 3′ to the 5′ end of mRNA (Hoshino et al., 1999; Uchida et al., 2002). Our results showed that luciferase expression from the A_{77} constructs was enhanced to a higher level than the construct without the A_{77}. These data support the concept that the poly(A) tract might form a “closed-loop” with its 5’ cap to promote translation of HLSV mRNA. A cap-poly(A)-dependent translation model is shown in Fig. 4.9 A. It shows that when PABP is tightly bound to eIF4G, the ribosome may be circulated back from the 3’ region to the 5’ cap to initiate another round of translation with the assistance of eRF3 (Hoshino et al., 1999; Uchida et al., 2002). In our model (Fig. 4. 9 A), the 40S ribosome might be blocked at the stem-loop region (ΔG =-30.8 kcal/mol) of the 3’TLS. However, it can be recruited back to the 5’ cap of the viral RNA via cap-poly(A)-mediated translation (Michel et al., 2000). The TLS region may function as a translational regulator, since the stem-loop region (ΔG = -30.8kcal/mol) may prevent ribosome from continuing the scanning.

4.9.4 Poly(A)-independent translation

Stem-loop “kissing” interactions between the 5’UTR and the 3’UTR of plant viruses have

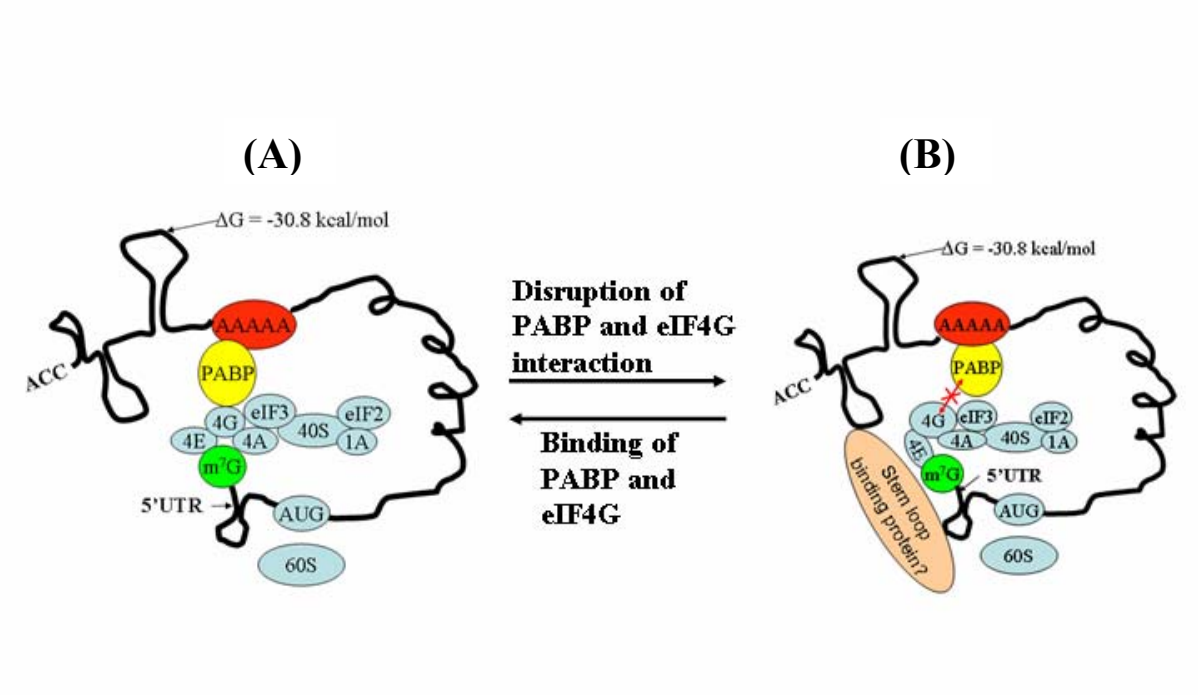

Fig. 4.9 Proposed models of (A) poly(A)-dependent and (B) poly(A)-independent translation of HLSV mRNA. PABP, poly(A) binding protein; 4G, 4E, 4A, 1A denote eIF4G, eIF4E, eIF4A, eIF1A respectively; AAAAA denotes HLSV internal poly(A) tract; 40S, 60S denote 40S, 60S ribosome; eIF2 denotes eIF2-GTP-Met-tRNA. Stem-loop binding protein is believed to strengthen the 5', 3' loop-loop "kissing" interaction.

been shown to be an efficient way of translation enhancement (Guo et al, 2001; Lipzig et al, 2002; Shen and Miller, 2004; Meulewaeter et al., 2004; Fabian and White, 2004). These "kissing" loops, which facilitate replication, are also found in the 3'UTR of animal viruses (Olsthoorn et al. 1999; Pilipenk et al., 1996; Goebel et al, 2001 a, b). In HLSV, the 5'UTR and 3'UTR could form a 9-nt base-pair between the two UTRs predicted by the M-fold RNA prediction program. Our data support that these base-pairs contributed to translational enhancement (Fig. 4.7). The stability of the 9-nucleotide base-pairing for the long distance "closed-loop" interaction might be further strengthened by host proteins. The "kissing" model could be quite stable as the "kissing" stem loops are more kinetically and thermodynamically favoured compared to equivalent base-pairing of linear RNAs (Guo et al., 2001). A 5'- to 3'- end interaction to facilitate efficient translation in eukaryotes can also be established by protein-protein interactions other than the initiation factors and PABP. In the case of AMV RNA and various cellular mRNAs, other factors, such as stem loop binding protein but not the PABP, are involved in efficient translation, (Barends et al., 2004; Ling et al., 2002; Mazumder et al., 2003; Neeleman et al., 2001; Wilkie et al., 2003; Sanchez and Marzluff, 2002). Taken together, the 5'- to 3'- stem-loop interaction might exist in the HLSV genome. Therefore, an alternate model is proposed in Fig. 4. 9 B. In this kissing "closed-loop" model, ribosome might start scanning from the 5'cap, passing through the poly(A) tract and continued to scan into the 3'TLS region. During the process, the ribosomes need to pass through a stem-loop immediately downstream of the poly(A) tract. The free energy of this stem-loop was predicted to be -30.8kcal/mol. As reported, the stem and loop structures with such a low free energy as ΔG= -30 kcal/mol located 50 or 60 nucleotide downstream of the AUG did not impair translation in COS cells or in cell-free extract (Kozak, 1986, 1991). It is possible that the ribosome could also scan through the stem-loop

region in the HLSV 3'TLS just downstream of the poly(A) tract. Only when the ribosome reaches the kissing stem-loop region would it return to the 5' cap of the viral RNA. During this process, host factors (probably stem-loop binding proteins) other than PABP would interact with the initiation factors to play an important role in the poly(A)-independent translation. This model is similar to those for TBSV (Fabian and White, 2004), BYDV (Guo et al., 2001) or TNV (Shen and Miller, 2004; Meulewaeter et al., 2004), in that the 5' and 3' RNA-RNA stem-loop interaction enhanced translation. In addition, studies on HLSV showed that as long as complementary nucleotides between the loops were maintained, the loop-loop base-pairing could tolerate nucleotide sequence modifications without major effect on the translational activity (Fig. 4. 7). This is in agreement with the results observed in TBSV (Fabian and White, 2004).

In this study, the functions of HLSV 5UTR and 3'UTR in regulating gene expression were analyzed. Using wheat germ extracts or kenaf (*Hibiscus cannabinus* L.) protoplasts, enhanced translation was observed when either 5'UTR or 3'UTR of HLSV was present. Predicted stem loops between the 5'UTR and the 3'UTR formed nine nucleotide base-pairs. The activity of the reporter luciferase was highest when m^7G (cap), 5'UTR and 3'UTR were present, while disruption of the base-pairing of the 5'UTR and the 3'UTR decreased the luciferase activity. After restoring the base-pairing, the luciferase activity was again increased. An extra base-pair between the two UTRs appeared to further enhance the luciferase activity. This indicates that base-pairing of the two UTRs contributes to translational enhancement. Further analysis suggests that the translational enhancement was highly cap-dependent. The base-pairing could form a "closed-loop" to enhance translation, while the poly(A) tract interacted with its 5'cap also forming a similar "closed loop" to enhance translation. Therefore, the 5' and 3' UTR interaction could promote both poly(A)-dependent and poly(A)-independent translation of HLSV mRNA.

To our knowledge, this is the first demonstration that a plant virus possesses such 5'and 3' translational enhancers which enhance both poly(A)-dependent and poly(A)-independent translation.

In conclusion, our results provided the first experimental evidence that a poly(A) tract of HLSV could indeed substitute for the UPD region for translation enhancement in tobamoviruses. This supports the notion earlier proposed by Gallie in 1990 (Gallie and Walbot, 1990). However, the HLSV might not be the same as TMV in term of enhancing translation. TMV is not polyadenylated, its UPD functions as a poly(A) (Gallie and Walbot, 1990). But the UPD need to fold into certain structure to perform this function. However, HLSV poly(A) did not need to fold into structure for the PABP to bind with it. When the TMV UPD fold into strcture, it might inhibit the ribosome to scan through it till the TLS region. But this might possibly happen in HLSV. So there might be a different way of translational enhancement in different virus. Here I only observed the additive translational enhancement of 5', 3'UTR in HLSV while it might be synergistic enhancing translation by TMV 5', 3'UTR. The nucleotide sequences and the forming of secondary structures could be major determinants of this. So in terms of translational enhancer, the HLSV 5', 3'UTRs might share some similarities with those of TMV, but not exactly use the same mechanism to enhance their viral protein translation.

CHAPTER 5

THE 3'TLS AND POLY(A) TRACT PROMOTE HLSV IRES TRANSLATION *IN VITRO* AND *IN VIVO* SEPARATELY

5.1 Introduction

In a former study, two putative IRES-like sequences present upstream of MP and CP ORFs of HLSV were identified (Srinivasan, 2003). Characterization these sequences have shown that they are functional as IRES elements *in vitro* in the wheat germ extract and *in vivo* in whole plant assays (Srinivasan, 2003). To obtain a better understanding the HLSV IRES-driven translation, it is important to analysis IRES translation in more detail. For example, its interaction with other elements in the genome, the translation strategy,the regulation mechanism, etc. Studies show that IRES-driven translation is achieved by the cleavage of eIF4G protein, a part of eIF-4F complex which brings together the 5' cap and 40S ribosomal subunit (Gradi et al., 1998). Under such conditions, viruses should have an alternate strategy to overcome the block in translation and be able to utilize the host cellular machinery for translating its proteins. IRES-dependent translation remains functional in these conditions as it requires only the C-terminal portion of eIF4G which is available after cleavage by viral proteases (Ohlmann et al., 1996). The IRES-driven mechanism may also aid in translation of mRNAs that are constrained by numerous upstream AUGs or RNA secondary structures in their 5' leader sequence (Chappell et al., 2001; Le Quesne et al., 2001). Plant tobamoviruses express 3' proximal proteins by production of sgRNA (Palukaitis and Zaitlin, 1986) and by utilizing an alternative cap-independent translational mechanism (Skulachev et al., 1999; Ivanov et al., 1997). TMV-Cr possesses IRES elements for driving the expression of MP and CP

ORFs whereas in TMV-U1, a 228 bp segment upstream of the MP gene was shown to promote internal initiation *in vitro*. Polypurine (A) rich sequences (PARSs) were identified to be responsible for TMV-Cr CP IRES (IRES $_{CP148}^{Cr}$) to be functional. In HCRSV,a carmovirus, a small sequence present upstream of its CP ORF which is complementary to 3' portion of 18S rRNA showed IRES-like activity and its 3'UTR functioned synergistically to enhance the IRES-translation (Koh et al., 2003). A marked translational synergy between the IRES, the 3'UTR and the poly(A) tail in FMDV RNA suggests that the 3'UTR and the poly(A) tail both promote IRES-mediated translation (Lopez et al., 2002). The interaction mechanism is not known but *in vitro* studies indicate the participation of eIF4G and PABP in EMCV translation (Michel, et al. 2000). In this study, further characterization of the HLSV 3'UTR on the influence of the two IRESs driven translation was carried out *in vitro* in wheat germ extract experiment and *in vivo* in whole plant assays.

5.2 HLSV IRES translation is less efficient than canonical cap-dependent translation *in vitro*

To obtain a better understanding the IRES-driven translation, it is first necessary to compare the efficiency of IRES-driven translation with the canonical cap-dependent translation. In order to do the comparison experiments, a GUS ORF following a T7 promoter was constructed and tested together with the IRES bicistronic contructs. The HLSV $IRES_{CP134}$ and $IRES_{MP165}$ segments, a non-PARS $(GUUU)_{16}$ spacer construct and a construct without any GUS ORF was tested together by *in vitro* translation methods. The final translation products were diluted 1000 times and 1 μl loaded for Western-blot by HRP antibody. From the results (Fig. 5.1), we can conclude that the canonical cap-

dependent translation is far more efficient than translation via either of the two HLSV IRESs. The cap at the 5'end could be more efficient in recruiting translational initiation factors eIF4G. The canonical cap-dependent translation is about 1000 times more efficient than IRES-driven translation from the results shown. However, there are still faint bands after 1000 times dilution in the two IRES lanes while no bands are present in non-PARS spacer $(GUUU)_{16}$ construct and the no GUS construct lane (Fig. 5.1). These suggest that HLSV IRESs-driven translations are functional *in vitro* in the wheat germ extract. However, the efficiency is very much lower than the canonical translation driven by a cap which could help to recruit the translational initiation factors more effectively.

5.3 HLSV CP IRES 134 translation is less efficient than TMV-Crucifer strain CP IRES 148 translation *in vitro*

Since the TMV-Cr IRES CP148 is a well characterized IRES element (Skulachev et al., 1999), it is necessary to know if the HLSV $IRES_{CP134}$ could have the same translational efficiency as the TMV-Cr $IRES_{CP148}$. To compare the efficiency of these two IRESs, experiments were conducted *in vitro* in the wheat germ extract system. and 2 µl translation products were loaded for Western blot analysis. The density of $IRES_{CP148}$ TMV-Cr was higher than that of the $IRES_{CP134}$ HLSV (Fig. 5.2). Through densitometry assay, the efficiency of $IRES_{CP134}$ HLSV is about 69% that of IRES $_{CP148}$ TMV cr (Fig. 5.2). This result suggest that the $IRES_{CP134}$ HLSV functional similar but less efficient as compared with the $IRES_{CP148}$ TMV-Cr.

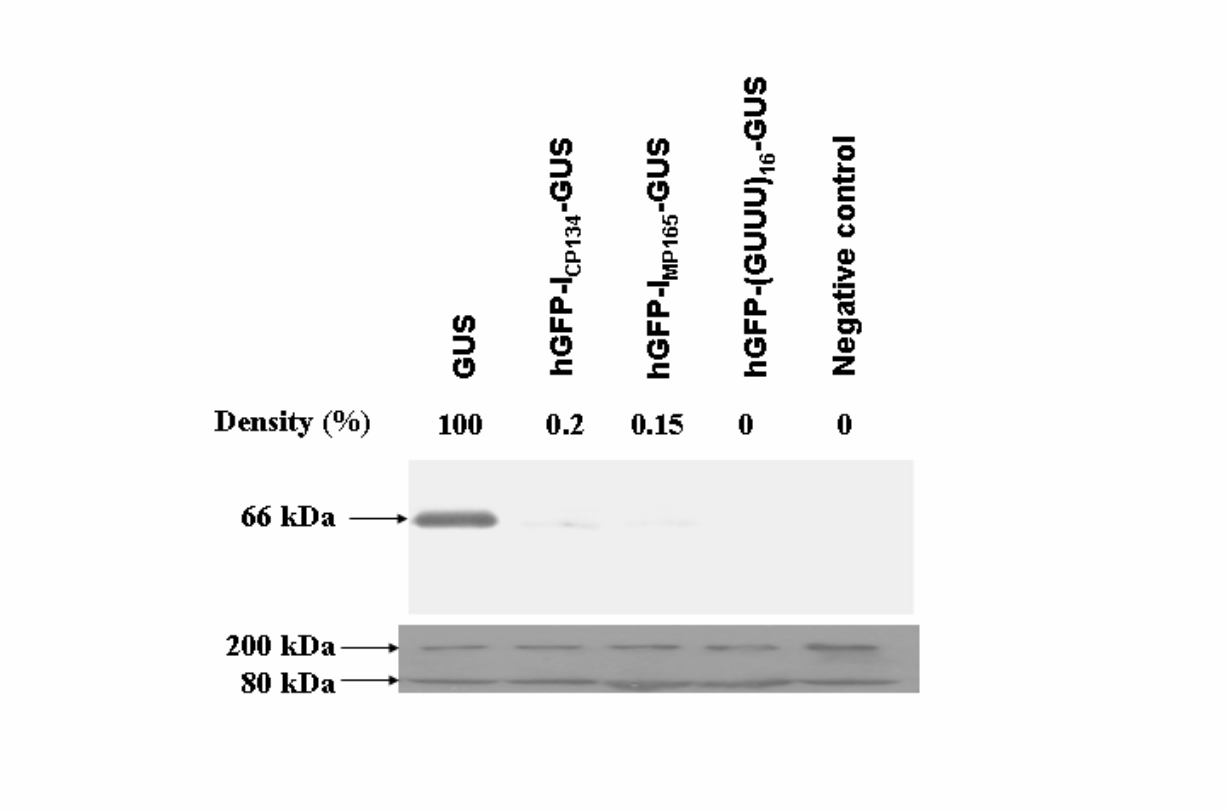

Fig. 5.1 The efficiency of HLSV IRES translation is less than canonical cap-dependent translation *in vitro*. The transctips of GUS, hGFP-I_{CP134}-GUS, hGFP-I_{MP165}-GUS, hGFP-$(GUUU)_{16}$-GUS with caps were produced and *in vitro* translation with same amount of transcripts were assembled. By setting the *in vitro* translation products of GUS transcripts density at 100%, the hGFP-I_{CP134}-GUS was 0.2%, hGFP-I_{MP165}-GUS was 0.15%, while no visible bands seen on hGFP-$(GUUU)_{16}$-GUS and negative control (dH_2O).

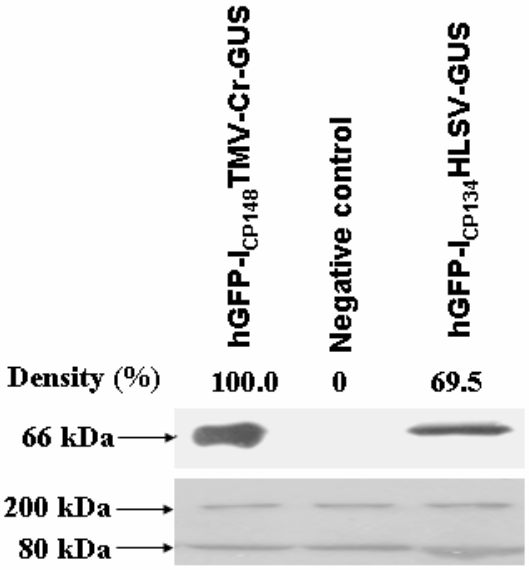

Fig. 5.2 The efficiency of HLSV IRES$_{CP134}$ translation is less than TMV-Cr IRES$_{CP148}$ translation *in vitro.* Comparison of *in vitro* translation products of hGFP-I$_{CP148}$TMV-Cr-GUS and hGFP-I$_{CP134}$HLSV-GUS transcripts was done. By setting the hGFP-I$_{CP148}$TMV-Cr-GUS density at 100%, the density of hGFP-I$_{CP134}$HLSV-GUS was 69.5%, which is less efficient than that of hGFP-I$_{CP148}$TMV-Cr-GUS. No visible band can be seen on dH_2O as negative control.

5.4 The full length HLSV 3'UTR promotes HLSV $IRES_{CP134}$-driven and $IRES_{MP165}$-driven translation *in vitro*

The 3'UTR could be involved in promoting IRES-driven translation in other studies (Koh et al, 2003; Lopez et al., 2002). In this study, the possible interactions of the HLSV 3'UTR and IRES were analyzed and the effects on IRES-driven translation were examined (Fig. 5.3). The 3'UTR could promote both CP and MP IRES-driven translations *in vitro* (Fig. 5.3). In addition, both the poly(A) and 3'TLS segments could promote the two IRES translation separately (Fig. 5.3). The 3'TLS is less efficient as compared with poly(A). However, it is still required for the enhancing effects. Thus the full length 3'UTR could have the highest enhancing effect on the two IRES-driven translations. In Fig. 5.3, it is obvious that the poly(A) promotes the $IRES_{CP134}$-driven translation more efficiently than the 3'TLS. But in $IRES_{MP165}$ translation, it is not very obvious from the Western blot compared to the enhancing efficiency of the poly(A) and the 3'TLS. However by assaying the GUS activity, the poly(A) promoted the IRES-driven translation by 21% while the 3'TLS promotes IRES translation by 12% (data not shown). All together, the results suggested that both poly(A) and 3'TLS could promote two HLSV IRESs-driven translation while the poly(A) could function better than the 3'TLS.

5.5 Domain D1 in the 3'TLS is more important than D2, D3 in promoting IRES translation *in vitro*

Since the 3'TLS could promote the two IRES-driven translations *in vitro*, further characterizations of the important domains of the 3'TLS was done. The 3'TLS could be folded into three stem-loop structures termed D1, D2 and D3 predicted by M-fold (Fig.

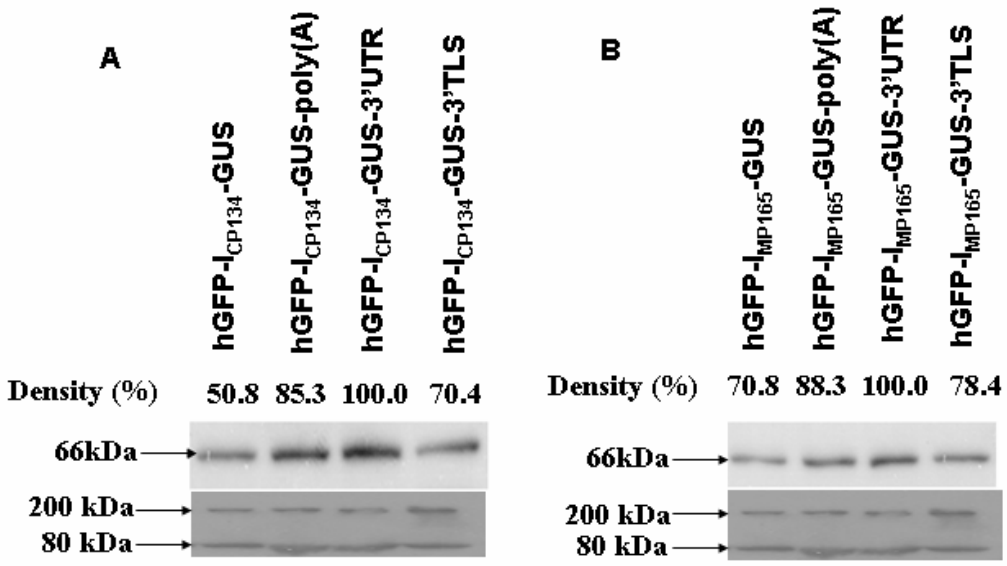

Fig. 5.3 The enhancement of full length HLSV 3'UTR, poly(A) or 3'TLS on IRES$_{CP134}$- and IRES$_{MP165}$-mediated translation *in vitro*. For IRES$_{CP134}$ mediated translation, by setting the *in vitro* translation products of hGFP-I$_{CP134}$-GUS-3'UTR transcripts density at 100%, the density of the hGFP-I$_{CP134}$-GUS was assayed as 50.2%, hGFP-I$_{CP134}$-GUS-poly(A) as 85.3%, hGFP-I$_{CP134}$-GUS-3'TLS as 70.4% respectively. For IRES$_{MP165}$ mediated translation, by setting the *in vitro* translation products of hGFP-I $_{MP165}$-GUS-3'UTR transcripts density at 100%, the density of hGFP-I$_{MP165}$-GUS was assayed as 70.8%, hGFP-I$_{MP165}$-GUS-poly(A) as 88.3%, hGFP-I$_{MP165}$-GUS-3'TLS as 78.4% respectively.

5.4A). To further analyze the effect of these domains on the effect of IRES-driven translation, the deletion of D1, D2 and D3 in the 3'TLS was performed in the bicistronic constructs as indicated (Fig. 5.4B). In transcripts also containing $IRES_{CP134}$, the results showed that the deletion of D1 affected the translation more drastically. However, deletion of D2 did not greatly affect the translation. Deletion of D3 enhanced the band intensity, possibly due to removal of the steric hindrance affecting the ability of D2 to base-pair with the IRES, caused by the presence of D3 (Fig. 5.4B), resulting in enhanced translation. In $IRES_{MP165}$-driven translation, deletion of D1 and D2 both affected the translation efficiency, compared to the intact 3'UTR. Deletion of D3 seemed not to affect the translation efficiency, which is similar to that of $IRES_{CP134}$-driven translation (Fig. 5.4B). Taken together, the results suggested that D3 hinders the IRES driven translation, while D1 and D2 may affect the IRES translational efficiency.

5.6 The HLSV 3'UTR promotes IRES-driven translation *in vivo*

The experiments done using bicistronic constructs in the wheat germ extract system demonstrated that the 3'UTR could promote HLSV IRESs-driven translation *in vitro*. Both the 3'TLS and the poly(A) tract were responsible for the enhancement of IRESs-driven translation *in vitro*. Subsequent experiments were designed to test if the 3'UTR of HLSV could functionally promote IRESs translation *in vivo* since a former study also showed that the IRESs of HLSV could function *in vivo* in whole plant assays by the agro-infiltration method (Srinivasan, 2003). This would indirectly indicate whether these IRESs may have an active role in the viral infection cycle and whether the 3'UTR and IRESs co-operate to enhance the IRESs-driven translation. The *in vivo* constructs were similar to *in vitro* constructs in architecture except that transcription was driven by a 35S

A.

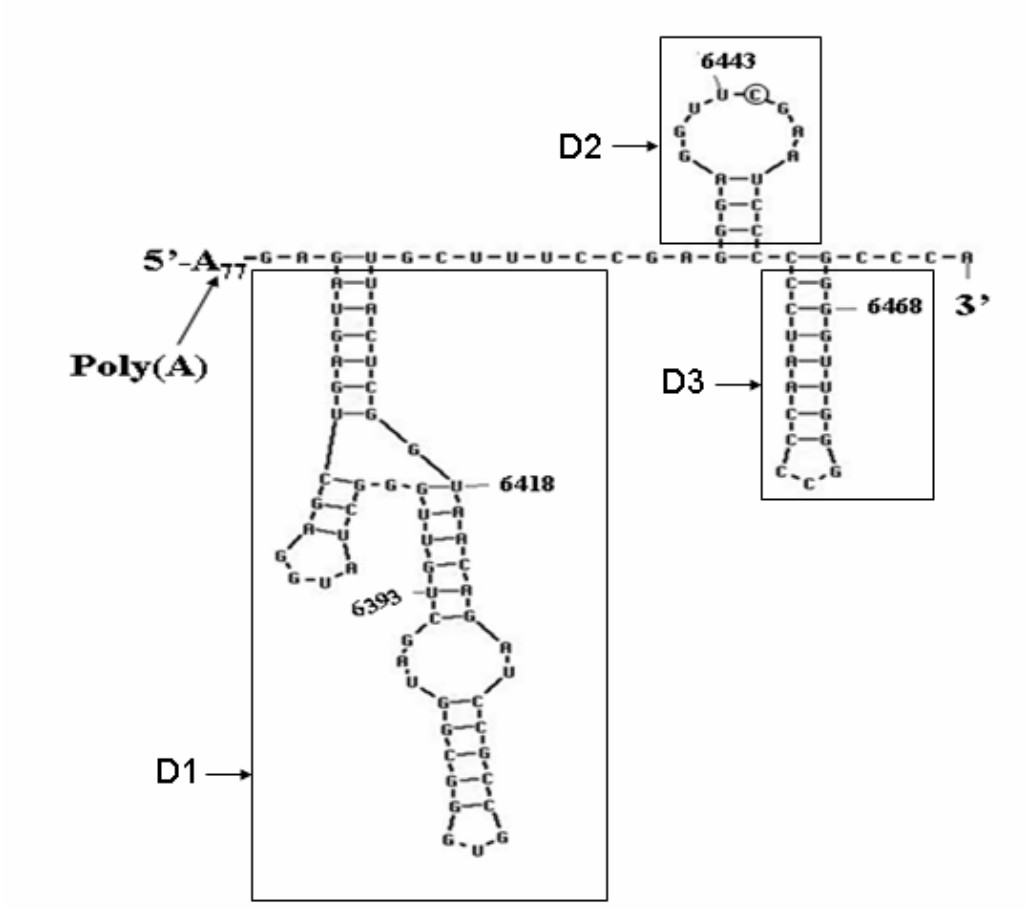

B.

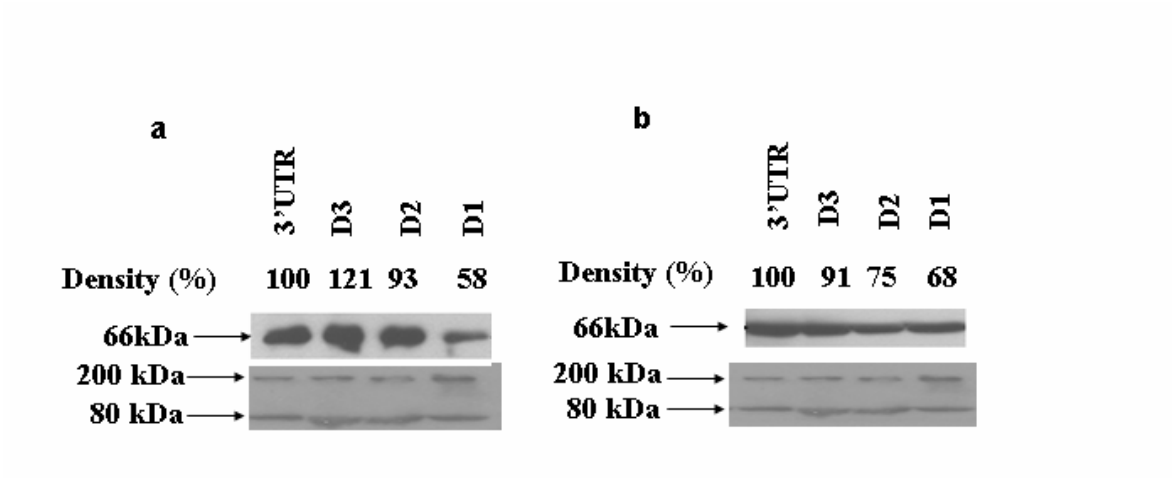

Fig. 5.4 The role of domain D1 in the 3'TLS vs D2, D3 promote IRES translation *in vitro.* A. Secondary structure of 3'TLS. B. Difference of deletion domains affects I_{CP134} (a) and I_{MP165} (b) translational efficiency *in vitro*. For $IRES_{CP134}$ mediated translation, by setting the *in vitro* translation products of hGFP-I_{CP134}-GUS-3'UTR transcripts density at 100%, the density of the hGFP-I_{CP134}-GUS-(3'UTR-D3) was assayed as 121%, hGFP-I_{CP134}-GUS-(3'UTR-D2) as 93%, hGFP-I_{CP134}-GUS-(3'UTR-D1) as 58% respectively. For $IRES_{MP165}$ mediated translation, by setting the *in vitro* translation products of hGFP-I_{MP165}-GUS-3'UTR transcripts density at 100%, the density of hGFP-I_{MP165}-GUS-(3'UTR-D3) was assayed as 91%, hGFP-I_{MP165}-GUS-(3'UTR-D2) as 75%, hGFP-I_{MP165}-GUS-(3'UTR-D1) as 68% respectively.

promoter. The 3'UTR was fused with the *in vivo* constructs of $IRES_{CP134}$ and $IRES_{MP165}$ and tested in *N. benthamiana* leaves (Fig. 5.5A). The observation of GUS activity by GUS staining and GUS assay facilitates the meaningful comparison of efficiencies of different IRES-UTR constructs *in vivo*.

From the results, *in vivo* GUS staining assays after transient expression of these constructs showed that the full length 35S-GFP-I_{CP134}-GUS-3'UTR construct could express GUS at the higher level compared to other constructs (Fig. 5.5 A, B). Constructs 35S-GFP-I_{MP165}-GUS and 35S-GFP-I_{CP134}-GUS still showed considerable GUS activity, which suggested that the IRESs were functionally active *in vivo* (Fig. 5.5 A, B). In the I_{MP165} constructs, the 3'UTR promoted the GUS activity by about 15% (Fig. 5.5B). In the I_{CP134} constructs, the 3'UTR promoted the GUS activity by about 20% (Fig. 5.5B). These effects also were observed in the GUS stained leaves (Fig. 5.5A).

5.7 Discussion

Viruses can employ different mechanisms in order to compete with the host for recruiting the cellular machinery for the synthesis of their viral proteins. The use of alternative mechanisms for translation of viral gene products offers a distinct advantage for the viral RNAs over the host mRNAs. In plant viruses, several sequences have been reported that are capable of recruiting ribosomes internally and lead to IRES-driven translation (Skulachev et al., 1999; Koh et al., 2003). Viruses that lack the 5' cap have IRES sequences which support efficient translation of their gene products (Levis and Astier-Manifacier, 1993). IRESs of different origins differ greatly in sequence, length, secondary structure organization, and functional requirements. Significant variability was revealed in sets of translation initiation factors and/or noncanonical transacting factors

A.

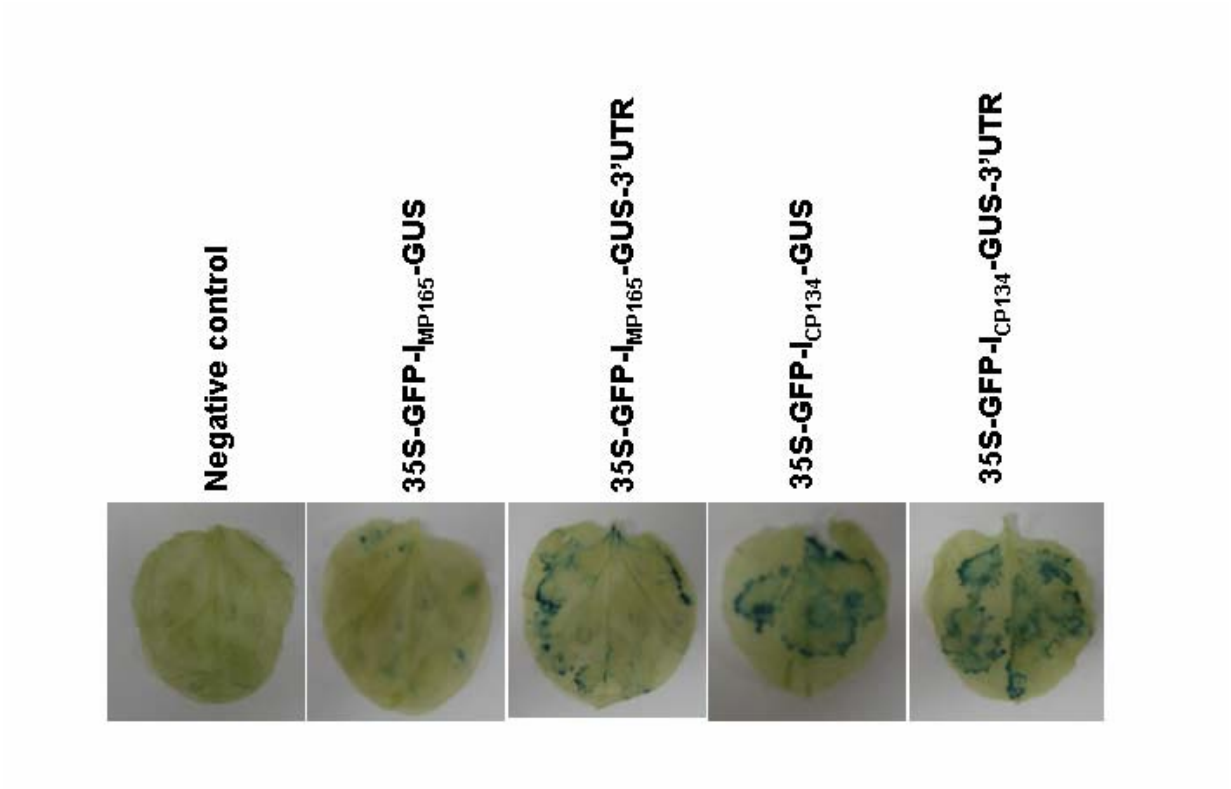
Negative control
35S-GFP-I$_{MP165}$-GUS
35S-GFP-I$_{MP165}$-GUS-3'UTR
35S-GFP-I$_{CP134}$-GUS
35S-GFP-I$_{CP134}$-GUS-3'UTR

B.

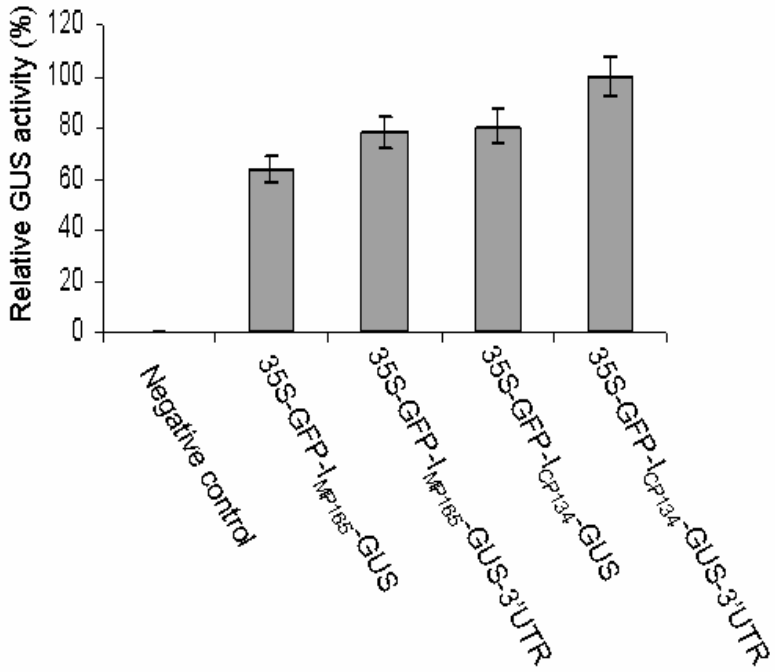

Fig. 5.5 GUS staining (A) and activity assay (B) on the 3'UTR promoting HLSV IRESs translation *in vivo* by agroinfiltration of *N. benthamiana* leaves. (A) GUS staining results of *N. benthaminana* were shown of those infiltrated leaves with dH_2O, 35S-GFP-I_{MP165}-GUS, 35S-GFP-I_{MP165}-GUS-3'UTR, 35S-GFP-I_{CP134}-GUS, 35S-GFP-I_{CP134}-GUS-3'UTR. (B) The relative GUS activity from the leaves of (A) were tested. Results showed that it was 0 from, dH_2O, 61% from 35S-GFP-I_{MP165}-GUS, 80% from 35S-GFP-I_{MP165}-GUS-3'UTR, 83% from 35S-GFP-I_{CP134}-GUS by setting relative GUS activity from 35S-GFP-I_{CP134}-GUS-3'UTR as 100%.

required for the activity of different IRES elements. The IRES activity could be cross-kingdom since animal virus (picornaviruses, hepatitis C virus) IRESs-mediated translation of cellular mRNAs has been reported in yeast. In addition, the IRES of EMCV was active both in animal and, moderately, in plant cells (Urwin et al., 2000). In HLSV, there are two IRES sequences that may operate actively in the genome (Srinivasan, 2003). Firstly, we compared the efficiencies of the two IRESs-driven translation with the canonical cap-dependent translation. Results showed that the cap-dependent translation is far more efficient than the two IRESs translation although the two IRESs were translationally active. Since the full-length eIF4G is required for cap-dependent translation, while only the C-terminal portion of eIF4G is available for IRES-mediated translation, we deduced from the results that the full-length eIF4G is more efficient in recruiting ribosomes than its C-terminal fragment. Studies have shown in the TMV-Cr strain that the $IRES_{CP148}$ functions *in vitro* and *in vivo* (Skulachev et al., 1999; Dorokhov et al., 2002). In this study, the activity of $IRES_{CP134}$ of HLSV was compared to $IRES_{CP148}$ TMV-Cr *in vitro*. Results suggested that the $IRES_{CP134}$ of HLSV was only 69% as efficient as that of the $IRES_{CP148}$ TMV-Cr in driving the IRES-mediated translation. The activities both the IRESs could be attributed to polypurine A rich sequences (PARS) present within the IRESs (Skulachev et al., 1999; Srinivasan, 2003). It has been suggested that PARSs naturally occurring in long 5'UTRs of plant mRNAs (*i*) confer IRES activity and (*ii*) confer this activity across kingdoms. The approach could thus be used to identify IRES elements in eukaryotic genomes as well as viral genomes or subgenomes. HLSV $IRES_{CP134}$ and $IRES_{MP165}$ were found to be active *in vitro* in the wheat germ extract system and *in vivo* in whole plant assays. Mechanisms underlying the

ability to promote internal initiation by such sequences are not been understood. Previous studies implicated two stem loop structures present within $IRES_{MP165}$ being responsible for its activity (Srinivansan, 2003). Sequences within IRES regions that are complementary to 18S rRNA have been shown to be determinants of IRES activity (Koh et al., 2003; Zhou et al 2003).

Studies have shown that the cap-poly(A) and 5'UTR-3'UTR interaction facilitate cap-dependent or cap-independent translation (Fabian and White, 2004; Guo et al., 2002). The IRES-driven translation starts translation internally. Whether this requires interaction with other element in the mRNA is still unknown. Few studies have addressed this issue. In this study, we have analyzed possible interactions of the 3'UTR and IRES elements in HLSV. In addition, the roles of the 3' UTR on the translation driven by two IRESs were analyzed. Our results showed that the 3'UTR could enhance $IRES_{CP134}$-driven and $IRES_{MP165}$-driven translation *in vitro* and *in vivo*. In the wheat germ extract system, the 3'UTR could promote $IRES_{CP134}$-mediated translation 96%, while $IRES_{MP165}$-mediated translation was stimulated by 41% (Fig. 5.3). This enhancement could be due to the IRES-UTR interaction to promote the recycling of internal translational initiators or regulators. Also, the circularized mRNA may help to recycle the 40S ribosomal subunit back to the IRES site for another round of recruitment, which is similar to the cap-poly(A) end-end communication. In addition, the 3'UTR of HLSV contains an internal poly(A) tract and a 3'TLS. In this study, the two parts were analyzed separately *in vitro* for their IRES translational enhancing effect. The results suggested that both the internal poly(A) tract and the 3'TLS could enhance the IRES-translation *in vitro*. The poly(A) tract enhanced the $IRES_{CP134}$-mediated translation by 68% and the $IRES_{MP165}$-mediated

translation by 25% separately. The 3'TLS enhanced the $IRES_{CP134}$ translation by 39% and the $IRES_{MP165}$ by 11% separately (Fig. 5.3). It is suggested that the internal poly(A) had a stronger enhancing effect on the IRES translation than did the 3'TLS. However, both played important roles in this enhancement. In a different study, a report using FMDV showed that the 3'UTR and poly(A) tract could promote its IRES translation *in vitro* and *in vivo* separately (Lopez et al., 2002). The maximum stimulation of FMDV IRES-dependent translation required the presence of the 3'UTR, suggesting a biological role in mediating a functional bridge with the IRES (Lopez et al., 2002). In contrast to the poly(A) tract stimulation of cap-dependent translation, the IRES-dependent stimulatory effect of the 3'UTR is not only resistant, but enhanced during co-expression of the FMDV Lb protease (Lopez et al., 2002). In recent reports, EMCV, HAV, poliovirus and hepatitis C virus (HCV) IRES-dependent translations had been shown to be stimulated by poly(A) sequences in cell-free extracts (Bergamini et al., 2000; Michel et al., 2001; Svitkin et al.,2001). In these cases, a protein-protein bridge was proposed to mediate this stimulation by their mutual interaction with the poly(A) tail and IRES sequences, bringing together the required signals present in both RNA ends. These findings indicate that interaction between eIF4G and PABP is not the only explanation for RNA terminal sequence communication in enhancing translation. The additional factors acting as a bridge between the RNA-binding proteins interacting with the IRES and the 3'UTR sequences should possibly exist. The 5'-3' crosstalk may likely be mediated by protein bridges involving RNA-RNA contacts. In several studies, the X region of the 3'UTR of HCV also has been reported to enhance HCV IRES-mediated translation (Michel et al., 2001; Ito et al., 1998; Ito and Lai, 1999). However, a down regulatory effect was

observed when the entire 3'UTR was present in full-length cDNA clones (Murakami et al., 2001). In another example, the interaction of hnRNP could potentially be involved in communicating between the 3' and 5' ends of mouse hepatitis virus RNA (Huang and Lai, 2001). These studies suggested that some particular interacting partners might interact with both the HLSV 3'UTR and the IRESs sequence in promoting the IRES-mediated translation.

On the other hand, most of the results for IRES-UTR interactions came from the *in vitro* observations. This is a major limitation for the study on HLSV IRES-UTR interaction. To what extent that it is relevant to the virus *in vivo* is hard to explain since till now there is not a suitable system to test this interaction *in vivo* for HLSV in terms of its IRES activity. However, the *in vitro* results suggest that this kind of IRES-UTR interaction might do exsit for enhancing viral proteins translation.

CHAPTER 6

FUTURE DIRECTIONS

6.1 Finding possible interactions between the poly(A) tract and PABP and its effect on translation

In general, tobamoviral 3'UTR consists of a TLS at the 3' terminus and a UPD upstream the TLS. The TLS is essential for minus-strand synthesis (Osman et al., 2000) and the UPD acts as a translational enhancer (Gallie et al., 1991). The presence of a unique 3' UTR region in HLSV makes it very unusual among tobamoviruses. It could also be folded into a TLS domain at the 3' terminus. The UPD upstream the TLS present in all other tobamoviruses is replaced by a poly-A tract (77-96 nt) in HLSV. The aim of this study is to characterize the functions of 3'UTR of HLSV. Based on the unique nucleotide sequence, the HLSV 3'UTR was determined to have important functions on the influence of protein expressions through analysis. The full-length HLSV cDNA clone was constructed and its transcripts were tested in *N. benthamiana*. With less than a minimum length of the internal poly(A) tract, the systemic movement of the transcripts in *N. benthamiana* was influenced although the virus still could accumulate viral RNA in the locally inoculated leaves. The lowCP expression of HLSV in *N. benthamiana* could be the major factor which influenced the systemic movement. The 5'-3'UTR loop-loop interaction was a putative translational enhancing element which was characterized in this study. This end-end communication to enhance translation is found in some other plant viruses like TNV (Shen and Miller, 2004), BYDV (Guo et al., 2001), TBSV (Fabian and White, 2004) and STNV (Lizig et al., 2002). However, this study provided a unique example of end-end communication which could possibly promote translation

through two different ways. This has not been reported in any other plant viruses and it may supplement the understanding of viral translation processes. In addition, the 3'UTR could promote the HLSV IRES translation, which was found in picornaviruses like FMDV (Lopez et al., 2002). The synergistic effect on translation between 3'UTR and IRES was found in a former study in HCRSV, a carmovirus which was characterized in our lab. In this study, the poly(A) and 3'TLS in its 3'UTR could promote IRES-driven translation separately, however, the 3'TLS is less efficient in promoting the IRES-driven translation than the poly(A) tract. This study coincides with the study of IRES translation in FMDV (Lopez et al., 2002). In former study, the UPD was identified to functionally substitute for the poly(A) tract in promoting translation. In the 3'UTR of HLSV, the internal poly(A) tract exists and acts as a translational enhancer. To our knowledge, this is a first observation of an internal poly(A) tract in the 3'UTR that acts as translational enhance element in a plant virus. In other studies, it was observed that a poly(A) tract 15-43 nucleotides is sufficient for associating itself with PABPs, subsequently resulting in translation of proteins as a circular complex by the interaction of PABPs with 5'-caps (Dreher, 1999). In this study, we have not identified whether the poly(A) tract is interacting with the PABPs or other factors to enhance translation. This could be a possible exploration to further analyze the translational mechanisms in future studies.

6.2 Analysis of poly(A) synthesis in the 3'UTR of HLSV

Sequencing the HLSV 3' terminus of several clones generated by conventional cDNA synthesis and cloning methods has confirmed that the internal poly(A) tract found within the 3' UTR region began at the same positions i.e. immediately after the CP stop codon. A putative polyadenylation signal AAUAUA was found 105 nt upstream of the poly(A)

tract in HLSV. In potexviruses such signals are present 120 nt upstream of the poly(A) tail (Abouhaidar, 1988). The poly(A) tail at the 3' end of viral sequences could be added by poly(A) polymerase present in the cytoplasm (Jupin et al., 1990) or by slippage of viral polymerases. Sequences found within vesicular stomatitis virus (VSV) has been shown to influence the backward slippage of polymerase which results in elongation of an A-tract (Barr et al., 1997). The mechanism by which a poly(A) tract is added in HLSV remains obscure. The presence of an internal poly(A) tract may favour template-dependent polymerase slippage. Whether the internal poly(A) tract of HLSV is the product of polymerase slippage remains to be investigated.

6.3 Substitution of the poly(A) tract to analyze its functions

In HLSV, the poly(A) tract is indeed a replacement for the pseudo-knots of TMV. In a comparison experiment, the TMV clones with the internal poly(A) tract of similar length in place of the pseudo-knots, while retaining the TMV TLS, could be constructed and tested for its translational efficiency in plant or animal cells. Also the infectivity of these construct could also be tested since studies showed that the double-helical segment I upstream of the TLS is indispensable for TMV replication (Takamatsu et al., 1990). Other domains within the pseudo-knots could be removed and replaced with the poly(A) tract with marginal effects on infectivity. Through these kinds of experiments, more evidence could be obtained as to whether these elements can be exchanged. These future studies may help to further elucidate the importance of the poly(A) in the 3'UTR of HLSV.

6.4 Finding binding factors between the 5'UTR and 3'TLS which may help promote translation

The 5'-3' loop-loop interaction was analyzed in terms of its contribution to the translation enhancement. However, the binding factors which may promote this loop-loop interaction is still unknown in this process. In a previous study, a single 102 kDa RNA binding protein that binds to those sequences within the 5' leader (Ω) and the UPD in the 3'UTR of TMV was identified (Tanguay and Gallie, 1996). Studies have shown that the 5' leader (Ω) and the 3' UTR of TMV are responsible for enhancing translation of its mRNA (Leathers et al., 1993; Gallie et al., 1987). This suggests a possible role for p102 in translational control and it may be necessary for efficient translation. These author also showed that the protein was conserved both antigenecally and in molecular weight throughout the plant kingdom. Therefore, p102 possibly plays a role in the translation of plant mRNAs that has been conserved throughout plant species, and that TMV has evolved to efficiently compete for this protein on entry into the host. Moreover, as p102 does not bind poly(A), and p102 and PABP are immunologically unrelated, PABP and p102 have distinct sequence specificities. In another study, the eukaryotic elongation factor 1A (eEF1A) was identified interacting with the UPD in the 3'UTR of TMV (Zeenko et al., 2002). Studies also showed that the 5' leader of TMV promotes translation through enhanced recruitment of eIF4F rather than eIFiso4F (Gallie, 2002). Studies on histone mRNA showed the stem-loop binding protein is required for its efficient translation *in vitro* and *in vivo* (Sanchez and Marzluff, 2002). The 3'UTR of HLSV could enhance translation. However, does the stem-loop binding protein or other binding proteins play important roles in this translational enhancement? Will it also utilize similar

machinery to fulfill its translational enhancement, i.e. whether it binds to stem-loop binding protein or eEF1A,p102,eIF4F to enhance translation? For future work, we need to identify the key binding factors which may play important roles in the translational process.

In summary, this piece of research focused on the HLSV untranslated regions, including both 5' and 3'. The secondary structure prediction of HLSV 3'UTR revealed it as poly(A) tract and a TLS. Research focused on the internal poly(A) in the 3'UTR and the putative polyadenylation signal in the CP region which might influence the infectivity of transcripts in the *N. benthamiana* plants. Although there are limitations because the study was done in the whole plant, the results from this study might also be indicative for the functions of HLSV 3'UTR. The length of poly(A) might be important for the virus infectivity. But the mechanism of how it influence infectivity is not clear. The results indicates that there might be a minimum length of the poly(A) for HLSV transcripts infectivity. It will make the study easier if an appropriate protoplasts system is workable for the HLSV transcripts. Also there might be a maximum length of although I've not concerned it in this study. Through study in the wheat germ extract and protoplasts, the 3'UTR of HLSV was identified to be a stronger translational enhancer while 5'UTR might not be. Some function overlap between HLSV 5'UTR and 3'UTR during enhancing translation. By comparing with TMV, HLSV 5'UTR and 3'UTR enhancing translation additively while TMV 5', 3'UTR enhances translation synergistically (Gallie, 2002). This might because of different viral UTRs function differently. It also might be the synergism that I've not tested out in my experiments. The 3'UTR also promotes the IRES-translation when tested *in vitro*. The relevance of the 3'UTR enhancing IRES

translation need to be justified since virologists might doubt its applicability for the virus *in vivo* during viral protein synthesis. However, 3'UTR enhancing IRES translation is a mechanism being identified in FMDV (Lopez et al, 2002) and it might be applicable to HLSV. In the end, this piece of research could broaden the knowledge of 3'UTR of viruses as translational enhancers.

REFERENCES

Abler, M., and Green, P. (1996). Control of mRNA stability in higher plants. *Plant Mol. Biol*. **32**, 63–78.

Abouhaidar, M. G. (1988). Nucleotide sequence of the capsid protein gene and 3' non-coding region of papaya mosaic virus RNA. *J. Gen.Virol.* **69,** 219-26.

Adkins, S., Kamenova, I., Achor, D., and Lewandowski, D.J. (2003). Biological and molecular characterization of a novel tobamovirus with a unique host range. *Plant Disease* **87**, 432-433.

Ali, N., and Siddiqui, A. (1995). Interaction of polypyrimidine tract-binding protein with the 5’ noncoding region of the hepatitis C virus RNA genome and its functional requirement in internal initiation of translation. *J. Virol.* **69**, 6367–6375.

Ali, N., and Siddiqui, A. (1997). The La antigen binds 5’ noncoding region of the hepatitis C virus RNA in the context of the initiator AUG codon and stimulates internal ribosome entry site-mediated translation. *Proc. Natl. Acad. Sci. U.S.A.* **94**, 2249–5422.

Alvarez, D.E., De Lella Ezcurra, A.L., Fucito, S., and Gamarnik, A.V. (2005). Role of RNA structures present at the 3’ UTR of dengue virus on translation, RNA synthesis, and viral replication. *Virology* **339**, 200–212.

Asurmendi, S., Berg, R.H., Koo, J.C., and Beachy, R.N. (2004). Coat protein regulates formation of replication complexes during tobacco mosaic virus infection. *Proc Natl Acad Sci U S A.* **101**, 1415-1420.

Bag, J. (2001). Feedback inhibition of poly(A)-binding protein mRNA translation. A possible mechanism of translation arrest by stalled 40 S ribosomal subunits. *J. Biol. Chem.* **276**, 47352–47360.

Barends, S., Rudinger-Thirion, J., Florentz, C., Giege, R., Pleij, C. W., and Kraal, B. (2004). tRNA-like structure regulates translation of Brome mosaic virus RNA. *J. Virol.* **78**, 4003-4010.

Barr, J.N., Whelan, S.P., and Wertz, G.W. (1997). cis-Acting signals involved in termination of vesicular stomatitis virus mRNA synthesis include the conserved AUAC and the U7 signal for polyadenylation. *J. Virol.* **71,** 8718-25.

Beaudoing, E., Freier, S., Wyatt, J.R., Claverie, J.M., and Gautheret, D. (2000). Patterns of variant polyadenylation signal usage in human genes. *Genome Res.* **10**, 1001-1010.

Bergamini, G., Preiss, T., and Hentze, M.W. (2000). Picornavirus IRESes and the poly(A) tail jointly promote cap-independent translation in a mammalian cell-free system. *RNA* **6**, 1781–1790.

Bernstein, P., Peltz, S.W., and Ross, J. (1989). The poly(A)-poly(A)-binding protein complex is a major determinant of mRNA stability *in vitro*. *Mol. Cell. Biol*. **9**, 659–670.

Bi, X., and Goss, D.J. (2000). Wheat germ poly(A)-binding protein increases the ATPase and the RNA helicase activity of translation initiation factors eIF4A, eIF4B, and eIF-iso4F. *J. Biol. Chem.* **275**, 17740–17746.

Blyn, L.B., Swiderek, K.M., Richards, O., Stahl, D.C., Semler, B.L., and Ehrenfeld, E. (1996). Poly(rC) binding protein 2 binds to stem-loop IV of the poliovirus RNA 5'noncoding region: identification by automated liquid chromatography–tandem mass spectrometry. *Proc. Natl. Acad. Sci. U.S.A.* **93**, 11115–11120.

Blyn, L.B., Towner, J.S., Semler, B.L., and Ehrenfeld, E. (1997). Requirement of poly(rC) binding protein 2 for translation of poliovirus RNA. *J. Virol.* **71**, 6243–6246.

Borman, A.M., Michel, Y.M., and Kean, K.M. (2000). Biochemical characterization of

cap-poly(A) synergy in rabbit reticulocyte lysates: the eIF4G-PABP interaction increases the functional affinity of eIF4E for the capped mRNA 5'-end. *Nucleic Acids Res*. **28**, 4068–4075.

Borman, A.M., Michel, Y.M., Malnou, C.E., and Kean, K.M. (2002). Free poly(A) stimulates capped mRNA translation in vitro through the eIF4G-PABP interaction. *J. Biol. Chem*. **277**, 36818–36824.

Bradford, M.M. (1976). A rapid and sensitive method for the quantitation of microgram quantities of protein utilizing the principle of protein-dye binding. *Anal. Biochem*. **72**, 248-254.

Brierley, I., P. Digard, and S. C. Inglis. (1989). Characterization of an efficient coronavirus ribosomal frameshifting signal: requirement for an RNA pseudoknot. Cell **57**, 537-547.

Brinton, M.A., Fernandez, A.V., and Dispoto, J.H. (1986). The 3'-nucleotides of flavivirus genomic RNA form a conserved secondary structure. *Virology* **153**, 113–121.

Brown, D.M., Kauder, S.E., Cornell, C.T., Jang, G.M., Racaniello, V.R., and Semler, B.L. (2004). Cell-dependent role for the poliovirus 3' noncoding region in positive-strand RNA synthesis. *J. Virol.* **78**, 1344–1351.

Brunt, A.A., Crabtree, K., Dallwitz, M.J., Gibbs, A.J., Watson, L., and Zurcher, E.J. (1996 onwards). Plant Viruses Online: Descriptions and Lists from the VIDE Database. Version: 20th August 1996.' URL http://biology.anu.edu.au/Groups/MES/vide

Bushell, M., Wood, W., Carpenter, G., Pain, V.M., Morley, S.J., and Clemens, M.J. (2001). Disruption of the interaction of mammalian protein synthesis eukaryotic initiation factor 4B with the poly(A)-binding protein by caspase- and viral protease-mediated

cleavages. *J. Biol. Chem*. **276**, 23922–23928.

Chappell, S.A., LeQuesne, J.P., Paulin, F.E., deSchoolmeester, M.L., Stoneley, M., Soutar, R.L., Ralston, S.H., Helfrich, M.H., and Willis, A.E. (2000). A mutation in the c-myc-IRES leads to enhanced internal ribosome entry in multiple myeloma: a novel mechanism of oncogene de-regulation. *Oncogene* **19**, 4437–4440.

Chappell, S.A., Owens, G.C., and Mauro, V.P. (2001). A 5' leader of Rbm3, a cold stress-induced mRNA, mediates internal initiation of translation with increased efficiency under conditions of mild hypothermia. *J. Biol. Chem.* **276**, 36917-36922.

Chiu, W.W., Kinney, R.M., and Dreher, T.W. (2005). Control of translation by the 5'- and 3'-terminal regions of the dengue virus genome. *J. Virol.* **79**, 8303–8315.

Chng, C.G., Wong, S.M., Mahtani, P.H., Loh, C.S., Goh, C.J., Kao, M.C., Chung, M.C., and Watanabe, Y. (1996). The complete sequence of a Singapore isolate of odontoglossum ringspot virus and comparison with other tobamoviruses. *Gene* **171**, 155-161.

Christensen, A.K., Kahn, L.E., and Bourne, C.M. (1987). Circular polysomes predominate on the rough endoplasmic reticulum of somatotropes and mammotropes in the rat anterior pituitary. *Am. J. Anat.* **178**, 1–10.

Claverie, J.M. (1997). Computational methods for the identification of genes in vertebrate genomic sequences. *Human Mol. Genet.* **6**, 1735–1744.

Colgan, D.F., and Manley, J.L. (1997). Mechanism and regulation of mRNA polyadenylation. *Genes. Dev.* **11**, 2755–2766.

Condeelis, J. (1995). Elongation factor 1-alpha, translation and the cytoskeleton. *Trends Biochem. Sci.* **20,** 169–170.

Conne, B., Stutz, A., and Vassalli, J.D. (2000). The 3' untranslated region of messenger RNA: a molecular 'hotspot' for pathology? *Nat. Med.* **6**, 637–641.

Copeland, P.R., Fletcher, J.E., Carlson, B.A., Hatfield, D.L., and Driscoll, D.M. (2000). A novel RNA binding protein, SBP2, is required for the translation of mammalian selenoprotein mRNAs. *EMBO J.* **19**, 306–314.

Craig, A.W., Haghighat, A., Yu, A.T., and Sonenberg, N. (1998). Interaction of polyadenylate-binding protein with the eIF4G homologue PAIP enhances translation. *Nature* **392**, 520–523.

Daughenbaugh, K., Fraser, C., Hershey, J., and Me, H. (2003). The genomelinked protein VPg of the Norwalk virus binds eIF3, suggesting its role in translation initiation complex recruitment. *EMBO J.* **22**, 2852–2859.

Dawson, W.O., Beck, D.L., Knorr, D.A., and Grantham, G.L. (1986). cDNA cloning of the complete genome of tobacco mosaic virus and production of infectious transcripts. *Proc. Natl. Acad. Sci. USA* **83**, 1832-1836.

de Melo Neto, O.P., Standart, N., and Martins de Sa, C. (1995). Autoregulation of poly(A)-binding protein synthesis in vitro. *Nucleic Acids Res.* **23**, 2198–2205.

Decker, C.J., and Parker, R. (1995). Diversity of cytoplasmic functions for the 3' untranslated region of eukaryotic transcripts. *Curr.Opin. Cell Biol.* **7**, 386–392.

Dehlin, E., Wormington, M., Korner, C.G., Wahle, E. (2000). Cap-dependent deadenylation of mRNA. *EMBO J.* **19**, 1079–1086.

Dever, T.E. (2002). Gene-specific regulation by general translation factors. *Cell* **108**, 545–556.

Dobrikova, E., Florez, P., Bradrick, S., and Gromeier, M. (2003). Activity of a type 1

picornavirus internal ribosomal entry site is determined by sequences within the 3' nontranslated region. *Proc. Natl. Acad. Sci. U.S.A.* **100**, 15125–15130.

Dreher, T.W. (1999). Functions of the 3'- untranslated regions of positive strand RNA viral genomes. *Ann. Rev. Phytopathol.* **37**, 151-174.

Edgil, D., Diamond, M.S., Holden, K.L., Paranjape, S.M., and Harris, E. (2003). Translation efficiency determines differences in cellular infection among dengue virus type 2 strains. *Virology* **317**, 275–290.

Edwalds-Gilbert, G., Veraldi, K.L., and Milcarek, C. (1997). Alternative poly(A) site selection in complex transcription units: mean to an end? *Nucleic Acids Res.* **25**, 2547–2561.

Fabian, M.R., and White, K.A. (2004). 5'-3' RNA-RNA interaction facilitates cap- and poly(A) tail-independent translation of tomato bushy stunt virus mrna: a potential common mechanism for tombusviridae. *J. Biol. Chem.* **279**, 28862-28872.

Felden, B., Florentz, C., McPherson, A., and Giege, R. (1994). A histidine accepting tRNA-like fold at the 3'-end of satellite tobacco mosaic virus RNA. *Nucleic Acids Res.* **22**, 2882-2886.

Florentz, C., Briand, J.P., and Giege, R. (1984). Possible functional role of viral tRNA-like structures. *FEBS Letters* **176**, 295-300.

Florez, P.M., Sessions, O.M., Wagner, E.J., Gromeier, M., and Garcia-Blanco, M.A., (2005). The polypyrimidine tract binding protein is required for efficient picornavirus gene expression and propagation. *J. Virol*. **79**, 6172–6179.

Fujiki, M., Kawakami, S., Kim, R.W., and Beachy, R.N. (2006). Domains of tobacco mosaic virus movement protein essential for its membrane association. *J Gen Virol.* **87**,

2699-2707.

Futterer, J., Kiss-Laszlo, Z., and Hohn, T. (1993). Nonlinear ribosome migration on cauliflower mosaic virus 35S RNA. *Cell* **73**, 789-802.

Futterer, J., Potrykus, I., Bao, Y., Li, L., Burns, T. M., Hull, R., and Hohn, T. (1996). Position-dependent ATT initiation during plant pararetrovirus rice tungro bacilliform virus translation. *J. Virol.* **70**, 2999–3010.

Futterer, J., Rothnie, H.M., Hohn, T., and Potrykus, I. (1997). Rice tungro bacilliform virus open reading frames II and III are translated from polycistronic pregenomic RNA by leaky scanning. *J. Virol.* **71**, 7984-7989.

Gallie, D. R., and Browning, K. S. (2001). eIF4G functionally differs from eIFiso4G in promoting internal initiation, cap-independent translation, and translation of structured mRNAs. *J. Biol. Chem.* **276**, 36951–36960.

Gallie, D. R., and Tanguay, R. (1994). Poly(A) binds to initiation factors and increases cap-dependent translation *in vitro*. *J. Biol. Chem*. **269**, 17166-17173.

Gallie, D.R. (1991). The cap and poly(A) tail function synergistically to regulate mRNA translational efficiency. *Genes Dev*.**5**, 2108–2116.

Gallie, D.R. (1998). A tale of two termini: a functional interaction between the termini of an mRNA is a prerequisite for efficient translation initiation. *Gene* **216**, 1–11.

Gallie, D.R. (2002). The 5'-leader of tobacco mosaic virus promotes translation through enhanced recruitment of eIF4F. *Nucleic Acids Res.* **30**, 3401-3411.

Gallie, D.R., and Kobayashi, M. (1994). The role of the 3'-untranslated region of non-polyadenylated plant viral mRNAs in regulating translational efficiency. *Gene* **142**, 159-165.

Gallie, D.R., and Walbot, V. (1990). RNA pseudoknot domain of tobacco mosaic virus can functionally substitute for a poly(A) tail in plant and animal cells. *Genes Dev.* **4**, 1149-1157.

Gallie, D.R., and Walbot, V. (1992). Identification of the motifs within the tobacco mosaic virus 5'-leader responsible for enhancing translation. *Nucleic Acids Res.* **20**, 4631-4638.

Gallie, D.R., Feder, J.N., Schimke, R.T., and Walbot, V. (1991). Functional analysis of the tobacco mosaic virus tRNA-like structure in cytoplasmic gene regulation. *Nucleic Acids Res.* **19**, 5031-5036.

Gallie, D.R., Sleat, D.E., Watts, J.W., Turner, P.C., and Wilson, T.M. (1987). The 5'-leader sequence of tobacco mosaic virus RNA enhances the expression of foreign gene transcripts *in vitro* and *in vivo*. *Nucleic Acids Res.* **15**, 3257-3273.

Gallie, D.R., Sleat, D.E., Watts, J.W., Turner, P.C., and Wilson, T.M. (1988). Mutational analysis of the tobacco mosaic virus 5'-leader for altered ability to enhance translation. *Nucleic Acids Res.* **16**, 883-893.

Garcia-Arenal, F. (1988). Sequence and structure at the genome 3' end of the U2-strain of *tobacco mosaic virus*, a histidine-accepting tobamovirus. *Virololy* **167**, 201-206.

Garcia-Luque, I., Ferrero, M.L., Rodriquez, J.M., Alonso, E., de la Cruz, A., Sanz, A.I., Vaquero, C., Serra, M.T., and Diaz-Ruiz., J.R. (1993). The nucleotide sequence of the coat protein genes and 3' non-coding regions of two resistance-breaking tobamoviruses in pepper shows that they are different viruses. *Arch Virol.* **131**:75-88.

Gautheret, D., Poirot, O., Lopez, F., Audic, S. and Claverie, J.M. (1998). Alternate polyadenylation in human mRNAs: a large scale analysis by EST clustering. *Genome Res.*

8, 524–530.

Gavis, E. (1997). Expeditions to the pole: RNA localization in Xenopus and Drosophila. *Trends Cell Biol.* **7**, 485–492.

Gehring, N.H., Frede, U., Neu-Yilik, G., Hundsdoerfer, P., Vetter, B., Hentze, M.W., and Kulozik, A.E. (2001). Increased efficiency of mRNA 3' end formation: a new genetic mechanism contributing to hereditary thrombophilia. *Nat. Genet.* **28**, 389–392.

Gil, P., and Green, P. (1996). Multiple regions of the Arabidopsis SAUR-AC1 gene control transcript abundance: the 3' untranslated region functions as an mRNA instability determinant. *EMBO J.* **15**, 1678–1686.

Gingras, A.C., Raught, B., and Sonenberg, N. (1999). eIF4 initiation factors: Effectors of mRNA recruitment to ribosomes and regulators of translation. *Annu. Rev. Biochem.* **68**, 913–963.

Girelli, D., Corrocher, R., Bisceglia, L., Olivieri, O., Zelante, L., Panozzo, G., and Gasparini, P. (1997). Hereditary hyperferritinemia-cataract syndrome caused by a 29-base pair deletion in the iron responsive element of ferritin L-subunit gene. *Blood* **90**, 2084–2088.

Goebel, S.J., Hsue, B., Dombrowski, T.F., and Masters, P.S. (2004). Characterization of the RNA components of a putative molecular switch in the 3' untranslated region of the murine coronavirus genome. *J. Virol.* **78**, 669-682.

Goebel, S.J., Taylor, J., and Masters, P.S. (2004). The 3' cis-acting genomic replication element of the severe acute respiratory syndrome coronavirus can function in the murine coronavirus genome. *J. Virol.* **78**, 7846-7851.

Goelet, P., Lomonossoff, G.P., Butler, P.J., Akam, M.E., Gait, M.J., and Karn, J. (1982).

Nucleotide sequence of *tobacco mosaic virus* RNA. *Proc. Natl. Acad. Sci. U S A.* **79**, 5818-5822.

Goodfellow, I., Chaudhry, Y., Gioldasi, I., Gerondopoulos, A., Natoni, A., Labrie, L., Laliberte, J.-F., and Roberts, L. (2005). Calicivirus translation initiation requires an interaction between VPg and eIF4E. *EMBO Rep*. **6**, 968–972.

Graber, J.H., Cantor, C.R., Mohr, S.C., and Smith, T.F. (1999). In silico detection of control signals: mRNA 3'-end-processing sequences in diverse species. *Proc. Natl. Acad. Sci. USA* **96**, 14055–14060.

Gradi, A., Svitkin, Y.V., Imataka, H., and Sonenberg, N. (1998). Proteolysis of human eukaryotic translation initiation factor eIF4GII, but not eIF4GI, coincides with the shutoff of host protein synthesis after poliovirus infection. *Proc. Natl. Acad. Sci. USA* **95**, 11089-11094.

Gray, N.K. and Wickens, M.P. (1998). Control of translation initiation in animals. *Annu. Rev. Cell Dev. Biol*. **14**, 399–458.

Grosset, C., Chen, C.Y., Xu, N., Sonenberg, N., Jacquemin-Sablon, H., and Shyu, A.B. (2000). A mechanism for translationally coupled mRNA turnover: Interaction between the poly(A) tail and a c-fos RNA coding determinant via a protein complex. *Cell* **103**, 29–40.

Gubler, U., and Hoffman, B.J. (1983). A simple and very efficient method for generating cDNA libraries. *Gene* **25**, 263-269.

Guo, L., Allen, E. M., and Miller, W.A. (2001). Base-pairing between untranslated regions facilitates translation of uncapped, nonpolyadenylated viral RNA. *Mol. Cell* **7**, 1103-1109.

Gustafson, G., and Armour, S. L. (1986). The complete nucleotide sequence of RNA beta from the type strain of barley stripe mosaic virus. *Nucleic Acids Res*. **14**, 3895-3909.

Gustafson,G., Armour, S.L., Gamboa, G.C., Burgett, S.G., and Shepherd, J.W. (1989). Nucleotide sequence of barley stripe mosaic virus RNA alpha: RNA alpha encodes a single polypeptide with homology to corresponding proteins from other viruses. *Virology* **170**, 370-377.

Gutierrez-Escolano, A.L., Vazquez-Ochoa, M., Escobar-Herrera, J., and Hernandez-Acosta, J. (2003). La, PTB, and PAB proteins bind to the 3' untranslated region of Norwalk virus genomic RNA. *Biochem. Biophys. Res. Commun*. **311**, 759–766.

Haenni, A.L., Joshi, S., and Chapeville, F. (1982). tRNA-like structures in the genomes of RNA viruses. *Prog. Nucleic. Acid. Res. Mol. Biol*. **27**, 85-104.

Hahn, C.S., Hahn, Y.S., Rice, C.M., Lee, E., Dalgarno, L., Strauss, E.G., and Strauss, J.H. (1987). Conserved elements in the 3' untranslated region of flavivirus RNAs and potential cyclization sequences. *J. Mol. Biol.* **198**, 33–41.

Hamamoto, H., Sugiyama, Y., Nakagawa, N., Hashida, E., Matsunaga, Y., Takemoto, S., Watanabe, Y., and Okada, Y. (1993). A new tobacco mosaic virus vector and its use for the systemic production of angiotensin-I-converting enzyme inhibitor in transgenic tobacco and tomato. *Biotechnology* **11**, 930-932.

Hann, L.E., Webb, A.C., Cai, J.M., and Gehrke, L. (1997). Identification of a competitive translation determinant in the 3' untranslated region of alfalfa mosaic virus coat protein mRNA. *Mol. Cell. Biol.* **17**, 2005– 2013.

Herbert, T.P., Brierley, I., and Brown, T.D. (1997). Identification of a protein linked to the genomic and subgenomic mRNAs of feline calicivirus and its role in translation. *J.*

Gen. Virol. **78**, 1033–1040.

Holden, K. L., and Harris, E. (2004). Enhancement of dengue virus translation: role of the 3' untranslated region and the terminal 3' stem-loop domain. *Virology* **329**, 119–133.

Hood, E.E., Gelvin, S.B., Melchers, S., and Hoekema, A. (1993). New Agrobacterium helper plasmids for gene transfer to plants (EHA105). *Trans. Res.* **2**, 208-218.

Hoshino, S., Imai, M., Kobayashi, T., Uchida, N., and Katada, T. (1999). The eukaryotic polypeptide chain releasing factor (eRF3/GSPT) carrying the translation termination signal to the 3'-Poly(A) tail of mRNA. Direct association of erf3/GSPT with polyadenylate-binding protein. *J. Biol. Chem*. **274**, 16677–16680.

Huang, P. and Lai, M.M. (2001). Heterogeneous nuclear ribonucleoprotein a1 binds to the 3'-untranslated region and mediates potential 5'-3'-end cross talks of mouse hepatitis virus RNA. *J. Virol.*, **75**, 5009-5017.

Hudder, A. and Werner, R. (2000). Analysis of a Charcot–Marie–Tooth disease mutation reveals an essential internal ribosome entry site element in the connexin-32 gene. *J. Biol. Chem.* **275**, 34586–34591.

Ikeda, R., Watanabe, E., Watanabe,Y., and Okada, Y. (1993). Nucleotide sequence of tobamovirus Ob which can spread systemically in N gene tobacco. *J Gen Virol.***74**, 1939-1944.

Imataka, H., Gradi, A., and Sonenberg, N. (1998). A newly identified N-terminal amino acid sequence of human eIF4G binds poly(A)-binding protein and functions in poly(A)-dependent translation. *EMBO J*. **17**, 7480–7489.

Isomura, Y., Matumoto, Y., Murayama, A., Chatani, M., Inouye, N., and M. Ikegami.

(1991). Molecular cloning, sequencing and expression in Escherichia coli of the odontoglossum ringspot virus coat protein gene. *J. Gen. Virol.* **72**, 2247-2249.

Ito, T., and Lai, M.M. (1999). An internal polypyrimidine-tract-binding proteinbinding site in the hepatitis C virus RNA attenuates translation, which is relieved by the 3'-untranslated sequence. *Virology* **254**, 288–296.

Ito, T., Tahara, S.M., and Lai, M.M. (1998). The 3'-untranslated region of hepatitis C virus RNA enhances translation from an internal ribosomal entry site. *J. Virol.*, **72**, 8789-8796.

Ivanov, P.A., Karpova, O.V., Skulachev, M.V., Tomashevskaya, O.L., Rodionova, N.P., Dorokhov, Y.L., and Atabekov, J.G. (1997). A tobamovirus genome that contains an internal ribosome entry site functional *in vitro*. *Virololgy* **232**:32-43.

Jacobson, A. (1996). Poly(A) metabolism and translation: the closed-loop model. Translational Control (Hershey, J. et al., eds). Cold Spring Harbor: Cold Spring Harbor Lab. Press.

Jacobson, A., and Peltz, S.W. (1996). Interrelationships of the pathways of mRNA decay and translation in eukaryotic cells. *Annu. Rev. Biochem.* **65**, 693–739.

Jansen, R.P. (2001). mRNA localization: message on the move. *Nat. Rev. Mol. Cell Biol.* **2**, 247–256.

Jefferson, R.A., Kavanagh, T.A., and Bevan, M.W. (1987). GUS fusions: beta-glucuronidase as a sensitive and versatile gene fusion marker in higher plants. *EMBO J*. **6**, 3901-3907.

Jeon, S., Allen-Hoffmann, B.L., Lambert, P.F. (1995). Integration of human papillomavirus type 16 into the human genome correlates with a selective growth

advantage of cells. *J. Virol.* **69**, 2989–2997.

Jiang, C., and Schuman, E.M. (2002). Regulation and function of local protein synthesis in neuronal dendrites. *Trends Biochem. Sci.* **27**, 506–513.

Jupin, I., Bouzoubaa, S., Richards, K., Jonard, G., and Guilley, H. (1990). Multiplication of beet necrotic yellow vein virus RNA 3 lacking a 3' poly(A) tail is accompanied by reappearance of the poly(A) tail and a novel short U-rich tract preceding it. *Virology* **178,** 281-284.

Kahvejian, A., Svitkin, Y.V., Sukarieh, R., M'Boutchou, M.N., and Sonenberg, N. (2005). Mammalian poly(A)-binding protein is a eukaryotic translation initiation factor, which acts via multiple mechanisms. *Genes Dev.* **19**, 104-113.

Kieft, J.S., Zhou, K., Jubin, R., and Doudna, J.A. (2001). Mechanism of ribosome recruitment by hepatitis C IRES RNA. *RNA* **7**, 194–206.

Kinzy, T. G., and Goldman, E. (2000). Nontranslational functions of components of the translational apparatus, p. 973–997. *In* N. Sonenberg, J. W. B. Hershey, and M. B. Mathews (ed.), Translational control. Cold Spring Harbor Laboratory Press, Cold Spring Harbor, N.Y.

Klausner, R.D., Rouault, T.A., and Harford, J.B. (1993). Regulating the fate of mRNA: the control of cellular iron metabolism. *Cell* **72**, 19–28.

Koh, D.C., Liu, D.X., and Wong, S.M. (2002). A six-nucleotide segment within the 3'untranslated region of *hibiscus chlorotic ringspot virus* plays an essential role in translational enhancement. *J. Virol.* **76**, 1144–1115.

Koh, D.C., Wong, S.M., and Liu, D.X. (2003). Synergism of the 3'-untranslated region and an internal ribosome entry site differentially enhances the translation of a plant virus

coat protein. *J. Biol. Chem*. **278**, 20565– 20573.

Komar, A. A., and Hatzoglou, M. (2005). Internal ribosome entry sites in cellular mRNAs: mystery of their existence. *J. Biol. Chem.* **280**, 23425-23428.

Kong, L.K., and Sarnow, P. (2002). Cytoplasmic expression of mRNAs containing the internal ribosome entry site and 3' noncoding region of hepatitis C virus: effects of the 3' leader on mRNA translation and mRNA stability. *J. Virol.* **76**, 12457–12462.

Kozak, M. (1983). Comparison of initiation of protein synthesis in procaryotes, eucaryotes, and organelles. *Microbiol. Rev.* **47**, 1-45.

Kozak, M. (1986). Regulation of protein synthesis in virus-infected animal cells. *Adv. Virus. Res*. **31**:229-292.

Kozak, M. (1989). The scanning model for translation: an update. *J. Cell. Biol.* **108**, 229-241.

Kozak, M. (1991). Structural features in eukaryotic mRNAs that modulate the initiation of translation. *J. Biol. Chem. 2*66, 19867-19870.

Kozak, M. (2001). Constraints on reinitiation of translation in mammals. *Nucleic. Acids. Res.* **29**, 5226-5232.

Kozak, M. (2002). Pushing the limits of the scanning mechanism for initiation of translation. *Gene* **299**, 1-34.

Laemmli, U.K. (1970). Cleavage of structural proteins during assembly of head bacteriophage T4. *Nature* **227**, 680-685.

Lartey, R.T., Voss, T.C., and Melcher, U. (1995). Completion of a cDNA sequence from a tobamovirus pathogenic to crucifers. *Gene* **166**, 331-332.

Latorre, P., Kolakofsky, D., and Curran, J. (1998). Sendai virus Y proteins are initiated

by a ribosomal shunt. *Mol. Cell. Biol.* **18**, 5021–5031.

Le Quesne, J.P., Stoneley, M., Fraser, G.A., and Willis, A.E. (2001). Derivation of a structural model for the c-myc IRES. *J. Mol. Biol.* **310**, 111-126.

Le, H., Browning, K.S., and Gallie, D.R. (2000). The phosphorylation state of poly(A)-binding protein specifies its binding to poly(A) RNA and its interaction with eukaryotic initiation factor (eIF) 4F, eIFiso4F, and eIF4B. *J. Biol. Chem*. **275**, 17452–17462.

Le, H., Tanguay, R.L., Balasta, M.L., Wei, C.C., Browning, K.S., Metz, A.M., Goss, D.J., and Gallie, D.R. (1997). Translation initiation factors eIF-iso4G and eIF-4B interact with the poly(A)-binding protein and increase its RNA binding activity. *J. Biol. Chem.* **272**, 16247–16255.

Leathers, V., Tanguay, R., Kobayashi, M., and Gallie, D.R. (1993). A phylogenetically conserved sequence within viral 3' untranslated RNA pseudoknots regulates translation. *Mol Cell Biol.* **13**, 5331-5347.

Lehrach, H., Diamond, D., Wozney, J.M., and Boedtker, H. (1977). RNA molecular weight determinations by gel electrophoresis under denaturing conditions, a critical re-examination. *Biochemistry* **16**, 4743-4751.

Lesemann, D. (1977). Virus group-specific and virus-specific cytological alterations induced by members of the tymovirus group. *Phytopathol. Z.* **90**, 315–321.

Lewandowski, D.J. (2005) Tobamovirus. In "Virus Taxonomy, Classification and Nomenclature of Viruses, Eighth Report of the International Committee on the Taxonomy of Virues" (C.M. Fauquet, M.A. Mayo, J. Maniloff, U.Desselberger and L.A. Ball, eds), Elsevier Academic Press, London, pp1009-1014.

Levis, C., and Astier-Manifacier, S. (1993). The 5' untranslated region of PVY RNA,

even located in an internal position, enables initiation of translation. *Virus Genes* **7,** 367-379.

Li, W., and Brinton, M.A. (2001). The 3' stem loop of the West Nile virus genomic RNA can suppress translation of chimeric mRNAs. *Virology* **287**, 49–61.

Liang, X.Z., Ding, S.W., and Wong, S.M. (2002). Development of a kenaf (*Hibiscus cannabinus L.*) protoplast system for replication study of hibiscus chlorotic ringspot virus. *Plant Cell Rep*. **20**, 982-986.

Ling, J., Morley, S.J., Pain, V.M., Marzluff, W.F., and Gallie, D.R. (2002). The histone 3'-terminal stem–loop-binding protein enhances translation through a functional and physical interaction with eukaryotic initiation factor 4G (eIF4G) and eIF3. *Mol. Cell. Biol.* **22**, 7853–7867.

Lo, M.K., Tilgner, M., Bernard, K.A., and Shi, P.Y. (2003). Functional analysis of mosquito-borne flavivirus conserved sequence elements within 3' untranslated region of West Nile virus by use of a reporting replicon that differentiates between viral translation and RNA replication. *J. Virol.* **77**, 10004–10014.

Lomakin, I.B., Hellen, C.U., and Pestova, T.V. (2000). Physical association of eukaryotic initiation factor 4G (eIF4G) with eIF4A strongly enhances binding of eIF4G to the internal ribosomal entry site of encephalomyocarditis virus and is required for internal initiation of translation. *Mol. Cell. Biol.* **20**, 6019–6029.

Lopez de Quinto, S., Saiz, M., de la Morena, D., Sobrino, F., and Martinez-Salas, E. (2002). IRES-driven translation is stimulated separately by the FMDV 3'-NCR and poly(A) sequences. *Nucleic Acids Res.* **30**, 4398–4405.

Luukkonen, B.G., Tan, W. and Schwartz, S. (1995). Efficiency of reinitiation of

translation on human immunodeficiency virus type 1 mRNAs is determined by the length of the upstream open reading frame and by intercistronic distance. *J. Virol*. **69**, 4086-4094.

Mans, R.M., Pleij, C.W., and Bosch, L. (1991). tRNA-like structures. Structure, function and evolutionary significance. *Eur. J. Biochem.* **201**, 303-324.

Matsuda, D., Bauer, L., Tinnesand, K., and Dreher, T. W. (2004). Expression of the two nested overlapping reading frames of turnip yellow mosaic virus RNA is enhanced by a 5' cap and by 5' and 3' viral sequences. *J. Virol*. **78**, 9325-9335.

Matthews, R.E.F. (1991). Plant Virology. San Diego: Academic. 3rd edition.

Mazumder, B., V. Seshadri, and P.L. Fox. (2003). Translational control by the 3'-UTR: the ends specify the means . *Trends Biochem. Sci.* **28**, 91-98.

Mendez, R. and Richter, J.D. (2001). Translational control by CPEB: a means to the end. *Nat. Rev. Mol. Cell Biol.* **2**, 521–529

Merrick, W.C., and Nyborg, J. (2000). The protein biosynthesis elongation cycle, p. 89–125. *In* N. Sonenberg, J. W. B. Hershey, and M. B. Mathews (ed.), Translational control. Cold Spring Harbor Laboratory Press, Cold Spring Harbor, N.Y.

Meshi, T., Ohno,T., Iba , H., and Okada, Y. (1981). Nucleotide sequence of a cloned cDNA copy of TMV (cowpea strain) RNA, including the assembly origin, the coat protein cistron, and the 3' non-coding region. *Mol. Gen. Genet.* **184**, 20-25.

Meulewaeter, F., Lipzig, R.V., Gultyaev, A.P., Pleij, C.W.A., Damme, D.V., Cornelissen, M., and Eldik, G.V. (2004). Conservation of RNA structures enables TNV and BYDV 5' and 3' elements to cooperate synergistically in cap-independent translation. *Nucleic Acids Res.* **32**, 1721-1730.

Meyuhas, O. (2000). Synthesis of the translational apparatus is regulated at the translational level. *Eur. J. Biochem.* 267, 6321–6330.

Michel, Y.M., Borman, A.M., Paulous, S., and Kean, K.M. (2001). Eukaryotic initiation factor 4G-poly(A) binding protein interaction is required for poly(A) tail-mediated stimulation of picornavirus internal ribosome entry segment-driven translation but not for X-mediated stimulation of hepatitis C virus translation. *Mol. Cell. Biol.*, **21**, 4097-4109.

Michel, Y.M., Poncet, D., Piron, M., Kean, K.M., and Borman, A.M. (2000). Cap-poly(A) synergy in mammalian cellfree extracts. Investigation of the requirements for poly(A)-mediated stimulation of translation initiation. *J. Biol. Chem.* **275**, 32268–32276;

Mitchell, P. and Tollervey, D. (2001). mRNA turnover. *Curr. Opin. Cell Biol.* **13**, 320–325.

Mizumoto, H., M. Tatsuta, M. Kaido, K. Mise, and T. Okuno. (2003). Cap-independent translational enhancement by the 3'untranslated region of *red clover necrotic mosaic virus* RNA1. *J. Virol.* **77**, 12113–12121.

Muckenthaler, M., Gray, N.K., and Hentze, M.W. (1998). IRP-1 binding to ferritin mRNA prevents the recruitment of the small ribosomal subunit by the cap binding complex eIF4F. *Mol. Cell* **2**, 383–388.

Mundry, K.W., Watkins, P.A., Ashfield, T., Plaskitt, K.A., Eisele-Walter, S., and Wilson, T.M. (1991). Complete uncoating of the 5' leader sequence of tobacco mosaic virus RNA occurs rapidly and is required to initiate cotranslational virus disassembly *in vitro*. *J. Gen. Virol.* **72**, 769-777.

Murakami, K., Abe, M., Kageyama, T., Kamoshita, N., and Nomoto, A. (2001). Down-regulation of translation driven by hepatitis C virus internal ribosomal entry site by the 3'

untranslated region of RNA. *Arch. Virol*., **146**, 729-741.

Murashige, T., and Skoog, F. (1962). A revised medium for rapid growth and bioassay with tobacco tissue cultures. *Physiol. Plant.* **15**, 473-497.

Neeleman, L., Olsthoorn, R.C., Linthorst, H.J., and Bol, J.F. (2001). Translation of a nonpolyadenylated viral RNA is enhanced by binding of viral coat protein or polyadenylation of the RNA. *Proc. Natl. Acad. Sci. USA*. **98**, 14286–14291.

Negrutskii, B.S., and Elskaya, A.V. (1998). Eukaryotic translation elongation factor 1 alpha: structure, expression, functions, and possible role in aminoacyl-tRNA channeling. *Prog. Nucleic Acid Res. Mol. Biol.* **60,** 47–78.

Oberg, B., and Philipson, L. (1972). Binding of histidine to tobacco mosaic virus RNA. *Biochem Biophys Res Commun.* **48**, 927-932.

Ohlmann, T., Prevot, D., Decimo, D., Roux, F., Garin, J., Morley, S.J., and Darlix, J.L., (2002). *In vitro* cleavage of eIF4GI but not eIF4GII by HIV-1 protease and its effects on translation in the rabbit reticulocyte lysate system. *J. Mol. Biol.* **318**, 9–20.

Ohlmann, T., Rau, M., Pain, V.M., and Morley, S.J. (1996). The C-terminal domain of eukaryotic protein synthesis initiation factor (eIF) 4G is sufficient to support cap-independent translation in the absence of eIF4E. *EMBO J.* **15**, 1371-82.

Ohme-Takagi, M., Taylor, C., Newman, T., and Green, P. (1993). The effect of sequences with high AU content on mRNA stability in tobacco. *Proc. Natl. Acad. Sci. USA* **90**, 11811–11815.

Ohno, T., Aoyagi, M., Yamanashi, Y., Saito, H., Ikawa, S., Meshi, T., and Okada, Y. (1984). Nucleotide sequence of the tobacco mosaic virus (tomato strain) genome and comparison with the common strain genome. *J. Biochem.* (Tokyo). **96**, 1915-1923.

Ohta, S., Mita, S., Hattori, T., and Nakamura, K. (1990). Construction and expression in tobacco of a b-glucuronidase (GUS) reporter gene containing an intron within the coding sequence. *Plant Cell Physiol.* **31**, 805-814.

Olivas, W., and Parker, R. (2000). The Puf3 protein is a transcript specific regulator of mRNA degradation in yeast. *EMBO J*. **19**, 6602–6611.

Olsthoorn R.C., Mertens, S., Brederodes, F.T., and Bol, J.F. (1999). A conformational switch at the 3'end of a plant virus RNA regulates viral replication. *EMBO J.* **18**, 4856-4864.

Osman, T.A., and Buck, K.W. (1996). Complete replication *in vitro* of tobacco mosaic virus RNA by a template-dependent, membrane-bound RNA polymerase. *J. Virol.* **70**, 6227-6234.

Osman, T.A., Hemenway, C.L., and Buck, K.W. (2000). Role of the 3' tRNA-like structure in tobacco mosaic virus minus-strand RNA synthesis by the viral RNA-dependent RNA polymerase in vitro. *J. Virol.* **74**, 11671-11680.

Otero, L.J., Ashe, M.P., and Sachs, A.B. (1999). The yeast poly(A)-binding protein Pablp stimulates *in vitro* poly(A)-dependent and cap-dependent translation by distinct mechanisms. *EMBO J*. **18**, 3153–3163.

Padilla-Noriega, L., Paniagua, O., and Guzman-Leon, S. (2002). Rotavirus protein NSP3 shuts off host cell protein synthesis. *Virology* **298**, 1–7.

Palukaitis, P., and Zaitlin, M. (1986). *Tobacco mosaic virus*: infectivity and replication. In: The Plant Viruses. **2**. The rod shaped plant viruses (eds) Van Regenmortel MHV and Fraenkel-Conrat, pp 105-131. Plenum Press, New York.

Paraskeva, E., Gray, N.K., Schlager, B., Wehr, K., and Hentze, M.W. (1999). Ribosomal

pausing and scanning arrest as mechanisms of translational regulation from cap-distal ironresponsive elements. *Mol. Cell. Biol.* **19**, 807–816.

Peng, S.S., Chen, C.Y., Xu, N., and Shyu, A,B. (1998). RNA stabilization by the AU-rich element binding protein, HuR, an ELAV protein. *EMBO J*. **17**, 3461–3470.

Perez, I., McAfee, J.G., and Patton, J.G. (1997). Multiple RRMs contribute to RNA binding specificity and affinity for polypyrimidine tract binding protein. *Biochemistry* **36**, 11881–11890.

Pesole, G., Liuni, S., Grillo, G., Licciulli, F., Mignone, F., Gissi, C., and Saccone, C. (2002). UTRdb and UTRsite: specialized databases of sequences and functional elements of 5' and 3' untranslated regions of eukaryotic mRNAs. Update 2002. *Nucleic Acids Res.* **30**, 335–340.

Pestova, T.V., Hellen, C.U., and Shatsky, I.N. (1996). Canonical eukaryotic initiation factors determine initiation of translation by internal ribosomal entry. *Mol. Cell. Biol.* **16**, 6859–6869.

Pestova, T.V., Kolupaeva, V.G., Lomakin, I.B., Pilipenko, E.V., Shatsky, I.N., Agol, V.I., and Hellen, C.U. (2001). Molecular mechanisms of translation initiation in eukaryotes. *Proc. Natl. Acad. Sci. U.S.A.* **98**, 7029–7036.

Pilipenko, E.V., Pestova, T.V., Kolupaeva, V.G., Khitrina, E.V., Poperechnaya, A.N., Agol, V.I., and Hellen, C.U. (2000). A cell cycle-dependent protein serves as a template-specific translation initiation factor. *Genes Dev.* **14**, 2028–2045.

Pilipenko, E.V., Poperechny, K.V., Maslova, S.V., Melchers, W.J., Slot, H.J., and Agol, V.I. (1996). Cis-element, oriR, involved in the initiation of (-) strand poliovirus RNA: a quasi-globular multi-domain RNA structure maintained by tertiary ('kissing') interactions.

EMBO J. **15**, 5428-5436.

Piron, M., Vende, P., Cohen, J., and Poncet, D. (1998). Rotavirus RNA-binding protein NSP3 interacts with eIF4GI and evicts the poly(A) binding protein from eIF4F. *EMBO J.* **17**, 5811–5821.

Pizzuti, A., Argiolas, A., Di Paola, R., Baratta, R., Rauseo, A., Bozzali, M., Vigneri, R., Dallapiccola, B., Trischitta, V., and Frittitta, L. (2002). An ATG repeat in the 3'-untranslated region of the human resistin gene is associated with a decreased risk of insulin resistance. *J. Clin. Endocrinol. Metab.* **87**, 4403–4406.

Pleij, C.W.A., Abrahams, J.P., van Belkum, A., Rietveld, K., and Bosch, L. (1987). The spatial folding of the 3' non coding region of aminoacylatable plant viral RNAs. In: Positive strand RNA Viruses. Brinton M and Rueckert R (eds) pp 299-316. Alan R. Liss, New York.

Pooggin, M.M., Futterer, J., Skryabin, K.G., and Hohn, T. (2001). Ribosome shunt is essential for infectivity of cauliflower mosaic virus. *Proc. Natl. Acad. Sci. USA.* **98**, 886–891.

Pooggin, M.M., Hohn, T., and Futterer, J. (2000). Role of a Short Open Reading Frame in Ribosome Shunt on the Cauliflower Mosaic Virus RNA Leader. *J. Biol. Chem*. **275**, 17288–17296.

Preiss, T., and Hentze, M.W. (1999). From factors to mechanisms: translation and translational control in eukaryotes. *Curr. Opin. Genet. Dev*. **9**, 515–521.

Qu, F., and Morris, T.J. (2000). Cap-independent translational enhancement of turnip crinkle virus genomic and subgenomic RNAs. *J. Virol.* **74**, 1085-1093.

Remm, M., Remm, A., and Ustav, M. (1999). Human papillomavirus type 18 E1 protein

is translated from polycistronic mRNA by a discontinuous scanning mechanism. *J. Virol.* **73**, 3062–3070.

Russo, M., Di Franco, A., and Martelli, G.P. (1983). The fine structure of Cymbidium ringspot virus infections in host tissues. III. Role of peroxisomes in the genesis of multivesicular bodies. *J. Ultrastruct. Res*. **82**, 52–63.

Sachs, A. (2000). Physical and functional interactions between the mRNA cap structure and the poly(A) tail. In: Sonenberg, N., Hershey, J.W.B., Matthews, M.B. (Eds.), Translational Control of Gene Expression, second ed. Cold Spring Harbor Laboratory Press, Cold Spring Harbor, NY, pp. 447–465.

Sachs, A. B , Sarnow, P., and Hentze, M. W. (1997). Starting at the beginning, middle, and end: translation initiation in eukaryotes. *Cell* **89**, 831-838.

Sambrook, J., Fritsch, E.F., and Maniatis, T. (1989). Molecular cloning: a laboratory manual, 2nd ed. Cold Spring Harbor Laboratory Press, New York.

Sanchez, R., and Marzluff, W.F. (2002). The stem-loop binding protein is required for efficient translation of histone mRNA in vivo and in vitro. *Mol. Cell Biol.* **22**, 7093–7104.

Sasaki, J., and Nakashima, N. (2000). Methionine-independent initiation of translation in the capsid protein of an insect RNA virus. *Proc. Natl. Acad. Sci. USA*. **97**, 1512-1515.

Schaad, M.C., Jensen, P.E., and Carrington, J.C. (1997). Formation of plant RNA virus replication complexes on membranes: role of an endoplasmic reticulum-targeted viral protein. *EMBO J*. **16**, 4049–4059.

Schmitz, J., Prufer, D., Rohde, W., and Tacke, E. (1996). Non-canonical translation mechanisms in plants: efficient *in vitro* and in planta initiation at AUU codons of the tobacco mosaic virus enhancer sequence. *Nucleic Acids Res.* **24**, 257-263.

Searfoss, A., Dever, T.E., and Wickner, R. (2001). Linking the 3' poly(A) tail to the subunit joining step of translation initiation: relations of Pab1p, eukaryotic translation initiation factor 5b (Fun12p), and Ski2p-Slh1p. *Mol. Cell. Biol*. **21**, 4900–4908.

Shatkin, A.J. (1976). Capping of eukaryotic mRNAs. *Cell* **9**, 645-653.

Sheets, M.D., Fox, C.A., Hunt, T., Vande Woude, G., and Wickens, M. (1994). The 3'-untranslated regions of c-mos and cyclin mRNAs stimulate translation by regulating cytoplasmic polyadenylation. *Genes Dev.* **8**, 926–938.

Shen, R., and Miller, W.A. (2004). The 3' untranslated region of tobacco necrosis virus RNA contains a barley yellow dwarf virus-like cap-independent translation element. *J. Virol.* 78, 4655-4664.

Shi, P.Y., Brinton, M.A., Veal, J.M., Zhong, Y.Y., and Wilson, W.D. (1996). Evidence for the existence of a pseudoknot structure at the 3' terminus of the flavivirus genomic RNA. *Biochemistry* **35**, 4222–4230.

Signori, E., Bagni, C., Papa, S., Primerano, B., Rinaldi, M., Amaldi, F., and Fazio, V.M. (2001). A somatic mutation in the 5'UTR of BRCA1 gene in sporadic breast cancer causes down-modulation of translation efficiency. *Oncogene* **20**, 4596–4600.

Silver, S., Quan, S., and Deom, C.M. (1996). Completion of the nucleotide sequence of sunn-hemp mosaic virus: a tobamovirus pathogenic to legumes. *Virus Genes* **13**, 83-85.

Singh, R.N., and Dreher, T.W. (1998). Specific site selection in RNA resulting from a combination of nonspecific secondary structure and -CCR- boxes: initiation of minus strand synthesis by turnip yellow mosaic virus RNA-dependent RNA polymerase. *RNA* **4**, 1083-1095.

Skulachev, M.V., Ivanov, P.A., Karpova, O.V., Korpela, T., Rodionova, N.P., Dorokhov,

Y.L., and Atabekov, J.G. (1999). Internal initiation of translation directed by the 5'-untranslated region of the tobamovirus subgenomic RNA $I_{(2)}$. *Virology* **263**,139-154.

Solis, I., and Garcia-Arenal, F. (1990). The complete nucleotide sequence of the genomic RNA of the tobamovirus tobacco mild green mosaic virus.*Virology***177**, 553-558.

Soto, M.J., Chen, L.F., Seo, Y.S., and Gilertson, R.L. (2005). Identification of regions of the Beet mild curly top virus (family Geminiviridae) capsid protein involved in systemic infection, virion formation and leafhopper transmission. *Virology* **341**, 257-270.

Srinivasan, K. G. (2003). Molecular characterization of a novel tobamovirus infecting hibiscus. Ph.D thesis, National University of Singapore.

Srinivasan, K.G., Min, B.E., Ryu, K.H., Adkins, S., and Wong, S.M. (2005). Determination of complete nucleotide sequence of Hibiscus latent Singapore virus: Evidence for the presence of an internal poly(A) tract. *Arch. Virol.* **150**, 153-166.

Srinivasan, K.G., Narendrakumar, R., and Wong, S.M. (2002). Hibiscus virus S is a new subgroup II tobamovirus: evidence from its unique coat protein and movement protein sequences. *Arch. Virol.* **147**, 1585-1598.

Stebbins-Boaz, B., Cao, Q., de Moor, C.H., Mendez, R., and Richter, J.D. (1999). Maskin is a CPEB-associated factor that transiently interacts with elF-4E. Mol. *Cell* **4**, 1017–1027.

Sutic, D.D., Ford, R.E., and Tosic, M.T. (1999). Handbook of plant virus diseases. CRC press LLC, Florida, USA.

Svitkin, Y.V., Imataka, H., Khaleghpour, K., Kahvejian, A., Liebig, H.D., and Sonenberg, N. (2001). Poly(A)-binding protein interaction with elF4G stimulates picornavirus IRES-dependent translation. *RNA*, **7**, 1743-1752

Tabaska, J., and Zhang, M.Q. (1999). Detection of polyadenylation signals in human DNA sequences. *Gene* **231**, 77–86.

Takamatsu, N., Watanabe, Y. Iwasaki, T., Shiba, T., Meshi, T., and Okada, Y. (1991). Deletion analysis of the 5' untranslated leader sequence of tobacco mosaic virus RNA. *J. Virol.* **65**,1619-1622.

Takamatsu, N., Watanabe, Y., Meshi, T., and Okada, Y. (1990). Mutational analysis of the pseudoknot region in the 3' noncoding region of tobacco mosaic virus RNA. *J. Virol*. **64**, 3686-3693.

Tan, S.H., Nishiguchi, M., Murata, M., and Motoyoshi, F. (2000). The genome structure of kyuri green mottle mosaic tobamovirus and its comparison with that of cucumber green mottle mosaic tobamovirus. *Arch. Virol.* **145**, 1067-1079.

Tang, C.K., and Draper, D.E. (1989). Unusual mRNA pseudoknot structure is recognized by a protein translational repressor. *Cell* **57**, 531-536.

Tanguay, R.L., and Gallie, D.R. (1996). Isolation and characterization of the 102-kilodalton RNA-binding protein that binds to the 5’ and 3’ translational enhancers of Tobacco mosaic virus RNA. *J. Biol. Chem.* **271**, 14316–14322.

Tarun, S., and Sachs, A.B. (1995). A common function for mRNA 5’ and 3’ ends in translation initiation in yeast. *Genes Dev*. **9**, 2997–3007.

Tarun, S.Z., and Sachs, A.B. (1996). Association of the yeast poly(A) tail binding protein with translation initiation factor eIF4G. *EMBO J.* **15**, 7168–7177.

Thompson, S.R., Goodwin, E.B., and Wickens, M. (2000). Rapid deadenylation and poly(A)-dependent translational repression mediated by the Caenorhabditis elegans tra-2 3’ untranslated region in Xenopus embryos. *Mol. Cell. Biol*. **20**, 2129–2137.

Tilgner, M., Deas, T.S., and Shi, P.Y. (2005). The flavivirus-conserved pentanucleotide in the 3' stem-loop of the West Nile virus genome requires a specific sequence and structure for RNA synthesis but not for viral translation. *Virology* **331**, 375–386.

Tsai, F.J., Lin, C.C., Lu, H.F., Chen, H.Y., and Chen, W.C. (2002). Urokinase gene 3'-UTR T/C polymorphism is associated with urolithiasis. *Urology* **59**, 458–461.

Tsuchihara, K., Tanaka, T., Hijikata, M., Kuge, S., Toyoda, H., Nomoto, A., Yamamoto, N., and Shimotohno, K. (1997). Specific interaction of polypyrimidine tract-binding protein with the extreme 3'-terminal structure of the hepatitis C virus genome, the 3'X. *J. Virol.* **71**, 6720–6726.

Tyc, K., Konarska, M., Gross, H.J., and Filipowicz, W. (1984). Multiple ribosome binding to the 5'-terminal leader sequence of tobacco mosaic virus RNA. Assembly of an 80S ribosome X mRNA complex at the AUU codon. *Eur. J. Biochem.***140**, 503-511.

Uchida, N., Hoshino, S., Imataka, H., Sonenberg, N., and Katada, T. (2002). A novel role of the mammalian GSPT/eRF3 associating with poly(A)-binding protein in Cap/Poly(A)-dependent translation. *J. Biol. Chem.* **277**, 50286–50292.

Ugaki, M., Tomiyama, M., Kakutani, T., Hidaka, S., Kiguchi, T., Nagata, R., Sato, T., Motoyoshi, F., and Nishiguchi, M. (1991). The complete nucleotide sequence of cucumber green mottle mosaic virus (SH strain) genomic RNA. *J Gen Virol.* **72**, 1487-1495.

Urwin, P., Yi, L., Martin, H., Atkinson, H., and Gilmartin, P.M. (2000). *Plant J.* **24,** 583–589.

van Belkum A, Abrahams, J.P., Pleij, C.W., and Bosch, L. (1985). Five pseudoknots are present at the 204 nucleotides long 3' noncoding region of tobacco mosaic virus RNA.

Nucleic Acids Res. **13**, 7673-7686.

van Lipzig, R., Gultyaev, A.P., Pleij, C.W.A., Montagu, M.V., Cornelissen, M., and Meulewaeter, F. (2002). The 5' and 3' extremities of the satellite tobacco necrosis virus translational enhancer domain contribute differentially to stimulation of translation. *RNA* **8**, 229-236.

Vende, P., Piron, M., Castagne, N., and Poncet, D. (2000). Efficient translation of rotavirus mRNA requires simultaneous interaction of NSP3 with the eukaryotic translation initiation factor eIF4G and the mRNA 3' end. *J. Virol.* **74**, 7064–7071.

Vilela, C., Velasco, C., Ptushkina, M., and McCarthy, J.E. (2000). The eukaryotic mRNA decapping protein Dcp1 interacts physically and functionally with the eIF4F translation initiation complex. *EMBO J.* **19**, 4372–4382.

von Der Haar, T., Ball, P.D., and McCarthy, J.E. (2000). Stabilization of eukaryotic initiation factor 4E binding to the mRNA 5'-Cap by domains of eIF4G. *J. Biol. Chem*. **275**, 30551–30555.

Wahle, E., and Keller, W. (1996). The biochemistry of polyadenylation. *TIBS* **21**, 247–250.

Wang, S., and Miller, W. A. (1995). A sequence located 4.5 to 5 kilobases from the 5' end of the barley yellow dwarf virus (PAV) genome strongly stimulates translation of uncapped mRNA. *J. Biol. Chem.* **270**, 13446-13452.

Wang, S., Browning, K. S., and Miller, W. A. (1997). A viral sequence in the 3'-untranslated region mimics a 5' cap in facilitating translation of uncapped mRNA. *EMBO J.* **16**, 4107-4116.

Warner, J.R. (1962). Electron microscope studies of ribosomal clusters synthesizing

hemoglobin. *Science* **138**, 1399–1403.

Waterworth, H.E., and Hadidi, A. (1998). Economic losses due to plant viruses. In: A.Hadidi, R.K.Khetarpal and H. Koganezawa (eds) Plant Virus Disease Control, pp.1-13 APS press,St Paul, MN.

Wei, C.C., Balasta, M.L., Ren, J., and Goss, D.J. (1998). Wheat germ poly(A) binding protein enhances the binding affinity of eukaryotic initiation factor 4F and (iso)4F for cap analogue. *Biochemistry* **37**, 1910–1916.

Wells, S.E., Hillner, P.E., Vale, R.D., and Sachs, A.B. (1998). Circularization of mRNA by eukaryotic translation initiation factors. *Mol. Cell* **2**, 135–140.

Wickens, M., Anderson, P., and Jackson, R.J. (1997). Life and death in the cytoplasm: messages from the 3' end. *Curr. Opin. Genet. Dev.* **7**, 220–232.

Wickens, M., Bernstein, D.S., Kimble, J., and Parker, R. (2002). A PUF family portrait: 3'UTR regulation as a way of life. *Trends Genet.* **18**, 150–157.

Widholm, J.M. (1972). The use of fluorescein diacetate and phenosafranine for determining viability of cultured plant cells. *Stain Tech.* **47**:189-194.

Wilkie, G. S., Dickson, K. S., and Gray, N. K. (2003). Regulation of mRNA translation by 5'- and 3'-UTR-binding factors. *Trends Biochem. Sci.* **28**, 182-188.

Wu, L., Jiang, L., Zhou, Z., Fan, J., Zhang, Q., Zhu, H., Han, Q., and Xu, Z. (2003). Expression of foot-and-mouth disease virus epitopes in tobacco by a tobacco mosaic virus-based vector. *Vaccine* **21**, 4390-4398.

Yamaji, Y., Kobayashi, T., Hamada, K., Sakurai, K., Yoshii, A., Suzuki, M., Namba, S., and Hibi, T. (2006). *In vivo* interaction between Tobacco mosaic virus RNA-dependent RNA polymerase and host translation elongation factor 1A. *Virology* **347**, 100-108.

Yang, A.D., Barro, M., Gorziglia, M.I., and Patton, J.T. (2004). Translation enhancer in the 3'-untranslated region of rotavirus gene 6 mRNA promotes expression of the major capsid protein VP6. *Arch. Virol*. 149, 303–321.

Yueh, A., and Schneider, R.J. (2000). Translation by ribosome shunting on adenovirus and hsp70 mRNAs facilitated by complementarity to 18S rRNA. *Genes Dev.* **14**, 414–421.

Zeenko, V.V., Ryabova, L.A., Spirin, A.S., Rothnie, H.M., Hess, D., Browning, K.S., and Hohn, T. (2002). Eukaryotic elongation factor 1A interacts with the upstream pseudoknot domain in the 3' untranslated region of *Tobacco mosaic virus* RNA. *J. Virol.* **76,** 5678-5691.

Zhang, B., Gallegos, M., Puoti, A., Durkin, E., Fields, S., Kimble, J., Wickens, M.P. (1997). A conserved RNA binding protein that regulates sexual fates in the *C. elegans* hermaphrodite germ line. *Nature* **390**, 477-484.